University of Glasgow | Institute of Neuroscience & Psychology

Predictive feedback to the primary visual cortex during saccades

Grace Edwards

THESIS SUBMITTED TO THE

UNIVERSITY OF GLASGOW FOR THE DEGREE OF

DOCTOR OF PHILOSOPHY

OCTOBER 2014

Contains studies performed in the:
Centre for Cognitive Neuroimaging,
Department of Psychology,
University of Glasgow,
Glasgow,
G12 8QB

For Granddad

Abstract

Perception of our sensory environment is actively constructed from sensory input and prior expectations. These expectations are created from knowledge of the world through semantic memories, spatial and temporal contexts, and learning. Multiple frameworks have been created to conceptualise this active perception, these frameworks will be further referred to as inference models. There are three elements of inference models which have prevailed in these frameworks. Firstly, the presence of internal generative models for the visual environment, secondly feedback connections which project prediction signals of the model to lower cortical processing areas to interact with sensory input, and thirdly prediction errors which are produced when the sensory input is not predicted by feedback signals. The prediction errors are thought to be fed-forward to update the generative models. These elements enable hypothesis driven testing of active perception. In vision, error signals have been found in the primary visual cortex (V1). V1 is organised retinotopically; the structure of sensory stimulus that enters through the retina is retained within V1. A semblance of that structure exists in feedback predictive signals and error signal production. The feedback predictions interact with the retinotopically specific sensory input which can result in error signal production within that region. Due to the nature of vision, we rapidly sample our visual environment using ballistic eye-movements called saccades. Therefore, input to V1 is updated about three times per second. One assumption of active perception frameworks is that predictive signals can update to new retinotopic locations of V1 with sensory input. This thesis investigates the ability of active perception to redirect predictive signals to new retinotopic locations with saccades. The aim of the thesis is to provide evidence of the relevance of generative models in a more naturalistic viewing paradigm (i.e. across saccades).

An introduction into active visual perception is provided in **Chapter 1**. Structural connections and functional feedback to V1 are described at a global level and at the level of cortical layers. The role of feedback connections to V1 is then discussed in the light of current models, which hones in on inference models of perception. The elements of inferential models are introduced including internal generative models, predictive feedback, and error signal production. The assumption of predictive feedback relocation in V1 with saccades is highlighted alongside the effects of saccades within the early visual system, which leads to the motivation and introduction of the research chapters.

A psychophysical study is presented in **Chapter 2** which provides evidence for the transference of predictive signals across saccades. An internal model of spatiotemporal motion was created using an illusion of motion. The perception of illusory motion signifies the engagement of an internal model as a moving token is internally constructed from the sensory input. The model was tested by presenting in-time (predictable) and out-of-time (unpredictable) targets on the trace of perceived motion. Saccades were initiated across the illusion every three seconds to cause a relocation of predictive feedback. Predictable in-time targets were better detected than the unpredictable out-of-time targets. Importantly, the detection advantage for in-time targets was found 50 – 100 ms after saccade indicating transference of predictive signals across saccade.

Evidence for the transfer of spatiotemporally predictive feedback across saccade was supported by the fMRI study presented in **Chapter 3**. Previous studies have demonstrated an increased activity when processing unpredicted visual stimulation in V1. This activity increase has been related to error signal production as the input was not predicted via feedback signals. In **Chapter 3**, the motion illusion paradigm used in **Chapter 2** was redesigned to be compatible with brain activation analysis. The internal model of motion was created prior to saccade and tested at a post-saccadic retinotopic region of V1. An increased activation was found for spatiotemporally unpredictable stimuli directly after eye-movement, indicating the predictive feedback was projected to the new retinotopic region with saccade.

An fMRI experiment was conducted in **Chapter 4** to demonstrate that predictive feedback relocation was not limited to motion processing in the dorsal stream. This was achieved by using natural scene images which are known to incorporate ventral stream processing. Multivariate analysis was performed to determine if feedback signals pertaining to natural scenes could relocate to new retinotopic eye-movements with saccade. The predictive characteristic of feedback was also tested by changing the image content across eye-movements to determine if an error signal was produced due to the unexpected post-saccadic sensory input. Predictive feedback was found to interact with the images presented post-saccade, indicating that feedback relocated with saccade. The predictive feedback was thought to contain contextual information related to the image processed prior to saccade.

These three chapters provide evidence for inference models contributing to visual perception during more naturalistic viewing conditions (i.e. across saccades). These findings are summarised in **Chapter 5** in relation to inference model frameworks, transsacadic perception, and attention. The discussion focuses on the interaction of internal generative models and trans-saccadic perception in the aim of highlighting several consistencies between the two cognitive processes.

Table of Contents

List of Figures

List of Publications

Vetter, P.*, **Edwards, G.*,** & Muckli, L. (2012). Transfer of Predictive Signals Across Saccades. *Frontiers in Psychology*, *3*: 176. 1-10.

Edwards, G., Vetter, P., Petro, L.S., & Muckli, L. (Submitted). Motion specific predictions relocate to new retinotopic positions in V1 with saccade.

Edwards, G., Vizioli, L., & Muckli, L. (In Preparation). Contextually relevant predictive feedback interacts with post-saccadic input to V1.

* signifies equal contribution

Acknowledgements[1]

Throughout my PhD I have looked to many people for guidance, and I'd like to take a moment to thank them.

I would like to start by thanking the boss, Prof. Lars Muckli. You have been hugely encouraging over the past five years, your diligence and positive outlook has been contagious. I have thoroughly enjoyed working with you! You have been both a great supervisor and friend.

Thank you also to Petra and Lucy; I really don't know where I would be without you both. Petra, thank you for being so honest and patient with me, it has been a brilliant way to learn. Lucy, thank you for everything, you saw me through thick and thin personally and professionally.

Phil, Paddy, Ash, & Cairsti – you guys have been a saviour this year. Thanks for suffering my complaints and making everything seem like less of a load. Also thank you for not blaming me for the hangovers.

Thank you to the Muckli lab: Fiona, Tyler, Matt, Luca, & Yulia. Thanks for making me laugh, making me exercise, and for the Pomodoro Technique!

I would also like to thank my friends outside of academia. You've all been very understanding. I can't wait to catch-up on the past year of your lives!

Finally, thank you to my family for all the support and love. Very special thanks to my parents for encouraging and motivating me. You have both been unendingly inspiring.

[1] This work was supported by BBSRC grant BB/G005044/1 and ERC grant StG 2012_311751-BrainReadFBPredCode.

Author’s Declaration

I declare that this thesis is my own work unless indicated otherwise in the text, carried out under normal terms of supervision. All collaborators are duly acknowledged.

This thesis has been composed by the undersigned. It has not been submitted or accepted in any previous application for any degree at this or any other university.

Grace Edwards

.....

Abbreviations

AC-PC	Anterior commissure – Posterior commissure
ANOVA	Analysis of variance
ART	Adaptive resonance theory
BOLD	Bold-oxygen-level dependent
CD	Corollary discharge
CI	Confidence interval
DCM	Dynamic causal modelling
EEG	Electroencephalography
ERP	Event-related potential
FDR	False discovery rate
FEF	Frontal eye field
FFA	Fusiform face area
fMRI	Functional magnetic resonance imaging
FOV	Field of view
GLM	General linear model
hMT/MT	Human medial temporal area/ medial temporal area
LGN	Lateral geniculate nucleus
LIP	Lateral intraparietal area
LOC	Lateral occipital complex
MEG	Magnetoencephalography
MST	Medial superior temporal
MVPA	Multivariate pattern analysis
ofMRI	optogenetic functional magnetic resonance imaging
PC/BC	Predictive coding/ Biased competition model
ROI	Region of interest
SC	Superior colliculus
SD	Standard deviation
SE/SEM	Standard error/ Standard error mean
STS	Superior temporal sulcus
TE	Echo time
TMS	Transcranial magnetic stimulation
TR	Repetition time
V1	Primary visual cortex (striate cortex)
V2, V3, V4, V5	Visual areas of the prestriate and extrastriate cortex

1 Chapter One – General Introduction

1.1 Active sensory perception

Catching a ball seems like a reflex response; however there are many contributing cognitive processes (Bennett, Gorassini, & Prochazka, 1994). In order to catch the ball, you not only have to perceive the ball flying through the air, but also take into account extenuating influences, such as wind, speed of throw, and weight of ball. This is all quite easily accomplished for those who have experience with catch, especially if you know the ball type (e.g. a tennis ball), as the ball's relationship to the environment has previously been established. Catching the ball is therefore actively constructed from sensory input and prior expectation (and an element of co-ordination).

In the 18th Century, the philosopher Bishop Berkeley observed that comprehension of the visual world was obscured by a constantly changing sensory environment, which could only be resolved using prior knowledge (Markov and Kennedy, 2013). This was an early insight to what is widely accepted today, that the brain actively constructs our sensory environment. For example, Gregory's (1970) Dalmatian dog picture demonstrates the use of prior expectations in constructing sensory input when it is ambiguous (Figure 1.1; Mumford, 1992; Bar, 2004). For those who have not observed the image, distinguishing the Dalmatian from the background is a complex task. However, once the dog is actively constructed from the low-level information (Figure 1.1 B), this internal representation will be used on viewing this image in the future, i.e. a prior expectation is created.

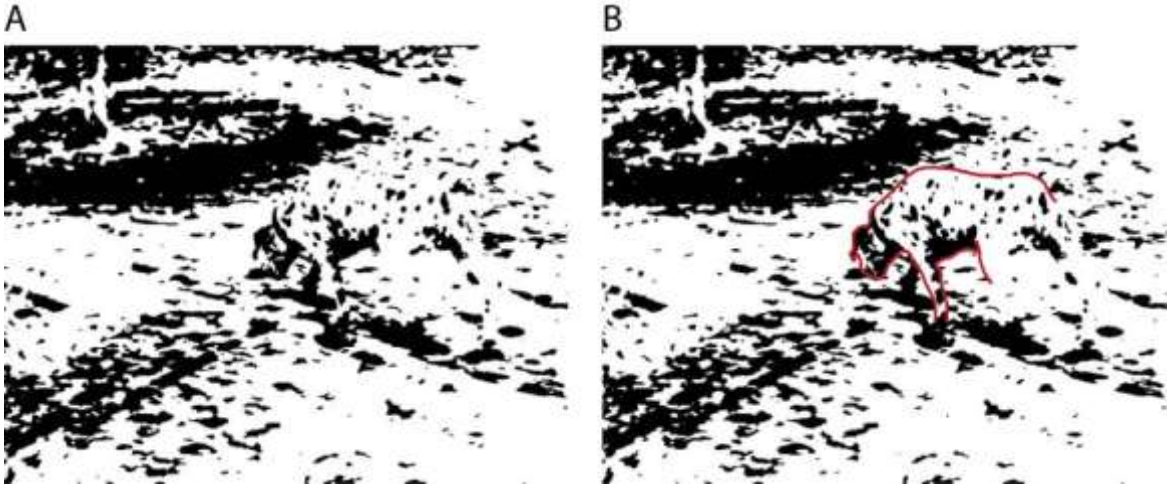

Figure 1.1 - Gregory's Dalmatian dog picture
A) Dalmatian dog blended into the background. B) Dalmatian dog revealed. Even though the Dalmatian can be constructed using top-down processing, the hind-legs are still too subjective to outline.

The effect of active perception on behaviour has also been investigated using a wide variety of experimental paradigms. In the case of ambiguous object presentation, cues from the surrounding environment can facilitate object recognition (Bar, 2004). Ganis & Kutas (2003) have found that objects which are congruent with a scene are quickly identified. Perceptual object completion also occurs when the object is partially occluded (van Lier, van der Helm, & Leeuwenberg, 1994; Sugita, 1999; Erlhagen, 2003; Wyatte, Jilk, & O'Reilly, 2014). An additional example of active perception includes perceptual biases which are induced when a cue (e.g. a tone) is coupled with a specific percept (Sterzer, Frith, & Petrovic, 2008; den Ouden et al., 2010). The cue then results in an increased likelihood of perceiving its coupled stimulus (den Ouden et al., 2010) even in an entirely ambiguous situation (Sterzer, Frith, & Petrovic, 2008). These examples demonstrate that the brain constructs the sensory environment using surrounding contexts and prior experience, influencing on our interaction with the environment.

Behavioural findings of active perception are complemented by brain imaging evidence. One sign of active perception in imaging studies is the increased activity associated with the perception of a surprising or unexpected sensory stimulus (Murray et al., 2002; Ulanorsky, Las, & Nelken, 2003; Alink et al., 2010; den Ouden et al., 2009; den Ouden et al., 2010; Wacongne et al., 2011; Kok, Jehee, & de Lange, 2012). For example increased activity has been found in the cat primary auditory cortex (A1) when a surprising auditory stimulus was delivered (Ulanorsky, Las, & Nelken, 2003). Using combined electroencephalography (EEG) and magnetoencephalography (MEG) in humans, Wacongne and colleagues (2011) also found evidence of surprise when a tone was missing in an expected sequence. Concurrent with an increased activation for the surprising stimulus is a reduced activation for an expected stimulus (Bastos et al., 2012). Short-term contingency between a visual stimulus and a tone have shown a decrease in activity related to predictable stimuli (den Ouden et al., 2010). As subjects learn that a certain tone predicts a particular stimulus (faces or places), the region which responds to the particular stimulus (fusiform face area or parahippocampal place area) reduces activity in response to the tone (den Ouden et al., 2010). It has also been found that motion direction reconstructed from signals in the visual cortex can be biased to a particular direction using top-down expectations (Kok et al., 2013). Face selective regions also decrease in activity when a face is presented on a continuous motion path as compared to discontinuous (Yi et al., 2008). Repetition suppression, which is a known decrease in activity related to repeated stimulus presentation, can be reduced in face processing region (FFA) when the face stimulus

repetition was unlikely (Summerfield et al., 2008). Finally a decreased neuronal response in the superior temporal sulcus (STS) of the monkey occurred when natural images were presented in a predicted sequence (Perrett et al., 2009). These are just a few examples from a wealth of studies on the active creation of our sensory environment from multiple regions of the brain. One region which has become increasingly studied for its role in the construction of visual perception is the primary visual cortex (V1). Typically, V1 is defined by classic receptive field properties, however research has demonstrated that V1 is heavily influenced by predictive signals fed back from higher cortical areas (Muckli, 2010). V1 is thought to integrate sensory feedforward input and cortical feedback signals. Multiple cognitive processes feed information back to V1, including attention, saccadic influences, imagery, memory, and predictive signals. Feedback is best discerned by studying the structural connectivity to V1, and the functional influences that manifest in V1.

1.1.1 V1 Structural Connectivity

The visual system has become a model for active perception (Rao & Ballard, 1999; Douglas & Martin, 2007). A wide variety of methods and analyses have been used to provide evidence of perceptual construction in the primary visual cortex (V1). V1 is an integration centre for both sensory input which is fed-forward from the thalamus, especially the lateral geniculate nucleus (LGN), and cognitive processing signals which are fed-back from multiple regions of the cortex (Douglas & Martin, 2007; Markov & Kennedy, 2013; Muckli & Petro, 2013; Figure 1.2). The structural connectivity of V1 provides a preliminary insight to how our visual world is constructed and perceived. V1 is part of the neocortex which is defined as having 6 layers (Douglas & Martin, 2007). The cortex and subcortex project to different layers of V1. Only 5% of excitatory synapses from LGN terminate in layer 4 (Douglas & Kennedy, 2007; Logothetis, 2008). The spiking activity that results from this sensory input accounts for 20% of the activation response in V1 (Carandini et al., 2005). The remaining activation must be related to intra-cortical input and feedback signals from other cortical regions (Douglas & Martin, 2007; Muckli & Petro, 2013). Tracer injection studies support the existence of large quantities of intra-cortical connections of pyramidal cells (Rockland & Lund, 1982; Sincich & Horton, 2005). Feedback connections to V1, which outnumber those from the thalamus, reinforce the likelihood of their effect on activation. V2, which is one level higher in the visual hierarchy, projects 10 times as many axons to V1 than the LGN. Each pyramidal cell in layer 1 of V1 receives approximately 400 excitatory synapses from non-V1 sources (Budd,

1998; Douglas & Martin, 2007; Muckli & Petro, 2013). Analysis of the hierarchical organisation of cortical areas in the macaque has demonstrated processing streams between higher cortical areas and V1 (Felleman & van Essen, 1991). Due to the relatively high number of feedback projections to V1, the feedback signals from other cortical areas seem significant in the processing of visual stimuli (Douglas & Martin, 2007; Larkum, 2013).

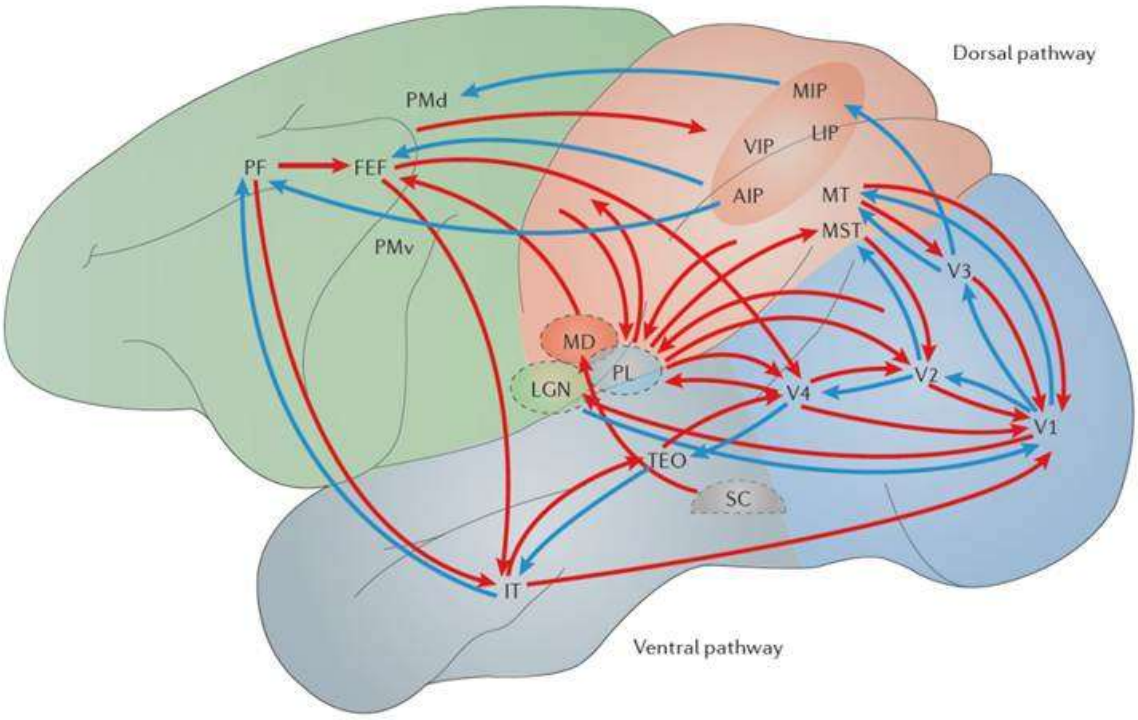

Figure 1.2 - Feedforward and feedback pathways across cortical and subcortical areas
This schematic illustration gives an example of some of the regions which project to V1 (and the projections between other cortical areas). Labelling in the frontal lobe – PF: prefrontal cortex; FEF: frontal eye fields; PMd: dorsal premotor area; PMv: ventral premotor area. Labelling in the parietal lobe – MIP: medial intraparietal area; LIP: lateral intraparietal area; VIP: ventral intraparietal area; AIP: anterior intraparietal area; MT: medial temporal area; MST: medial superior temporal cortex. Labelling in occipital lobe – V1: primary visual cortex; V2, V3, V4: extrastriate visual areas. Labelling in temporal lobe – TEO: tectum opticum; IT: inferior temporal area. Subcortical labelling – SC: superior colliculus; LGN: lateral geniculate nucleus; MD: medial dorsal nucleus; PL: pulvinar (figure with permission from Gilbert & Li, 2013).

1.1.2 Functional feedback to V1

V1 afferent connectivity indicates that its activity is made up of feedforward sensory input, feedback higher cortical input, and lateral interactions. In order to determine the effect of feedback signals from higher cortical areas to V1, neuroimaging experiments have been employed to examine specific cognitive functions fed-back to V1. A memory and imagery based paradigm produced by Albers and colleagues (2013) showed that mental imagery led to patterns in early visual areas that enabled identification of stimuli held in working memory or within imagination. These patterns of stimuli were accompanied by an activity

enhancement in the prefrontal and parietal cortex which may have retained the imagery and memory representations (Albers et al., 2013). Vetter and colleagues (2014) found that activation patterns in V1 held complex natural auditory information and imagined auditory information – such V1 input must be fed back from multisensory areas (Vetter, Smith, & Muckli, 2014). The top-down influence of attention has also been found at a level of V1 (Gilbert & Sigman, 2007; Harris & Thiele, 2011; Verghese et al., 2014). Attention has been found to reduce gamma oscillations in V1 (Chalk et al., 2010) and that spotlight attention is fed-back from dorsal parietal regions to the V1 to gate processed information in object perception (Saalmann, Pigarev, Vidyasagar, 2007). Feedback carrying prior expectations has also been discovered in V1 from paradigms which investigate predictive feedback. V1 is retinotopically organised, which means that the spatial structure of retinal stimulation is preserved (Sereno et al., 1995; Hadjikhani et al., 1998). Predictive feedback elements of a scene should then also project to a specific spatial location of V1 (Sterzer, Haynes, & Rees, 2006; Akselrod, Herzog, & Öğmen, 2014). The portion of V1 processing an occluded region of the visual field have been reported to contain information pertaining to the surrounding context (Smith & Muckli, 2010), along with topographic representations of occluded objects (Ban et al., 2013). Perceived illusory motion has been found to cause activation along the illusory moving trace in V1 (Muckli et al., 2005; Sterzer, Haynes, & Rees, 2006; Alink et al., 2010; Edwards, et al., in prep) and activation was present for regions of V1 processing illusory shapes (Kok & de Lange, 2014). Murray and colleagues also used depth illusions to demonstrate feedback signals to V1. A larger cortical area was activated for a ball which was made to appear larger due to depth cues (Murray, Boyaci, & Kersten, 2006). Colour memory has also been discovered from activity patterns at the level of V1 from grey-scale images. These activation patterns correlate with patterns in V4 which is known to process colour, this indicates that colour information may be fed-back to V1 from V4 (Bannert & Bartels, 2013).

Other approaches for investigating feedback to V1 include cooling which has been used in monkeys (Hupé et al., 2001) and cats (Schmidt et al., 2011). Cooling is a method of inactivating regions by circulating chilled methanol through implanted hypodermic loops resulting in localised hypothermia and blocked functioning of neurons (Lomber et al., 1999; Hupé et al., 2001). Hupé and colleagues demonstrated that cooling the motion processing region MT in monkeys affects the response of V1 neurons rapidly after stimulation onset (Hupé et al., 2001). In cats, cooling of the motion processing region (posteromedial suprasylvian sulcus) demonstrated it was imperative for discriminating between global and local motion in V1 (Schmidt et al., 2011). Feedback has also been

studied in ferrets using voltage sensitive dyes to demonstrate motion dependent feedback between areas 19/21 and 17/18 (Ahmed et al., 2008). Motion related feedback has also been found in humans using EEG (Wibral et al., 2009). Wibral and colleagues revealed three components, the earliest around 60 ms over the early visual cortex which was sensitive to initial stimulus, next at 90 ms spatially coherent to hMT/V5+ related to motion content, and finally the latest component at 110 ms which was sensitive to the retinotopic position of the stimulus causing reactivation of the early visual cortex. The final component was interpreted as evidence of predictive feedback from hMT/V5+ to early visual cortices once the motion had been processed in the second component (Wibral et al., 2009). Recurrent feedback has also been demonstrated using transcranial magnetic stimulation (TMS) in humans (Corthout et al., 1999; Camprodon et al., 2010; Koivisto et al., 2011; Wyatte, Jilk, & O'Reilly, 2014). It was found that application of TMS to V1/V2 between 90-210 ms after stimulation offset effected categorisation of natural scenes. TMS to the lateral occipital complex (LOC) only affected categorisation at 150 ms. Therefore the effects of TMS interruption of V1/V2 after LOC indicates recurrent feedback from LOC to V1/V2 is important for the categorisation task (Koivisto et al., 2011). The multitude of feedback examples presented demonstrates a number of cortical processing feeding into V1 from higher cortical areas.

1.1.3 Feedforward and feedback connections in cortical layers

The two previous sections focus on structural connections and functional activity in V1 in a more global sense. However, cortical connections have been found to be layer specific and recent research on functional activity has supported the layer specificity of feedback and feedforward projections into V1. These details are elaborated in this section, incorporating layer specific connections and functional activation.

Seminal studies of the sensory cortex were provided by Mountcastle (1957) and Hubel and Wiesel (1968). Mountcastle (1957) found evidence of radial columns extending from the white matter to the surface of the cortex in the somatosensory region of cats and monkeys. This structural finding was suggested to form functional columns (Powell & Mountcastle, 1957). Hubel and Wiesel (1968) were able to distinguish cortical layers within the columns in the striate cortex of primates. Many microelectrode recordings in V1 gave the same result of the uniform columns and layers, which has been found throughout the striate cortex (Douglas & Martin, 2007). The function of these cortical columns is best discerned by looking at the structural connections of the columns (Douglas & Martin, 2007). Binzegger and colleagues (2004) analysed the excitatory connections of the cat visual

cortex and found that many synapses could not be accounted for in area V1. It was suggested that local and thalamic neurons were the source (Binzegger, Douglas, & Martin, 2004), however synapses from other sources, such as feedback projections from higher cortical regions, could also terminate in the cortical column (Vezoli, et al., 2004; Douglas & Martin, 2007). Evidence collected over the years, has demonstrated that feedforward sensory input terminates in the middle layers (mainly layer 4), and feedback from other parts of the cortex project to outer layers (supragranular and infragranular layers; Figure 1.3; Coogan & Burkhalter, 1990; Felleman & Van Essen, 1991; Shipp, 2007; Larkum, 2013). This is a fairly basic description as structural analysis of the cortical layers within each column demonstrates that supragranular layers receive thalamic input which is first projected to layer 4. Infragranular layers contain the feedback projections to subcortical regions, including the thalamus, which are thought to have modulatory effects (Rockland & Pandya, 1979; Vezoli et al., 2004; Markov & Kennedy, 2013; Larkum, 2013). Further studies have shown that 80% of neurons projecting a point on the cortical surface have originated within one and a half millimetres. The residual 20% originate from 25-80 areas, mainly close cortical areas and few from distant areas (Markov et al., 2011).

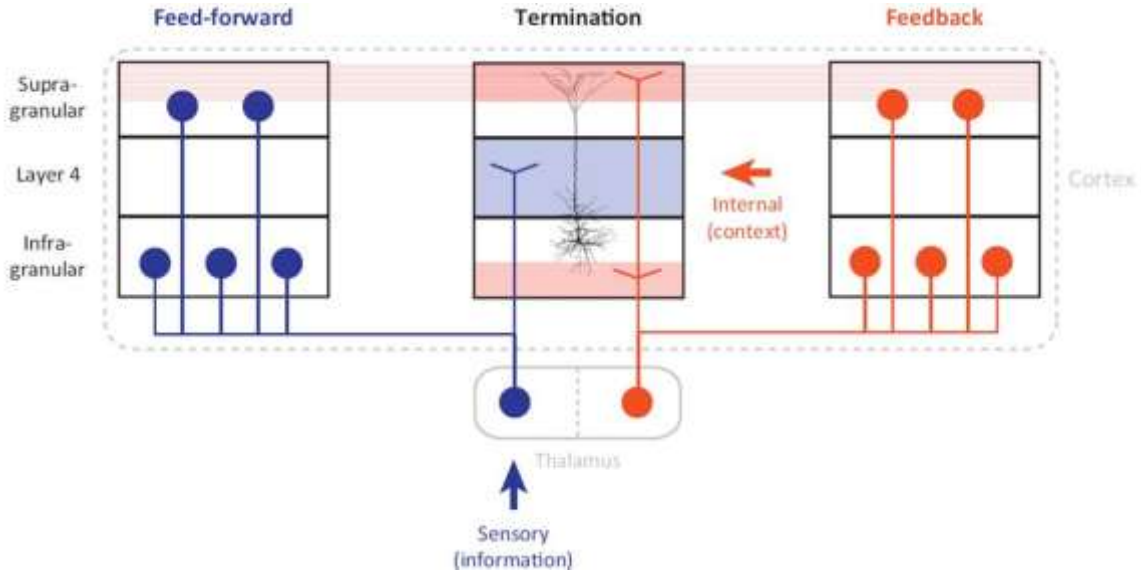

Figure 1.3 - Long-range projections within and into the neocortex
Illustrates the layers of the cortex where feedforward and feedback connections terminate. The feedforward connections (blue) carry information pertaining to the sensory input. The feedback connections (orange) project internal signals from higher cortical areas (figure with permission from Larkum, 2013).

These structural findings have been supported by research in brain oscillations within layers (Roopun et al., 2006; Buffalo et al., 2011; Jensen, Bonnefond, & VanRullen, 2012; Spaak et al., 2012; Bastos et al., 2012; Markov & Kennedy, 2013). Buffalo and colleagues

(2011) found gamma oscillations in supragranular layers, and alpha in infragranular. Differing oscillatory synchronization in layers suggest distinct neuronal dynamics (Bastos et al., 2012). Support for which is indicated by alpha oscillations modulating attention in a feedback manner (Jensen, Bonnefond, & VanRullen, 2012; Spaak et al., 2012). These findings indicate that there are two sets of feedforward and feedback connections which terminate in the supragranular and infragranular layers separately (Markov & Kennedy, 2013). More recently, high-field high-resolution fMRI studies have enabled the investigation of activation at cortical layers (Koopmans, Barth & Norris, 2010; Koopmans et al., 2011; Olman et al., 2012; Olsen et al., 2012; de Martino et al., 2013) with the goal of determining different neuronal computations through the laminae (Olman et al., 2012). It has been demonstrated that the inhibitory feedback from layer 6 of V1 to the LGN and intrinsically to layers 2 and 5 (Olsen et al. 2012). Current research from the Muckli laboratory has demonstrated layer specific differences between the processing of stimulation that incorporates both feedforward and feedback signals versus stimulation with no feedforward input (Muckli, HBM 2014). Muckli and colleagues classified between images using activation patterns at 6 depths of V1 which approximately correspond to the 6 layers of the cortex. In feedback-only conditions it was found that correct classification between images occurred more readily in the superficial cortical layers. This is in line with anatomical findings which indicate that feedback connections from higher cortical areas projected to superficial layers (Budd, 1998; Douglas & Martin, 2007; Bastos et al., 2012; Muckli & Petro, 2013).

1.2 The role of feedback in the brain

1.2.1 Classical models of perception

The classical notion of perception is that feedforward retinal information is analysed at successive levels of the visual hierarchy (Riesenhuber & Poggio, 1999). In this view, the role of feedforward processing is dominant as it is thought that the feedforward connections are recruiting the receptive fields through the visual hierarchy (Marr, 1982). According to the feedforward theory of cortical function, feedback signals play no part (Riesenhuber & Poggio, 1999; Dura-Bernal, Wennekers, & Denham, 2012) or a minor role of selective attention by biased competition (Desimone & Duncan, 1995; Desimone, 1998). One model which relies on feedforward connections only is the HMAX model. HMAX is the standard model within the group of models known as Multi-Stage Hubel-Wiesel networks which were created on the biophysiological principles of the V1 simple and

complex cells (Dura-Bernal, Wennekers, & Denham, 2012). HMAX was originally developed to explain data on the invariance properties and shape tuning of neurons of the inferotemporal cortex in macaque monkeys (Logothetis, Pauls, & Poggio, 1995). HMAX stands apart from the other Multi-Stage Hubel-Wiesel networks as it is modelled on the physiological and psychophysical parameters of the visual system ventral pathway, and is therefore most realistic (Dura-Bernal, Wennekers, & Denham, 2012). However, as highlighted by the authors of the HMAX, ignoring the feedback connectivity which is known to exist across the cortex is a serious limitation of the HMAX (Serre et al., 2007). Other examples of feedforward models incorporate feedback signals, but only in a supporting role of feedforward processing, for example biased competition. Biased competition focuses on the attention competition for internal representation of sensory input, and postulates that this competition is resolved by some internal neural mechanism, i.e. feedback (Desimone & Duncan, 1995). In this case feedback enables processing of specific feedforward information through attention. Biased competition is an example of gain control, where attention-related feedback leads to a non-equally distributed gain which filters the feedforward signal resulting in relevant stimuli being processed (Desimone & Duncan, 1995).

1.2.2 Models of active sensory perception

The theoretical inference model perspective incorporates feedback signals in a more complex manner during active construction of perception (Lee & Mumford, 2003; Clark, 2013; Pickering & Clark, 2014). As described earlier, active perception is the construction of our environment using both sensory input and prior expectations. Models of active perception explain prior expectations in terms of feedback and feedforward loops through the cortical hierarchy. These models were based on proposals such as Grenander's pattern theory where feedback connections enable the 'explaining away' of sensory representations and the Helmholtz machine which saw feedback connections employed for implementing priors (Lee & Mumford, 2003).

One of the first explanations for recognising new sensory input from previously experienced input was developed in the Adaptive Resonance Theory in 1980 (ART; Grossberg, 2013). ART describes feedback signals from generative models of recognised objects as being projected to early cortical areas. If the feedback signals matched the sensory input, an enhanced signal was produced, however if the signals did not match, the signal would be erased. The erased signal indicates an updating of the generative model is necessary, which has been demonstrated in a computational model in real time (Zacharie,

2007). In 1991, David Mumford proposed a computational architecture of the neocortex from a hierarchical view and which employed the thalamus in sensory stimulus processing. The thalamo-cortical loop in Mumford's framework suggests that the thalamus acts as an 'active blackboard' where multiple representations are projected about the current sensory stimulus. These representations are combined by thalamic neurons and are then fed-forward to the input layer of the neocortex (Mumford, 1991). A subsequent article on this framework incorporated cortico-cortical loops and focused on the relationship between higher and lower cortical areas (Mumford, 1992). Higher areas send templates of expected input to lower level cortical areas through deep pyramidal cells. The lower levels merge the templates with thalamic input and communicate any elements not predicted by the template back to higher areas from its superficial pyramidal cells (Mumford, 1992). A few years later, Mumford's framework was followed by hierarchical predictive coding which was proposed by Rao and Ballard (1999). Rao and Ballard created a simulation model in which lower level visual neurons signal the difference between sensory input and predictions communicated from higher cortical areas in response to viewing natural scenes (Figure 1.4). The difference between input and feedback predictions was termed an error signal and could be communicated back to higher cortical areas. Essentially, predictions in the predictive coding framework have an inhibitory effect as they descend from higher cortical areas while prediction errors are excitatory, which stood in stark contrast to the ART model (Rao & Ballard, 1999; Lee & Mumford, 2003; Grossberg, 2013). Rao and Ballard's simulation of neurons which naturally developed the tuning properties of V1/V2 was also replicated by Jehee and colleagues (2006). In addition, Jehee et al. model developed receptive field properties similar to MST when the computational network of neurons were presented with motion input (Jehee et al., 2006). These results support predictive coding in higher cortical levels of the visual hierarchy. In 2003, Mumford followed up his original proposal by introducing hierarchical cortical computation using Bayesian inference (Lee & Mumford, 2003). Bayesian inference uses mathematical and computational models of computer vision. When applied to cortical computation, Bayesian application to the theory results in feedback predictions based on probability (Lee & Mumford, 2003). Using the Bayesian scheme for modelling cortical function, Karl Friston expanded the current models by suggesting a unified theory of the brain which is based on minimising surprise (Friston, 2010). This theory was termed the free-energy principle and works from a similar idea of homeostasis, i.e. maintaining an internal state (Friston, 2010). Minimisation of surprise (or free energy) is a result of correct prediction from higher cortical areas (Markov & Kennedy, 2013). Spratling (2008) has suggested a similar theory

which is formulated on a different architecture of connectivity. Essentially, Spratling's PC/BC model is a reformulation of the predictive coding model using features of the biased competition model. Here the prediction error is created within each cortical region and inhibitory predictions suppress inputs of neighbouring prediction cells rather than supressing outputs (Spratling, 2010).

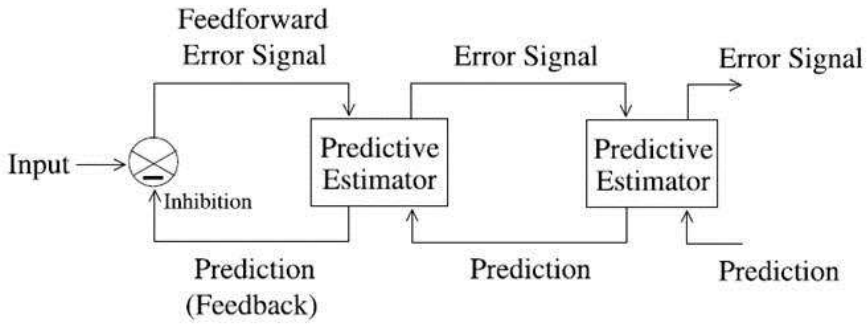

Figure 1.4 - Hierarchical predictive coding model – Rao & Ballard (1999)
Inhibitory predictions are carried by feedback down to lower cortical areas. Excitatory prediction errors are carried by feedback to higher cortical areas. Predictive estimators through the hierarchy correct the estimate of input signal to generative new predictions (figure adapted with permission from Rao & Ballard, 1999).

1.2.3 Classical feedforward models vs. Inference models

The shift of modelling feedback in cortical function from the classical idea of HMAX to the more complex of predictive coding and free energy principle is supported by multiple studies. In order for feedforward models (or feedforward models which give a small role to feedback signals) to account for visual perception, the sensory organ must be stimulated with sensory input. However, many studies have demonstrated how feedback signals contribute to behavioural perception and activation of lower cortical areas without sensory input. Visual illusions of moving stimuli can be perceived without real motion input (Muckli et al., 2005; Schwiedrzik et al., 2007) and the path of the illusory motion can also cause activation in V1 without feedforward stimulation (Muckli et al., 2005; Sterzer, Haynes, & Rees, 2006; Alink et al., 2010). Some cortical models which incorporate feedback in a small role have even been suggested as have evolved from predictive coding Bayes-optimal schemes, specifically biased competition (Feldman & Friston, 2010). Feedback signals in biased competition plays the role of attending to competing sensory input (Desimone & Duncan, 1995). Attention can be considered as a method of optimising representation of uncertainty (i.e. error signals), which is consistent with predictive coding (Feldman & Friston, 2010). Spratling (2008) also fused predictive coding and biased

competition in favour of a modelling approach of biased competition which simplified the assumptions of predictive coding models. This reconciliation becomes clear when attention is considered as optimising uncertain representations of sensory input (Feldman & Friston, 2010).

1.2.4 Internal model generation and updating

The above theories of cortical function differ in interpretation of connectivity and functional activity, however the common elements of all the most recent frameworks are inhibitory feedback cortical predictions and excitatory feedforward error signals. Predictions are a result of internal generative models of our sensory environment. These models are a consequence of day-to-day experience, for example, individuals assume that light comes from above and that objects are convex over concave (Champion & Adams, 2007). Internal generative models are not only affected by semantic memories of our environment, but also spatial context, temporal context, and short-term associations, to name a few (de Wit, Machilsen, & Putzeys, 2010). In these proposals of cortical function, feedback connections have the central function of communicating predictions created by internal generative models of the sensory world from higher cortical areas through the hierarchical levels to explain away immediate future sensory input (Mumford, 1992; Rao & Ballard, 1999; Lee & Mumford, 2003). Predictions sent through feedback connections to lower cortical areas are therefore biasing inference of something about the sensory input (Markov & Kennedy, 2013). When sensory input is not adequately predicted by internal models, error signals are fundamental in updating internal generative models. Prediction errors measure the success of the selected internal model, and have the ability to communicate failed predictions back to higher cortical areas where the models are created. The predictive coding framework suggests that prediction errors are reduced by synaptic strengthening, i.e. plasticity (den Ouden, Kok, & de Lange, 2012). Therefore prediction errors result in physiological changes in cortical connectivity. Specifically, dopaminergic firing during reward prediction errors has been suggested to form relations between action and sensory input, likened to a learning signal (Friston et al., 2012). The precision of prediction errors is based on the quality of sensory information. It has been suggested that precise prediction errors are given more weight using top-down attention (Feldman & Friston, 2010; Hohwy, 2012).

1.2.5 Anatomical feasibility of inference models

After the ART proposal, inference models suggest slightly different connectivity architecture, however the interactions between feedback predictions and feedforward errors remains comparable. One anatomically feasible consideration of prediction and prediction error interaction was provided by den Ouden and colleagues (2012; Figure 1.5). The authors suggested that prediction errors are produced in granular layer 4 of the neocortex (den Ouden, Kok, & de Lange, 2012). The prediction errors are created by subtracting the prediction of agranular layers from the sensory input which is provided by lower levels of the visual hierarchy. Prediction errors result in the updating of predictions which are then communicated forward to higher cortical areas via superficial layers (L2/L3) and backward to lower areas via infragranular layers (L5/L6; Rockland & Pandya, 1979; Vezoli et al., 2004) to update lower level predictions (den Ouden, Kok, de Lange, 2012). This proposed architecture deviates from some models with excitatory feedback (Rao & Ballard, 1999; Friston, 2005) by incorporating the mathematically simplifying assumptions provided by Spratling (2008). It should be reiterated that prediction errors still cause an excitatory response with unpredicted stimuli; however this error is carried in both a feedforward and feedback manner and therefore, the neuronal architecture required for their implementation is different. Importantly, for this structure to be plausible, the segregation of feedforward and feedback should be evident. Markov and colleagues (2013) used a double tracing paradigm which demonstrated that when feedforward and feedback projecting neurons were simultaneously traced, the two populations were separate and had different targets (Markov & Kennedy, 2013). As mentioned previously, there are also distinct oscillatory features of feedforward and feedback layers, which add to evidence of their segregation (Buffalo et al., 2011).

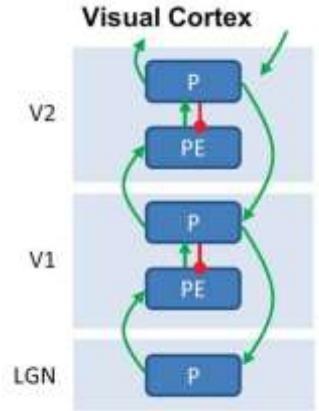

Figure 1.5 - Den Ouden, Kok & de Lange's (2012) potential implementation of prediction (P) and prediction error (PE) interaction
Prediction errors are a mismatch between input (excitatory green arrow) and predictions (inhibitory red projection). Prediction errors update predictions within each region. Prediction units send

excitation forward to higher cortical regions to update generative models, and backward to lower levels to update predictions (adapted image with permission from den Ouden, Kok, & de Lange (2012).

1.3 Evidence for inference models in V1

There are three criteria of inference model frameworks, namely the internal generative model of our sensory environment, the inhibitory prediction fed-back to lower cortical areas, and the excitatory error signal produced in lower cortical areas when the prediction is incorrect. These testable elements enable hypothesis driven investigation of predictive coding in the cortex. Within this thesis, the focus is on the primary visual cortex, which some inferential perception theories have been based upon, namely the original predictive coding framework (Rao & Ballard, 1999; Jehee et al., 2006; Douglas & Martin, 2007). An abundance of evidence has been accumulated in support of this framework within the visual cortex.

Murray and colleagues (2002) found evidence for inhibitory predictive feedback when subjects performed a fixation task whilst they were presented with coherent or incoherent shapes. When coherent shapes were presented, subjects showed a significant increase in activation of the lateral occipital complex (LOC) with a simultaneous decrease in activation found in V1. The LOC has been shown to be important for object and shape perception (Malach et al., 1995; Kanwisher et al., 1996). According to the results, V1 activity was dependent on the degree to which neurons in LOC were tuned for the sensory stimulus, therefore upon information being fed-back from higher to lower visual areas. These findings reflect predictions about coherent shape sensory input communicated from LOC to V1 which caused inhibition in V1 when the coherent shape was presented (Murray et al., 2002). It has also been found that coherent motion causes less activation in V1 than incoherent motion (McKeefry et al., 1997; Harrison et al., 2007; Bartels, Zeki, & Logothetis, 2008).

1.3.1 Activation difference for predictable and unpredictable sensory input

In order to study the activity enhancement related to prediction errors, paradigms have been developed which incorporate predictable and unpredictable stimuli. One of these paradigms incorporates a visual illusion called apparent motion (Muckli et al., 2002; Muckli et al., 2005; Schwiedrzik et al., 2007; Alink et al., 2010; Vetter, Edwards, &

Muckli, 2012; Akselrod, Herzog, & Öğmen, 2014). Apparent motion is the illusion of a moving token between two alternating flashing stimuli (Korte, 1915; Kolers, 1963; Shepard & Zare, 1983). Previously it has been shown that the illusory moving token causes activity in V1 in the region processing the apparent motion trace (Muckli et al., 2005; Sterzer, Haynes, & Rees, 2006; Akselrod, Herzog, & Öğmen, 2014). Recently, retinotopic activity has been found which reflects curved apparent motion paths when the percept of the path is altered using faint path cues (Akselrod, Herzog, & Öğmen, 2014). Using dynamic causal modelling (DCM), this activity was found to originate from hMT/V5+ higher in the hierarchical visual system (Sterzer, Haynes, & Rees, 2006). Therefore, hMT/V5+, which also has large enough receptive fields to process the entire apparent motion stimulus, is involved in the creation of the spatiotemporally specific model. Spatiotemporal predictions related to the illusory moving token are then fed-back to the early visual cortex. Alink and colleagues (2010) tested this hypothesis by presenting targets along the apparent motion trace which are either in-time (spatiotemporally congruent) or out-of-time (spatiotemporally incongruent) with the illusory moving token. When apparent motion was presented without target, activation increased in V1 where the apparent motion trace was being processed, which indicates a filling-in of the illusory moving token (Muckli et al., 2005; Sterzer, Haynes, & Rees, 2006). The in-time targets caused significantly less activation than the out-of-time targets in V1 at the target processing region between the apparent motion inducers (Alink et al., 2010; Figure 1.6). This study provides evidence of an error signal by the increased activation for the out-of-time targets which violate the spatiotemporal model created for the apparent motion percept. Psychophysical studies have shown that subjects are better at detecting the in-time targets than the out-of-time targets which also demonstrates their spatiotemporal predictability (Schwiedrzik et al., 2007; Vetter, Edwards, Muckli, 2012). Others have also used DCM to show that the increased activity in V1 suggested to be related to prediction errors was also related to associative plasticity (den Ouden et al., 2009). Overtime it was found that connectivity changed significantly as a function of error signal production (den Ouden et al., 2009). Predictive spatiotemporal learning has also been demonstrated in mouse V1 (Gavornik & Bear, 2014).

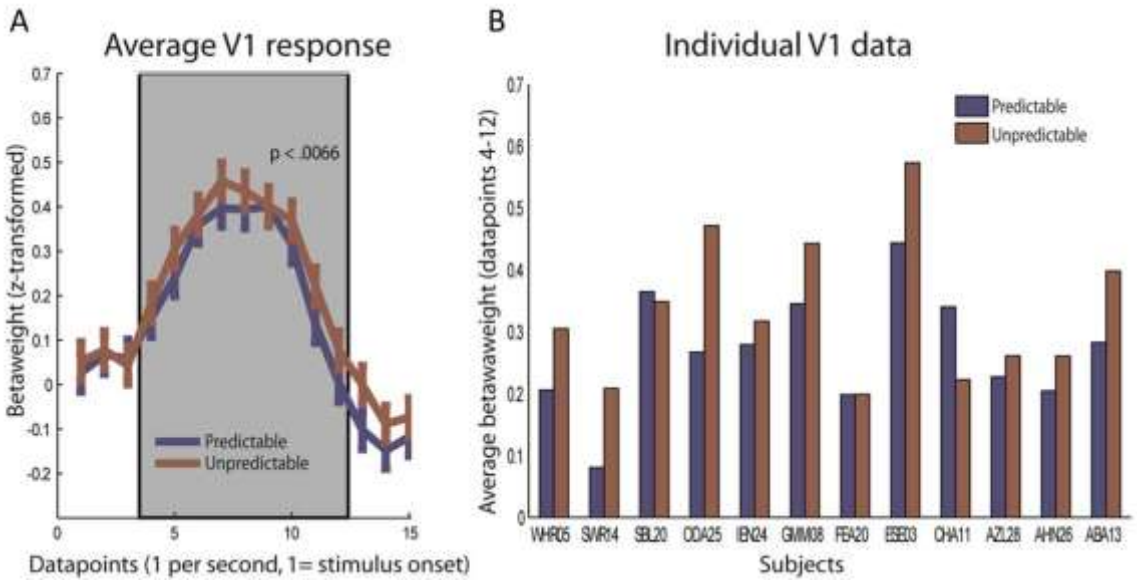

Figure 1.6 - BOLD response in V1 to predictable in-time and unpredictable out-of-time stimuli presented along an apparent motion trace
A) Group event-related BOLD response. B) Single subject peak BOLD amplitude (adapted with permission from Alink et al., (2010).

1.3.2 Contextual feedback evidence in V1

The apparent motion paradigm serves to illustrate spatiotemporal predictions and prediction errors communicated to V1. Recently, studies have been examining the pattern content of regions in V1 which are suppressed due to predicted sensory input. These activity patterns have enabled investigation of the context of predictive feedback from generative models. Activity patterns are studied using multivariate pattern analysis (MVPA). Activity patterns are created by retaining the activity of each voxel in an area, rather than averaging across the voxels to get an overall activity amplitude (Kriegeskorte & Bandettini, 2007). This pattern of voxel activity is specific to the stimulus being processed. Therefore the overall activation of a region can be the same for two stimuli, but the activity pattern can be different providing information on what the subject has perceived. Kok and colleagues (2012) found that the pattern of activity in V1 for the stimulus was more decipherable when the stimulus was predicted. This indicates that the internal representation was improved by the predictability of the stimulus, which provides more evidence of feedback predictions of sensory stimulation. Contextual information has also been detected using MVPA in regions of V1 which are not stimulated by sensory information. Smith & Muckli (2010) found that the cortical region in V1 representing the occluded portion of an image held a representation of the surrounding image (Figure 1.7).

This demonstrates that the higher visual cortex fills in expected contextual information and that this information is fed-back to the occluded processing region in V1 (Smith & Muckli, 2010). Others have also demonstrated that occluded portions of objects are represented in the early visual cortex (Ban et al., 2013). Feedback predictions have also been studied in ferrets in the absence of visual stimulation (Berkes et al., 2011). It was found that the spontaneous activity which occurred without stimulation was very similar to activity when the ferrets viewed natural scenes. The similarity became stronger through development and the activity was specific to the feedforward natural scenes stimulation (Berkes et al., 2011). This demonstrates that the spontaneous activity was geared towards the visual stimulus the ferrets learned in their environment overtime.

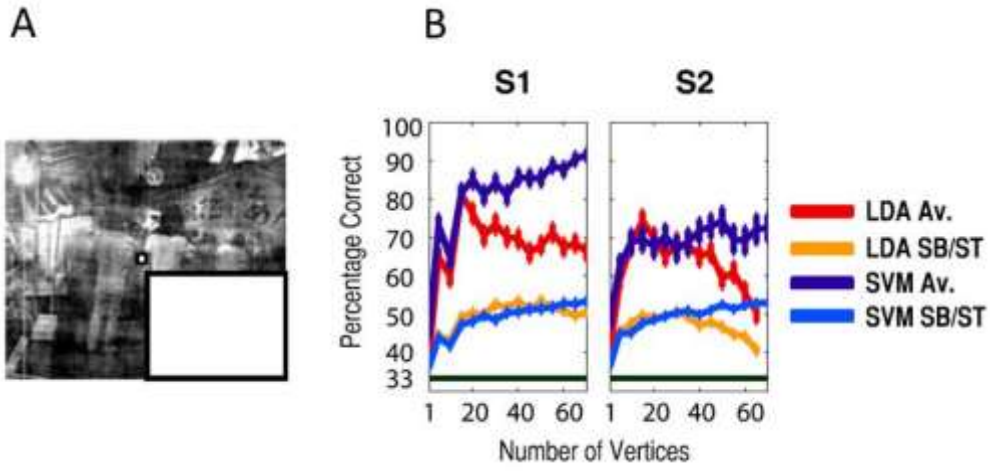

Figure 1.7 - Single subject pattern classification in V1 region processing an occluded quadrant of an image
A) Example of stimuli with bottom right corner occluded. B & C) Averaged and single block pattern classification using two different classifiers (LDA & SVM) for two subjects (adapted with permission from Smith & Muckli, 2010).

These examples of predictive feedback signals to V1 are strongly suggestive of the active construction of our visual environment. The evidence presented demonstrates that internal generative models of the environment influence our sensory processing at the level of the primary visual cortex. However, research to date has focused on predictive feedback to V1 during steady fixation. In reality, humans move their eyes multiple times per second (Melcher, 2011). This results in the repositioning of sensory input within V1 with each eye-movement (Adams, Sincich, & Horton, 2007). As described previously, V1 is retinotopic and predictive feedback has been found to project to the relevant processing regions of V1 (Akselrod, Herzog, & Öğmen, 2014). Therefore predictive signals should also relocate to new regions of V1 with saccades (i.e. eye-movements). A large body of

research has been collected on saccadic effects in V1; however the influence of saccades on predictive feedback to V1 is unknown. Saccades are discussed below with reference to V1 processing, further highlighting the need to test for predictive feedback across eye-movements.

1.4 Saccadic eye-movement effects on V1

1.4.1 Fixation vs. saccade studies

In previous years, it has been customary to study the V1 neuronal response with fixation paradigms. In this case, V1 neurons are stimulated either by flashing or bringing stimuli into their receptive fields, rather than the more naturalistic method of using free viewing or saccade paradigms. Paradigms using steady fixation are valuable as reproducible retinal stimulation can be created which allows reliable neural averaging across trials in V1. However, the steady fixation approach to studying V1 is limited as saccades are restricted and therefore V1 is not studied in an ecologically valid setting (Olshausen & Field, 2005). By removing saccades, the natural rhythm between fixations and saccades which gives a temporal dynamic to visual processing is also extinguished. The limitations highlighted here surely result in an incomplete description of the function of V1 (MacEvoy, Hanks, & Paradiso, 2008).

Previously, the receptive field response found in V1 was determined as similar between fixating on a stimulus via saccade and flashing the stimulus onto the receptive field manually (Richmond, Hertz, & Gawne, 1999). However, this study focused only on orientation tuning approach. Those who used single unit recordings in V1 found contrasting evidence which demonstrates that saccades alter the basic receptive field properties of V1 in comparison to a flashed stimulus (Livingstone, Freeman, & Hubel, 1996; Gallant, Connor, Van Essen, 1998; MacEvoy, Hanks, & Paradiso, 2008). Differences found in how stimulation is perceived (with or without saccades) highlight the importance of studying V1 with the most naturalistic approach possible (Olshausen & Field, 2005).

1.4.2 The purpose of saccades

Saccadic eye-movements enable active vision. Active vision is the ability to actively search our visual environment using saccades (Schroeder et al., 2010), which should not be confused with active perception (i.e. integrating feedforward sensory stimulus with

generative models of our environment) discussed previously. Information must be combined across saccades, otherwise the visual system would need to re-perceive the visual environment with each eye-movement, and therefore the benefits of the ability to saccade would be lost (Melcher & Colby, 2008). Another issue is the time taken to re-perceive after each saccade. In object recognition, the first pass of visual processing takes approximately 100ms from the retina (Thorpe & Fabre-Thorpe, 2001). As we move our eyes approximately 150,000 times per day, visual perception would be catching-up to sensory input for four hours per day (Melcher & Colby, 2008). Finally, the smooth and continuous perception we perceive despite ballistic eye-movements is another indication that information is integrated across saccades (Melcher, 2011).

Stemming from this logic, multiple theories have been suggested for the integration of sensory information across saccades. The most plausible of which is trans-saccadic perception, which was derived from human psychophysics, primate neurophysiology, and neuroimaging (Melcher & Colby, 2008). According to Melcher & Colby (2008), trans-saccadic perception is compiled of five main components based on a large body of research. Firstly, trans-saccadic perception is enabled by a predictive process which remaps visual information by updating input spatial location with each saccade, called dynamic receptive field remapping. Each eye-movement is accompanied by a corollary discharge which is a neural copy of the self-induced movement (Sperry, 1950). This discharge facilitates remapping by indicating the amount and direction that external stimuli will move across the retina during the saccade (Melcher & Colby, 2008; Crapse & Sommer, 2008). Dynamic receptive fields are activated in order to receive sensory input at the imminent fixation location, just prior to and during the saccade (Parks & Corballis, 2008). Dynamic receptive fields therefore allow remapping salient objects to new receptive fields with saccadic eye-movement ready for continued processing (Melcher & Colby, 2008; Irwin & Robinson, 2014). It is important to mention that an element of working memory is necessary to remap the representations of salient objects (Prime et al., 2007). The second principle is closely linked to dynamic receptive fields, which is the ability to predict the outcome of a saccade (i.e. where the saccade will land, and therefore where the sensory input will relocate; Wexler, 2005). The third component is the intermediate processing stage, which is the ability to determine an object from abstract shapes, contours, and colours using higher cortical areas within the visual hierarchy (Harrison & Bex, 2014), for example, incorporating the lateral occipital complex (LOC) for object perception (Malach et al., 1995; Kanwisher et al., 1996). This feature-integration in the intermediate

processing stage highly suggests the incorporation of generative models (Harrison & Bex, 2014). The fourth component is the effect of remapping on the intermediate processing stage, which is more substantial in higher cortical areas (Tolias et al., 2001; Nakamura & Colby, 2002; Merriam, Genovese, & Colby, 2007). This higher cortical remapping essentially determines what information will be carried across saccade (Melcher & Colby, 2008). Finally, the fifth component incorporates the perception of gist. Gist is defined as the general meaning of a scene which can be determined rapidly from one glimpse (Gombrich, 1979). Although the gist of a scene cannot be remapped with saccade, the combination of known gist with the previous four components enables the detection of inconsistencies in perceptual experience (Melcher & Colby, 2008). Evidence for saccade related information transference across hemispheres has been found in human EEG studies. Bellebaum and Daum (2006) studied the memory trace remapped across hemispheres due to saccades and found an early and late positive wave localised to the posterior parietal cortex (PPC). The early positivity was located contralateral to saccade direction and was related to the mechanical process of remapping. The late positivity which was found ipsilateral to the saccade direction was also reported in subsequent studies (i.e. Peterburs et al., 2011), and related to the sensory memory of the remapped stimulus (Bellebaum & Daum, 2006).

These five components work within trans-saccadic perception in order to combine sensory input across saccade. During trans-saccadic perception a saccadic suppression of neurons occurs. Saccadic suppression ensures the blur of the eye-movement is not perceived (Wurtz, 2008; Irwin & Robinson, 2014).

1.4.3 Receptive field remapping in V1

Dynamic remapping of receptive fields with saccades has been found in the lateral intraparietal area (LIP; Duhamel, Colby, & Goldberg, 1992), the frontal eye fields (Goldberg & Bruce, 1990; Umeno & Goldberg, 1997), and extrastriate visual cortex (Tolias et al., 2001; Nakamura & Colby, 2002). Until 2007 (Merriam, & Genovese, Colby, 2007), research suggested that very little (if any) remapping occurred in the primary visual cortex. Nakamura & Colby (2002) found that receptive fields shifted progressively less down the visual hierarchy, only one in 64 neurons (2%) exhibited remapping in the macaque V1 (Figure 1.8 A; Nakamura & Colby, 2002). The human fMRI study conducted by Merriam and colleagues (2007) provided evidence to the contrary. Although V1 still showed less receptive fields remapping than the extrastriate visual cortex, 22% of voxels demonstrated remapping with saccade (Figure 1.8 B; Merriam, Genovese, & Colby, 2007).

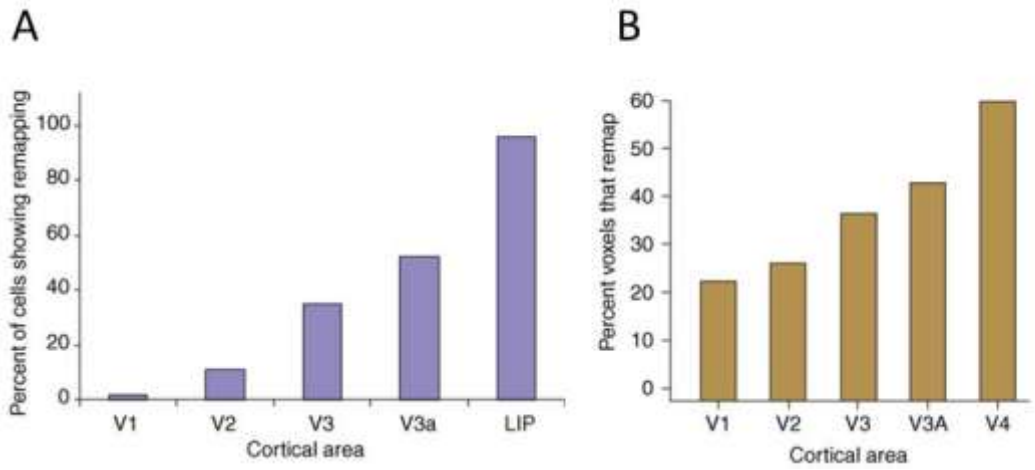

Figure 1.8 - Dynamic receptive field remapping through the visual processing areas
A) Single cell recordings illustrate remapping in macaque monkeys through the visual system. B) Significant change in hemodynamic response in remapped location where no stimulus was present in striate and extrastriate visual cortex (adapted with permission from Melcher & Colby, 2008).

1.4.4 Saccade suppression and excitation in V1

The main effects of saccades reported in V1 have been saccadic suppression (Sylvester, Haynes, & Rees, 2005; Vallines & Greenlee, 2006) followed by excitation (Kagan, Gur, & Snodderly, 2008; MacEvoy, Hanks, & Paradiso, 2008; Hass & Horowitz, 2011; Ibbotson & Krekelberg, 2011; Ruiz & Paradiso, 2012). Saccadic suppression of the early visual cortex has been found to begin around 75 ms prior to saccade onset (Vallines & Greenlee, 2006) similar to that found in psychophysical research (Latour, 1962; Zuber & Stark, 1966; Volkmann, Schick, & Riggs, 1968; Riggs et al., 1982; Diamond, Ross, & Morrone, 2000). Sylvester and colleagues (2005) found that saccades caused an increase in activity in V1 and LGN when subjects were in complete darkness; however, with visual stimulation, suppression of these areas was reported. This indicates that visual stimulation is necessary for saccadic suppression to occur (Sylvester, Haynes, & Rees, 2005). Saccadic suppression has been reported to last until approximately 50 ms after saccade offset in the monkey parietal cortex (Deubel, Schneider, & Bridgeman, 1996). Suppression until 50 ms after saccade was also reported in the LGN (Royal et al., 2006; Wurtz, 2008; Ibbotson & Krekelberg, 2011). This is supported by detection tasks in which a reduction in target detection occurs prior and during saccade until 50-100 ms after saccade offset (Vetter, Edwards, & Muckli, 2012).

Although the Sylvester and colleagues' (2005) study is convincing, some have suggested saccadic suppression is more limited in V1 (Wurtz, 2008). Originally no suppression was observed (Fischer, Boch, & Bach, 1981), followed by research that suggested a few neurons did not respond during saccade (Battaglini et al., 1986). Other research has

suggested that saccades modulate V1 by causing an increase in activity 100 ms prior to saccade rather than suppression (Supèr et al., 2004). Sylvester and colleagues (2005) suggest that saccadic suppression is dependent on visual input, which could account for opposing findings.

Several studies have found that saccades modulate V1 by causing a late excitation after saccade (Kagan, Gur, & Snodderly, 2008; MacEvoy, Hanks, & Paradiso, 2008; Hass & Horowitz, 2011; Ibbotson & Krekelburg, 2011; Ruiz & Paradiso, 2012). It is thought that the saccadic suppression prior and during saccade and the increased activity after saccade facilitates the integration of information across saccades. Saccadic suppression causes a decrease in perceptual sensitivity just prior and during eye-movement which ensures that the motion of the eye-movement is not processed, resulting in visual stability (Helmholtz, 1867; Holt, 1903; Ilg & Hoffman, 1993; Bremmer et al., 2009). The enhancement after saccade could be related to biasing perception of saccade target (Kagan, Gur, & Snodderly, 2008). These findings seem to suggest that saccades manipulate sensitivity to sensory input to enable smooth visual processing (Hall & Colby, 2001; Melcher & Colby, 2008; Ibbotson & Krekelberg, 2011; Wurtz, Joiner, & Berman, 2011).

1.4.5 Feedback relocation with saccade in V1

The saccade-related alterations to visual processing regions indicate that integrating information across saccade is taxing and effects cortical function at the level of V1. Continuously changing sensory input in V1 may affect the location of feedback signals to V1 from higher cortical areas. Adams and colleagues (2007) provided a powerful example of input changes to V1 along saccadic motion paths. The eye-movement path of one of the authors was recorded while freely observing a painting (Figure 1.9 – a screenshot of the video). The snapshots of the painting in the visual field were then reverse transformed to be mapped onto an inflated surface of V1, which resulted in a dynamic video of how the visual scene moved around V1 during free-viewing (Adams, Sincich, & Horton, 2007). This example of changing input to V1 through saccades motivates the question: can predictions be projected to new retinotopic regions across saccade?

Figure 1.9 - Still image from video of input change in V1 during free-viewing of painting
The red fixation cross indicates the fixation location during the screenshot. A reverse transformation was performed to translate objects from the visual field on to a flattened retinotopic map of V1 (left and right V1 present at bottom of screenshot). In the short video, the sequential eye-movements capture the rapid information change across V1 (screenshot of video with permission from Adams, Sincich, & Horton, 2007).

1.5 Thesis rationale

Evidence for active perception has demonstrated that sensory perception is a construct of sensory input and previous experience. Active perception enables rapid and efficient processing of the sensory environment (Kveraga, Ghuman, & Bar, 2007). In the visual domain, structural connectivity and functional activity support the primary visual cortex's (V1) ability to integrate sensory input and feedback cortical connections locally. According to inference model theorists, these feedback connections from higher cortical areas contain predictions which are created by internal generative models. For correct predictive feedback to cause inhibition in early cortical areas, the feedback signals must be spatially specific to sensory input within retinotopic V1 (Sterzer, Haynes, & Rees, 2006; Akselrod, Herzog, & Öğmen, 2014).

However, as Mumford stressed is his 1991 article on the thalamus as an active blackboard for internal representations of the sensory environment, one definitive obstacle for this

hypothesis is continuously changing visual input (Mumford, 1991). The extent of changing sensory input in natural viewing has been demonstrated in V1 by Adams and colleagues (2007). These studies highlight an important assumption that predictive feedback can relocate to new retinotopic regions of V1 in order to integrate sensory input and feedback predictions.

The aim of this thesis is to study the effect of eye-movements on predictive feedback to V1. More specifically, the studies presented in the following three Chapters aim to provide evidence for the relocation of predictive feedback in V1 with saccades. Feedback signal relocation would ensure that predictive feedback is relevant in more naturalistic viewing conditions, and therefore further support the inference theorists' framework for visual perception.

To effectively tackle the question of how saccadic eye-movements' influence predictive feedback, I concentrated on paradigms which have previously been used to study predictive feedback in V1 and redesigned them to include saccades. These experiments are explained in full in **Chapters 2**, **3**, and **4**.

Chapter 2 focuses on the transference of predictive signals across saccades in a behavioural experiment. The apparent motion paradigm (Muckli et al., 2005) with targets (Schwiedrzik et al., 2007; Alink et al., 2010; Vetter, Grosbras, & Muckli, 2013) was employed for this study, and saccades were incorporated. This chapter investigated detectability of predictable in-time and unpredictable out-of-time targets presented along the apparent motion trace at different time-points related to the saccade. If predictable targets presented within apparent motion directly after saccade are better detected then evidence for prediction transfers with saccade is obtained.

Accompanying the behavioural study, **Chapter 3** explores neural evidence of predictive feedback in V1 across saccades. Neural activity in response to predictable and unpredictable targets presented along the apparent motion trace directly after saccade was examined to determine predictive feedback relocation in V1. fMRI is suitable for studying feedback signals as the blood-oxygen-level-dependent (BOLD) signal is similar to local field potential fluctuations (Logothetis et al., 2001). Therefore, BOLD reflects input and intracortical processing (Muckli et al., 2005). We expected to find a decreased activity for the predictable in-time targets directly after saccade. This decreased activity would indicate that predictive feedback has relocated and is projecting to a new retinotopic position.

Chapter 4 employs naturalistic stimuli and a combination of univariate and multivariate statistics to investigate contextual feedback relocation in V1 with saccade. The importance of incorporating contextually rich natural images in saccade experiments has recently been highlighted (MacEvoy, Hanks, & Paradiso, 2008; Temereanca et al., 2012). Therefore, **Chapter 4** aims to provide confirmation of predictive feedback relocation across saccade and increase the reliability of this effect by incorporating contextually rich scenes and multivariate techniques.

The research conducted in **Chapters 2, 3** and **4** are concluded in **Chapter 5** – the general discussion chapter. **Chapter 5** reviews the main findings throughout the thesis and discusses these results within the current literature. Specifically **Chapter** 5 examines the challenges highlighted throughout the thesis, for example the incorporation of predictive feedback within trans-saccadic perception and the role of attention within both these fields.

2 Transfer of predictive signals across saccades

2.1 Abstract

Predicting visual information facilitates efficient processing of visual signals. Higher visual areas can support the processing of incoming visual information by generating predictive models that are fed back to lower visual areas. Functional brain imaging has previously shown that predictions interact with visual input already at the level of V1 (Alink et al., 2010; Harrison et al., 2007). Given that fixation changes up to four times a second in natural viewing conditions, cortical predictions are effective in V1 only if they are fed back in time for the processing of the next stimulus and at the corresponding new retinotopic position. Here, we tested whether spatio-temporal predictions are updated before, during or shortly after an interhemifield saccade is executed, and thus, whether the predictive signal is transferred swiftly across hemifields. Using an apparent motion illusion, we induced an internal motion model that is known to produce a spatio-temporal prediction signal along the apparent motion trace in V1 (Muckli et al., 2005). We presented participants with both visually predictable and unpredictable targets on the apparent motion trace. During the task, participants saccaded across the illusion whilst detecting the target. As found previously, predictable stimuli were detected more frequently than unpredictable stimuli. Furthermore, we found that the detection advantage of predictable targets is detectable as early as 50-100 ms after saccade offset. This result demonstrates the rapid nature of the transfer of a spatio-temporally precise predictive signal across hemifields, in a paradigm previously shown to modulate V1.

2.2 Introduction

Comparing incoming sensory stimulation with previously generated predictions is an efficient strategy for processing the wealth of visual information. Predicted stimuli can be processed more efficiently and unpredicted surprising stimuli are allocated more processing resources. The brain constantly constructs predictive models of the world which are updated in anticipation of planned movements. With respect to vision, both Descartes and later Helmholtz made an important discovery about the visual system: When external pressure is used to displace the eyeball, the visual scene moves. However, when we saccade our eyes, the visual world remains stable (Descartes, 1642; v. Helmholtz, 1962). This was the first evidence that internal models do not anticipate the mechanically induced change of the visual stimulus but are updated in anticipation of voluntary eye movements.

An internal copy of the motor command, called efference copy, is used to update these internal predictions (Sperry, 1950). In hierarchical models of cortical processing, it is conceptualized that higher cortical areas incorporate planned motor signals and provide spatio-temporal predictions for lower level visual areas. Lower visual areas can use these top-down predictive signals to anticipate expected change and process visual information more rapidly and efficiently (Alink et al., 2010; Bar, 2007; Friston, 2009; Gilbert & Sigman, 2007; Harrison et al 2007; Kveraga, Ghuman and Bar, 2007; Merriam & Colby, 2005). For example, predictions developed from previous experience can allow an individual to correctly perceive the entire shape of an object when it is partially occluded (Erlhagen, 2003; Johnson and Olshausen, 2005; Sugita, 1999; van Lier, van der Helm & Leeuwenberg, 1994).

Many models have suggested that predictions are generated in higher cortical areas. Mumford (1992) proposed that flexible templates are formed in higher cortical areas and sent down to lower cortical areas where they explain away the bottom-up input signal. In such a predictive model, only the non-explained, surprising incoming signal is fed forward whereas all other signals explainable by spatio-temporal context are filtered out at the earliest possible cortical processing stage. In 1999, Rao and Ballard modelled a hierarchical predictive coding architecture in which higher levels of the model predict responses of the next lower level using feedback. Feedforward connections from lower to higher cortical areas communicate any errors between the predicted response and the actual response. As a consequence of this architecture, new synaptic connections are formed reflecting learned associations (den Ouden et al., 2009). Several models have been proposed demonstrating the importance of the bidirectional influence between higher and lower cortical areas for perception and recognition (Bar et al., 2006; Lamme et al., 2006; Meyer 2012). A more formal account of predictive coding has been developed by Friston (2005, 2009; 2010).

For predictive coding to facilitate visual processing it is important that the predictive signal transfers across hemifields rapidly, ensuring that it continues to aid visual recognition across visual fields. This study aims to demonstrate whether a predictive signal is transferred across hemifields and, more precisely, how quickly after saccade completion we can detect prediction effects previously related to V1 processing (Alink et al., 2010).
Previous evidence indicated that the transfer of information across saccades is rapid and accelerates visual perception by about 40 ms (Hunt and Cavanagh, 2009). When subjects

saccaded towards a ticking clock and reported the time displayed on the clock, subjects' response was 39 ms earlier than the actual time. Hunt and Cavanagh (2009) attributed this effect to anticipatory sensory enhancement in the target area in which the eyes fall after saccade. Peterburs and colleagues (2011) found three ERP components which were related to saccadic updating. The antecedent potential building from 80 – 40 ms prior to saccade was thought to be associated with the planning of the impending saccade, consistent with previous findings in monkey lateral intraparietal area (LIP) and frontal eye field (FEF) (Duhamel, Colby, & Goldberg, 1992; Umeno & Goldberg, 2001). The next component in the time course related to spatial updating was a negative ERP 30 - 70 ms post-saccade onset. Finally the last component to occur in relation to the saccade arrived 200-500 ms after the saccade onset. On closer inspection of this late updating, Peterburs and colleagues (2011) found evidence in the ERP traces to suggest that positive ERP activity in the time-window between 100-150 ms after onset was related to interhemispheric transfer. Bellebaum & Daum (2006) also found an early post-saccadic component at 50 ms after offset which was thought to be imperative for saccadic updating. Allowing for approximately 80 ms for saccade duration (Baloh et al., 1975; see also Results below), Peterburs and colleagues' (2011) evidence suggests predictive coding transfer should occur within 20-70 ms after saccade offset if it is indeed relevant for efficient processing.

In this experiment we used an apparent motion paradigm which has previously been proven useful to demonstrate the effect of a predictive mechanism (Alink et al., 2010; Schwiedrzik et al., 2007). Visual illusions reflect the fact that the brain draws inferences from the visual input and that prior beliefs (or predictions) are used to construct the percept (Brown & Friston, 2012; Goebel et al., 1998). Apparent motion is an illusion of motion induced by two stationary stimuli that blink on and off alternately. It gives rise to an illusory object moving between the inducing stimuli along the shortest path (Attneave & Block, 1974; Goebel et al., 1998; Kolers, 1963; Larsen et al., 2006; Liu, Slotnick & Yantis, 2004; Muckli et al., 2002; Muckli et al. 2005; Shepard & Zare, 1983). Long distance apparent motion is a particularly suitable paradigm as higher visual areas have larger receptive fields which enable them to process the spatio-temporal dynamics of the illusion, thus creating a prediction with regard to where the illusory motion token is at a certain time (Alink et al., 2010).

In the experimental paradigm used here, targets were presented on the apparent motion trace either in-time or out-of-time with the illusory motion token. Targets were similar in

visual features to those stimuli inducing apparent motion. In-time targets fitted the predicted time and place of the illusory motion token better than those presented out-of-time. Moreover, we have shown that participants are significantly more accurate in detecting the more predictable in-time targets than the unpredictable out-of-time targets (Schwiedrzik et al., 2007). However, it should be noted that both in-time and out-of-time targets are masked by illusory motion and are detected less frequently than control stimuli that are not embedded in apparent motion (Schwiedrzik et al., 2007). Our previous brain imaging results with the same paradigm showed that the effect of prediction interacts with incoming information at the level of V1 (Alink et al., 2010). Alink and colleagues found that unpredictable, out-of-time targets caused a higher activation in V1 than predictable, in-time targets even though these targets were detected less frequently. In line with predictive coding frameworks (Mumford, 1992; Rao & Ballard, 1999; Friston 2005, 2009, 2010), the decreased BOLD signal in response to predictable targets was interpreted as consistent with the notion that predicted information is processed more efficiently and thus causes less neural activation. The increased BOLD signal in response to unpredictable targets was thought to be a result of prediction errors being communicated to higher level areas. Alink and colleagues' experiments were performed under conditions of central fixation and it is unclear whether predictability effects would also occur when cortical predictions need to be transferred across an eye movement. Since V1 has a precise retinotopic structure, feedback must interact with incoming information at a high spatial and temporal precision. It is unclear whether a predictive signal can quickly transfer to new retinal coordinates or even across visual hemifields.

Here, we combine our previous apparent motion paradigm with inter-hemifield saccades to investigate the transfer of the predictive signal to the other hemifield. In contrast to a related study by Szinte and Cavanagh (2011), we added in-time and out-of-time targets on the apparent motion trace to investigate effects of visual predictions. By presenting targets along the apparent motion trace immediately after a saccade we were able to determine how long it takes for the predictive signal to transfer to the new retinal position.

2.3 Materials and Methods

2.3.1 Subjects

30 subjects were recruited via the online departmental subject pool, 27 were included in the final analysis (see section "Task" for reasons of exclusion; mean age 25, range 19-38

years, 19 females). 14 subjects performed version A of the experiment and 13 subjects version B. Of those, 3 subjects took part in both versions. All subjects had normal or corrected-to-normal eye sight, no history of brain damage and signed informed consent.

2.3.2 Stimuli

Two white rectangles (2.1˚ each, 12.3˚ vertically apart) were flashed alternately to induce apparent motion (see Fig. 2.1). Each apparent motion stimulus was displayed for five frames (67 ms) followed by an inter-stimulus interval of another five frames, resulting in a frequency of 3.75 Hz. Targets were the same shape and colour, but slightly smaller (1.7˚) than the inducing stimuli, to ensure they fall on the apparent motion trace and to account for cortical magnification. Targets were presented on the apparent motion trace at either an upper or lower position (2.5˚ from the midline) in either the 2^{nd} or 4^{th} frame of the ISI. The targets were presented for 13.3 ms (1 refresh rate) either in time with a linearly moving illusory token or out of time (i.e. at the same time but at the wrong target position, Fig. 2.1b). Targets occurred equally often at the upper and lower target position and during both upward and downward apparent motion. Each trial consisted of 10 cycles of apparent motion. Apparent motion stimulation was continuous and the onsets and offsets of trials were not noticeable. The apparent motion stimulus was placed at the centre of the screen with two fixation crosses (0.62˚ each, one green, one red) at either side (7˚ eccentricity). Fixation crosses changed colour every 2.66 s (10 cycles of apparent motion), always at the beginning of cycle 6 of each trial. In version A of the experiment, targets were displayed in the cycle immediately before and immediately after the colour change of the fixation cross (cycles 5 and 6) and also in between the colour change (cycle 1). In version B of the experiment, targets were displayed in cycles 7, 8, 9 and 10, i.e. 2 - 4 cycles after the colour change of the fixation cross (see explanation below). Apparent motion stimulation was interrupted with a natural scene display once a minute, enabling subjects to rest their eyes for 20 seconds and preventing apparent motion breakdown due to adaptation (Anstis & Giaschi, 1985). Stimuli were created using Presentation (Neurobehavioural Systems, Inc., Albany, USA) and presented on a 16 inch Sony Trinitron CRT Monitor (resolution: 1024 by 768, refresh rate: 75 Hz). The setup was similar to Szinte and Cavanagh (2011), however we used a larger vertical distance of the apparent motion stimulus and a much slower saccading rhythm.

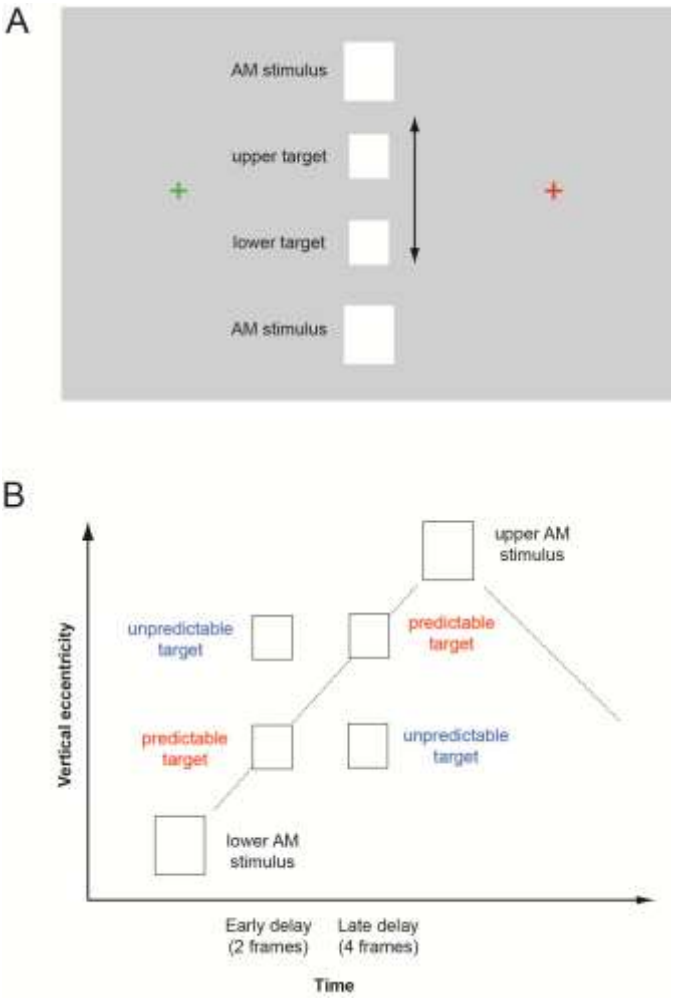

Figure 2.1 - Apparent motion stimulus & illustration of target presentation
A) Schematic depiction of the stimulus display (not in scale). The two apparent motion stimuli flashed in alternation (at 3.75 Hz). During the ISI, a target was flashed at either an upper or lower position on the apparent motion trace. The target was of the same shape and luminance as the apparent motion stimuli though slightly smaller. Subjects maintained their eyes at the red fixation cross and saccaded across the illusion when the fixation cross changed colour (every 2.66 s). B) Time-space diagram of the stimulus display. Predictable targets were flashed in-time with a linearly moving illusory token whereas unpredictable targets were flashed out-of-time with an illusory token, i.e. at the same time as the corresponding predictable target but at the wrong place. Targets were presented either at an early or late delay, and either during upward or downward apparent motion.

2.3.3 Task & Procedure

Each subject was seated in a dark room at a distance of 70 cm from the computer monitor using a chin rest and a forehead support. Eye movements (EyeLink, SR Research, Ontario, Canada) were recorded throughout.

2.3.3.1 Pre-test

Prior to the main experiment, a 10 min pre-test was conducted to familiarise subjects with the task, determine their optimal stimulus contrast, and their baseline performance without

saccades. Here, the same apparent motion stimulus was presented in the right visual field (7˚ eccentricity) with a single white fixation cross at the centre. The subjects' task was to keep their eyes at the central fixation cross and detect the targets on the apparent motion trace. The background grey values were varied block-wise in 5 steps (Michelson contrasts derived from luminance measurements with a photometer (Minolta): 0.80; 0.69; 0.56; 0.43; 0.29) to determine subjects' individual stimulus contrast for highest detectability of in-time targets compared to out-of-time targets. This optimal contrast value was then used throughout the main saccading experiment. On average, a mean Michelson contrast of .052 (SEM .027) was employed. Mean detection rates across the 5 contrast values are plotted in Fig. 2.2. Replicating previous findings (Schwiedrzik et al., 2007), in-time targets were detected better than out-of time targets (repeated measures ANOVA: $F(1,23) = 42.09$, $p < .001$). Overall, detection rates increased with decreasing contrast ($F(4,92) = 3.21$, $p = .016$; no interaction). However, contrast blocks were not counterbalanced, so this could reflect a training effect instead of an effect of contrast.

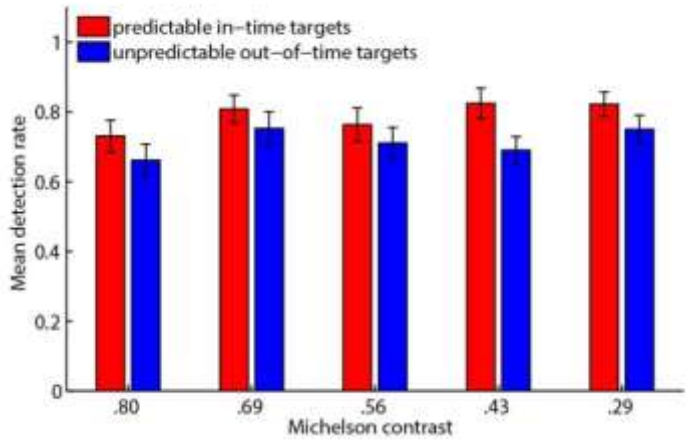

Figure 2.2 - Results of the pre-test
Here, subjects performed the task without saccading, with a fixation cross at the centre and the apparent motion display at an eccentricity of 7˚ to the right. Contrast between background and stimuli were varied in five steps to determine the optimal stimulus contrast for each subject individually. Replicating previous results (Schwiedrzik et al., 2007), mean detection rates were higher for in-time targets than for out-of-time targets ($p < .001$). Error bars indicate 1 SEM.

2.3.3.2 Main experiment

In the main experiment, participants were instructed to fixate their eyes on the red fixation cross and saccade over the central illusion when the cross changed colour, whilst never to rest their eyes directly at the illusion. At the same time, participants detected targets on the apparent motion trace and responded via a button press. Three subjects with frequent saccades to the centre of the screen were excluded from the analysis. The experiment was

broken up into four runs of 10 minutes and lasted in total about 1.5 h including pre-test, practice trials and breaks.

2.3.4 Experimental Design

Two versions of the experiment were run. In version A we anticipated that subjects would rhythmically saccade from left to right without much saccade latency after cue, similarly to Szinte & Cavanagh (2011). Thus, we presented the targets mainly in the cycle before and after the fixation cross colour change. However, after initial data analysis we realised that subjects reaction to the timing of the cross colour change was comparably slow and that subjects in fact showed a significant saccade latency (about 300 ms, see Results below). Therefore, we took this delay in saccading into account in version B of the experiment and presented the targets between 346 and 1303 ms after the saccade cue. We pooled the data from both versions of the experiment in the final data analysis to achieve maximum data coverage across all time windows.

Across all time windows, a total of 1300 trials were presented. To increase statistical power across all time windows, 40% of trials contained in-time targets, 40% contained out-of-time targets and 20% contained no target. Note that our critical measure was not overall detection rate, but the difference between in-time and out-of-time target detection. Target presence, target timing (in-time or out-of-time), target position along the apparent motion trace, and target presentation time window were randomised and counter-balanced.

2.3.5 Analysis

Eye-tracking data was analysed using SR Research Data Viewer. Only trials with large horizontal saccades occurring within 500 ms after saccade cue were included. From all trials containing a target, detection rates were derived as the proportion of trials where a button press occurred between 150 and 1200 ms after target onset. Trials were sorted with respect to target time distance from individual saccade offset (for each trial and each subject). Note that as we were interested in the re-occurrence of a predictive effect after saccade, saccade offset was our critical point of reference rather than saccade onset as used in several other studies (e.g. Peterburs et al., 2011).

Detection rates for in-time and out-of-time targets were binned into 50 ms and 100 ms time windows (or bigger, see Fig. 2.3a) and averaged, first within subjects, then across subjects. Data were only included in a bin if more than 3 trials per subject and more than 3 subjects

contributed to that bin (outlier reduction). Relative differences in detection rates were computed on a single subject level as detection rate (in-time) – detection (out-of-time) / (detection rate (in-time) + detection rate (out-of-time))

Note that our experimental design implied that we could not compute d'. Subjects only responded to the presence of a target but not its absence due to the fact that apparent motion stimulation was on-going and the onset and offset of trials were not noticeable. That is, while we could compute hits, misses and false alarms, correct rejections are not captured with this experimental design.

2.4 Results

Mean latency between saccade cue and saccade onset was 307.9 ms (SEM 7.3), mean saccade duration was 89.3 ms (SEM 6.7).

Detection rates for in-time and out-of-time targets, pooled within large time-windows according to mean saccade latency and mean saccade duration, are plotted in Fig. 2.3b. As expected, in-time targets were detected more accurately than out-of-time targets (repeated measures ANOVA; $F(1,26) = 110.26$, $p < .001$). Detection rates decreased after saccade cue and during saccades, leading to a main effect of time window ($F(3,78) = 25.13$, $p < .001$). This effect interacted with target timing ($F(3,78) = 2.77$, $p = .047$). Post-hoc comparisons (paired sample t-tests) for individual time windows revealed a significant detectability difference between in-time and out-of-time targets before the saccade cue and after saccade offset ($p < .05$, Bonferroni-corrected). At the uncorrected level, the detectability difference was also significant in the time window between saccade cue and saccade onset ($p = .027$), and marginally significant during saccade ($p = .060$). Note that the number of trials, and thus statistical power varied across time windows due to their variable length. The average percentage of trials contributing to the individual time windows were as follows: 68% (before and between saccades), 15% (after saccade cue), 5% (during saccade) and 12% (0 – 200ms after saccade offset).

Detection rates were binned into 100 ms (Fig. 2.3c) and 50 ms time windows (Fig. 2.3d). Note that bins always included data centred around a specific time point. For example, in the data binned by 100 ms, the data point at 50 pooled over targets occurring from 0 (saccade offset) to 100 ms. Paired-sample t-tests (uncorrected) revealed that the detection advantage of in-time targets disappeared within 100 – 200 ms after saccade cue (Fig. 2.3c) and reappeared as early as 50-100 ms after saccade offset (Fig. 2.3d).

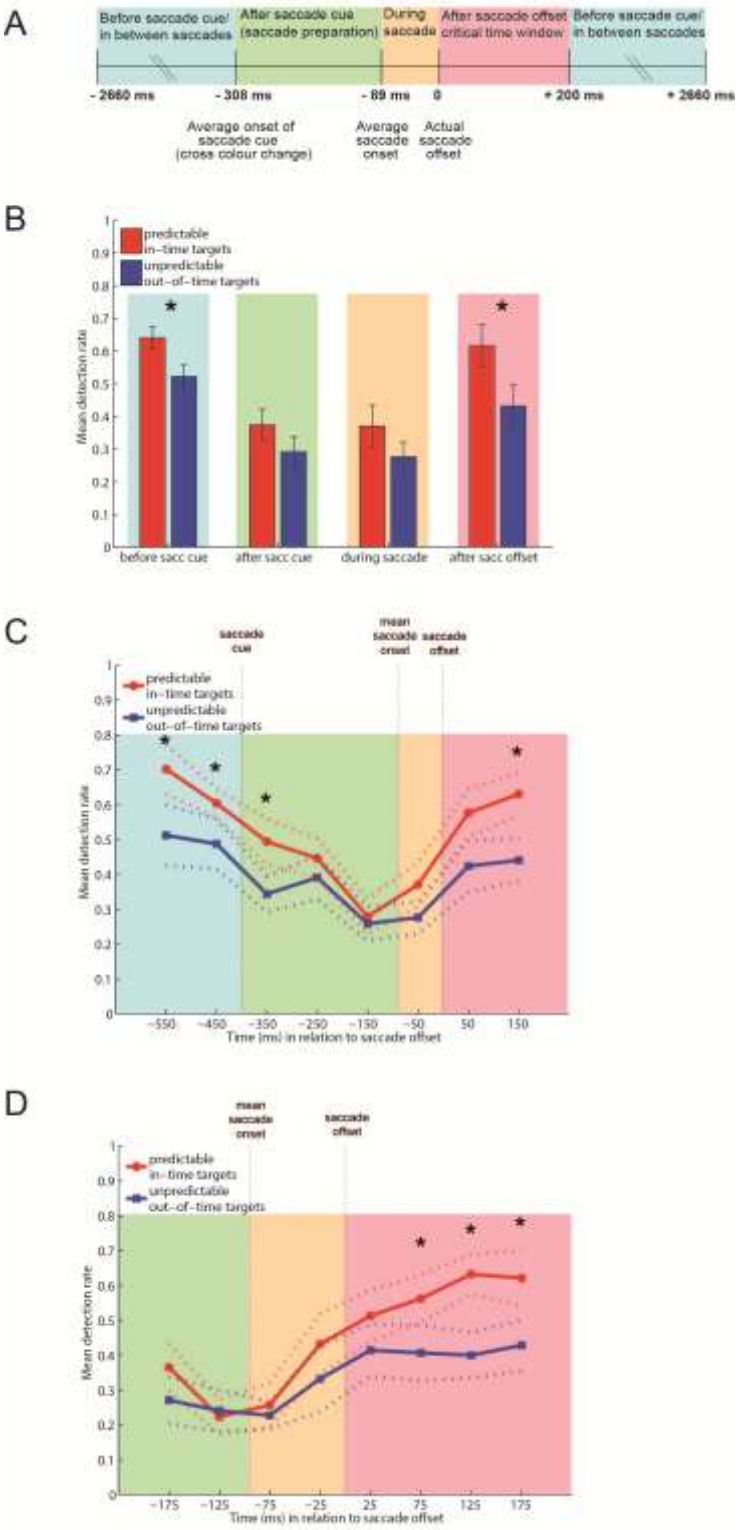

Figure 2.3 - Results of the main experiment
A) Diagram of the time windows of interest. Detection rates were analysed for target occurrence relative to subjects' individual saccade offset. B) Mean detection rates for predictable in-time and unpredictable out-of-time targets for the data averaged across the four large time windows of interest. Error bars indicate 1 SEM. C) Mean detection rates averaged across bins of 100 ms from 600 ms before and 200 ms after saccade offset (zoom). Note that bins always included data centered around the time point labelled on the x-axis. For example, the data point at 50 contains detection rates for targets occurring from 0 (saccade offset) to 100 ms after saccade offset. D) Detection rates averaged across bins of 50 ms (further zoom) from 150 ms before to 200 ms after saccade offset. Dashed lines indicate data +/- 1 SEM, stars indicate $p < .05$.

In Fig. 2.4, the relative difference between in-time and out-of-time target detection rate is plotted for single subjects, for the data binned by 100 ms (Fig. 2.4a) and for the data binned by 50 ms (Fig. 2.4b). Note that some data points overlap and that the number of data entries varies across bins due to differences in individual saccade latencies, differential target presentation in relation to saccade offset and outlier reduction (see "Analysis" section above). The plots show a positive difference in detection rates (i.e. better detection for in-time than for out-of-time targets) in the majority of subjects in those time window in which we found a significant effect (cf. Fig. 2.3 c and d).

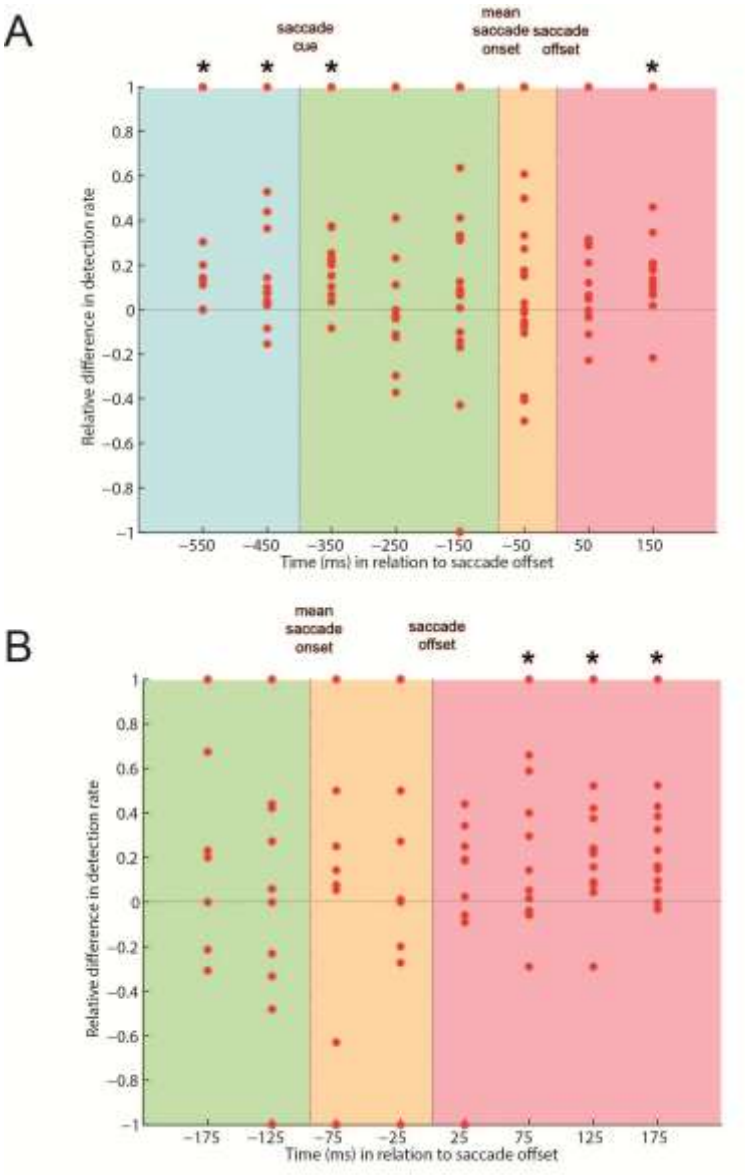

Figure 2.4 - Relative difference in detection rates between predictable in-time and unpredictable out-of-time targets for single subjects
Data were binned by 100 ms (A) and by 50 ms (B) across the same time windows as in Fig. 2.3 C and D. Data points above the midline at 0 depict a positive difference, i.e. in-time targets were better detected than out-of-time targets in that particular subject. Vice versa for negative differences. Note that data points for several subjects may overlap and that data entries varied across individual bins (see "Results"). As in Fig. 2.3 C and D, bins always included data centered around the time point labelled on the x-axis.

A control analysis showed that the detectability difference between in-time and out-of-time targets did not change over the four runs of the experiment (repeated-measures ANOVA; $F(3,27) = 2.916$, $p > .05$). Therefore, targets became neither more nor less predictable within the experimental session, precluding a potential confound of training as raised e.g. by deWit, Machilsen & Putzeys (2010).

2.5 Discussion

Subjects were required to detect targets presented along the apparent motion trace whilst saccading across the illusion. As a main effect, targets that appeared in-time with the motion illusion were detected more frequently than those appearing out-of-time, replicating previous results (Hidaka et al., 2011; Schwiedrzik et al., 2007). The increased detection rate of in-time targets is an indication that the visual system generates an illusion-related prediction along the apparent motion path. Predicted in-time targets are processed more efficiently, detected better, and cause less fMRI brain activity in V1 (Alink et al., 2010). Previous results indicate that predictions of moving tokens are generated with the contribution of hMT/V5+ and are fed back to retinotopic visual areas (Sterzer, Haynes & Rees, 2006; Wibral et al., 2009). Simulations of area V1 show that combined cortical feedback and lateral interaction can lead to precise spatial predictions (Erlhagen, 2003).

The main aim of our experiment was to determine the length of time taken by the predictive signal on the apparent motion trace to transfer across saccades and to re-occur at the new retinotopic position. This effect should occur swiftly (i.e. between 20-70 ms) after saccade offset to facilitate visual processing (Bellebaum & Daum, 2006; Peterburs et al., 2011), given that the next saccade is often initiated already after 250 ms in natural viewing conditions. Our results show that the predictive detection advantage of in-time targets is present as early as 50-100 ms after saccade offset. The transfer of the predictive signal occurs timely for visual processing in the next fixation period. This finding suggests that a spatio-temporally precise internal model is transferred across saccades and updated within 50-100 ms. This fast time window relates to the earliest time window in which stable vision is possible after saccades due to saccadic suppression. It is also too early to allow for an entirely new rebuilt apparent motion illusion in the new hemifield and subsequent post-diction to take place. For rebuilt and post-diction, at least half a cycle of apparent motion (133 ms) would need to be presented in the new hemifield (see discussion below).

Interestingly, the same time window of 50 ms and above was found to be critical for the release of saccadic suppression (Deubel, Schneider & Bridgeman, 1996). Subjects are unable to detect relatively large displacements of saccadic target stimuli if they occur during saccade or up to 50 ms after saccade offset. Our data is in accordance with this finding: Projecting the predicted target position to a new post-saccadic retinotopic position takes about 50 - 100 ms. Before this time period, spatio-temporal target displacements will go largely unnoticed because the precise location is not yet transferred. Indeed, Deubel and colleagues (1996) found that when the target stimulus remains off ('blanked') for 50 ms or longer after saccade offset, subjects recover the ability to detect target displacements. Furthermore, the earliest ERP time component related to trans-saccadic updating and integrating of visual information starts at 50 ms after saccade offset (Bellebaum & Daum, 2006). The authors relate the parietal ERP component starting at 50 ms to the updating process that matches the efference copy of the motor command to the stimulus location. It is plausible to assume that this reflects the process that transfers the prediction to the new retinotopic position at which it will facilitate processing of in-time targets.

Our data also show that the overall detection of targets is reduced during saccade and until 50 ms after saccade offset. In theory, we cannot exclude the possibility of an in-time prediction effect during these time windows, but the low detection rates do not allow for sufficient statistical power (see "Results").

It seems that the visual prediction system has learned its delay times and found ways to compensate the lost 50 ms by correcting its forward prediction. Hunt and Cavanagh (2009) showed that subjects who follow the arms of a fast moving clock with peripheral vision will predate the fixation of the clock by 40-60 ms – a process that might be thought of as a temporal filling-in process to avoid discontinuities introduced by each saccadic eye-movement and its saccadic suppression. Other motion illusions are related to this temporal filling-in: Movement into the blind spot is extrapolated in its expected coordinates even when no retinal signal is received (Maus & Nijhawan, 2008). A common demonstration of forward adjustment of predictions is the flash lag illusion (Nijhawan, 2008). It seems that we act on predictions corrected forward in time unless there is a strong signal overwriting this prediction. Weak error signals as our out-of time stimulus are likely to remain unnoticed like a small signal in a noisy pattern. Strong unexpected transients, however, allow for an immediate update (Maus et al., 2010).

To perceive apparent motion during saccadic eye-movements, the visual system has to keep track of the spatiotopic position of the moving illusion and correct for eye-movement induced shifts at retinotopic positions. Szinte and Cavanagh (2011) measured the precision with which spatiotopic coordinates of the apparent motion illusion are updated while saccadic eye-movements are performed. If the remapping compensation is perfect, vertical apparent motion should appear precisely vertical even if a horizontal saccade is performed across the illusion. However, the findings of Szinte and Cavanagh (2011) suggest differently: the trans-saccadic remapping of the apparent motion end points leads to an overcompensation of the eye-movement amplitude by 5%, and the illusion appears tilted by up to 9 degrees. Interestingly, the compensation was tested at nine different positions and it was found to vary between positions individually, suggesting that the compensation does not follow an overall global correction but depends on locally acquired experience.
Our experiment does not inform us about the spatial precision with which a signal is transferred (apart from the fact that the transfer is precise enough for the in-time/out-of-time difference to take effect). Also, it should be noted that the horizontal saccadic rhythm was much slower in our paradigm compared to Szinte and Cavanagh (2011) and that the illusion did not appear tilted, suggesting that no overcompensation occurred.

The decrease in mean detection rate seen in Fig. 2.3c prior and during saccade could be explained by trans-saccadic suppression and peri-saccadic mislocalisation. During trans-saccadic suppression there is a general reduction in visual sensitivity which can occur even prior to saccade onset (Vallines & Greenlee, 2006). Peri-mislocalisation could also account for a decrease in target detection as objects which are flashed close to saccade onset are largely mislocalised on the retina from their actual physical position (Ostendorf et al., 2007). This mislocalisation may occur due to spatiotemporal mismatch between the saccade and extraretinal eye position information (Ross et al., 2001). Both these models of vision breakdown over saccades could predict a decrease in detection rate of both in-time and out-of-time targets within the illusion.
Szinte and Cavanagh's findings as well as evidence by Rolfs et al. (2011) suggest that there is a close interplay between the remapped visual information and attention. Our observed prediction effect could be explained by smoothly moving visuo-spatial attention, similar to what Shiori and colleagues (2002) demonstrated behaviourally. That is, subjects' attention may have been trained on the dynamics of the illusory motion as they were instructed to detect targets along the apparent motion trace. As attention is transferred across saccades as much as visual information (Rolfs et al., 2011), this may lead to a better

detection rate of in-time targets as they appear in the focus of attention. Our results are consistent with dynamical concepts of a fast moving attentional searchlight: such a moving searchlight predicts the location where a stimulus is expected – which is closely related to a moving token or a motion prediction.

However, our results cannot be explained with conventional notions of a static visuo-spatial attention searchlight, as it cannot account for in-time/out-of-time differences. Even when visuo-spatial attention is focused on a centre task, the apparent motion illusion in the periphery remains strong (Kohler et al., 2008) and brain activity along the apparent motion trace is increased (Muckli et al. 2005). Gilbert and Sigman (2007) highlight the wealth of top-down influences and note that "the notion of attention itself may be inadequate as a descriptor of the full range of top-down influences that are exerted".

We propose that the predictive signal is transferred from one hemifield to the next. An alternative would be to assume that the signal could be rebuilt anew or that the presence of an in-time target was inferred by post-diction. Our data show that rebuilding of a detectability advantage of in-time targets must occur until 50 -100 ms after saccade offset. For post-diction to be effective in the new hemifield, both the upper and lower apparent motion stimuli must have been presented and perceived for the in-time/out-of-time detectability difference to take effect. Given that half an apparent motion cycle lasted 133 ms, it is unlikely that an entire rebuilt of the predictive signal could have occurred within 50 – 100 ms after saccade offset.

It is worth mentioning that our results are not in contrast to Yantis and Nakama (1998). Yantis and Nakama (1998) showed that target discrimination degrades if targets are presented on the apparent motion trace, but they did not investigate in-time versus out-of-time differences of target stimuli on the apparent motion path. In line with Yantis and Nakama (1998), also our apparent motion illusion induces motion masking and overall reduces the detectability of both in-time and out-of-time stimuli (Schwiedrzik et al., 2007). When apparent motion is not induced, both types of stimuli are detected equally well. In the presence of the illusion, in-time stimuli are less masked by apparent motion than out-of-time-stimuli. Moreover, Yantis showed that high precision object discrimination is reduced on the apparent motion trace, whereas our paradigm just required the detection of a simple flash without the need of high spatial frequency analysis. High precision object discrimination may be incompatible with the apparent motion illusion as is exemplified by interference of inconsistent stimulus features on the apparent motion path with motion

masking: for example, orthogonally oriented Gabor patches along the apparent motion trace slow down the perceived speed of the motion illusion (Georges et al., 2002)

Motion induced blindness provides another example in which static stimuli not fitting to the motion percept are overwritten by a top-down motion prediction even though the non-perceived stimulus induced a stronger V1 signal (Schölvinck & Rees, 2010). One of the most convincing demonstrations of predictive coding overwriting the physical stimulus is given by Hidaka, Nagai and Gyoba (2009). Three blinking bars triggered a strong apparent motion prime that was followed by a test stimulus of two blinking bars that could either consistently continue the apparent motion direction or that blinked in opposite sequence. In both cases, subjects see consistent apparent motion, indicating that motion prediction overwrites the non-fitting opponent motion. Both the out-of-time stimulus of our study and the apparent motion stimulation in the opponent direction of Hidaka et al.'s (2009) study are less detectable as they are overwritten by top-down predictions.

2.6 Conclusions

Our findings are an additional piece of evidence for the theory of a predictive mechanism in the visual system. Predictive signals transfer rapidly across hemifields. At around 50 - 100 ms after saccade offset, the apparent motion illusion, including its predicted path, is remapped to the corresponding retinotopic position in the other hemifield. The time interval corresponds well to other forms of interhemifield update. Consistent with previous research it seems that predictive codes help to maintain information across saccades. Our results suggest that the visual brain does not passively wait to be stimulated but rather constantly forms predictions to allow for consistency across saccades and over space and time.

3 Motion specific predictions relocate to new positions in V1 with saccade.

3.1 Abstract

Predictive coding theories of vision propose that higher visual areas use internal models of the environment to predict upcoming sensory input to V1. These predictions are carried by cortical feedback down the visual system where they are compared to sensory inputs. However, patterns of sensory input to V1 constantly update with saccades. We test if predictions feed back to new retinotopic locations in V1 in time to interact with *post-saccadic* sensory input. We used functional brain imaging and eye-tracking, whilst presenting an apparent motion illusion. The apparent motion illusion creates an internal model of motion which is fed-back to V1 by prediction signals. In line with predictive coding, we observed attenuated BOLD signal to predicted stimuli presented on the trace directly after saccade. Therefore, predictions update their retinotopic position in time for post-saccadic input. These data confirm the relevance of cortical predictions in vision.

3.2 Introduction

Predictive coding accounts of vision propose that higher cortical areas use internal generative models of the world to predict sensory inputs (Mumford, 1992; Rao & Ballard, 1999; Friston, 2005; Bastos et al., 2012; Clark, 2013). These predictions are fed back to V1 where they are compared to the real sensory inputs (Alink et al., 2010). However, there is one critical assumption of predictive coding which remains to be tested, and which challenges its ecological function. Humans saccade approximately three times per second, changing the retinotopic pattern of sensory inputs to V1 (Adams, Sincich, & Horton, 2007). Therefore for cortical predictions to be beneficial to sensory processing, the predictions of sensory input descending the hierarchy must update to new retinotopic locations in V1 in time for post-saccadic input (Mumford, 1991; Melcher, 2011).

Central to our study is the creation of an internal model in the brain during which sensory predictions are fed back to V1 from higher areas. The apparent motion illusion offers a paradigm for such a model. Apparent motion is an illusion of a moving token between two alternating flashing stimuli (Kolers, 1963; Shepard & Zare, 1983). Apparent motion is integrated in V5 (Muckli et al., 2002; Sterzer, Haynes, & Rees, 2006; Wibral et al., 2009;

Vetter, Grosbras, & Muckli, 2013) which feeds back a spatiotemporal prediction about the moving token to retinotopic V1. In V1, the predictive feedback induces activation along the non-stimulated illusory motion trace (Muckli et al., 2005; Sterzer, Haynes, & Rees, 2006; Larsen et al., 2006; Ahmed et al., 2008; Alink et al., 2010; Akselrod, Herzog, & Öğmen, 2014). To probe the spatio-temporal specificity of the predictive feedback, we presented targets in-time (contextually congruent) or out-of-time (incongruent) with the illusory motion token on the apparent motion trace. Out-of-time targets are detected less well than in-time targets (Schwiedrzik et al., 2007; Vetter, Edwards, & Muckli, 2012) and cause increased BOLD activation in V1 (Alink et al., 2010). Under predictive coding theories, this activation increase is indicative of an error signal as out-of-time targets are less predictable in the context of the illusory moving token. Here, we investigated if such illusion-related predictions are fed back to new retinotopic locations in V1 in time for post-saccadic processing. To this end, we presented the apparent motion illusion to one visual field, and induced an interhemifield saccade transferring the prediction to new retinotopic coordinates in the opposite visual field. The relocation of the predictive feedback was tested in the post-saccade region using in-time and out-of-time targets. Our data confirm that cortical predictions feed back to V1 in time for the processing of a new stimulus and at the updated retinotopic location.

3.3 Materials and Methods

Two fMRI experiments were performed with two groups of subjects. All parameters were consistent across experiments except viewing distance. Subjects who received stimulation through goggles (experiment 1) had a larger viewing distance of objects presented (Figure 3.1A & 3.1B). Eye-tracking was used for trial exclusion in the second experiment.

3.3.1 Subjects

Twenty-five healthy subjects with normal or corrected-to-normal vision (11 male; 19-34 years) were recruited using the University of Glasgow, School of Psychology subject pool. Experiments were conducted with written consent and approval from the ethics committee of the College of Science and Engineering, University of Glasgow. Two subjects were removed from analysis due to excessive head-motion in experiment 1 (leaving n = 13). One subject was removed for failing to meet saccade criterion in experiment 2 (leaving n = 9).

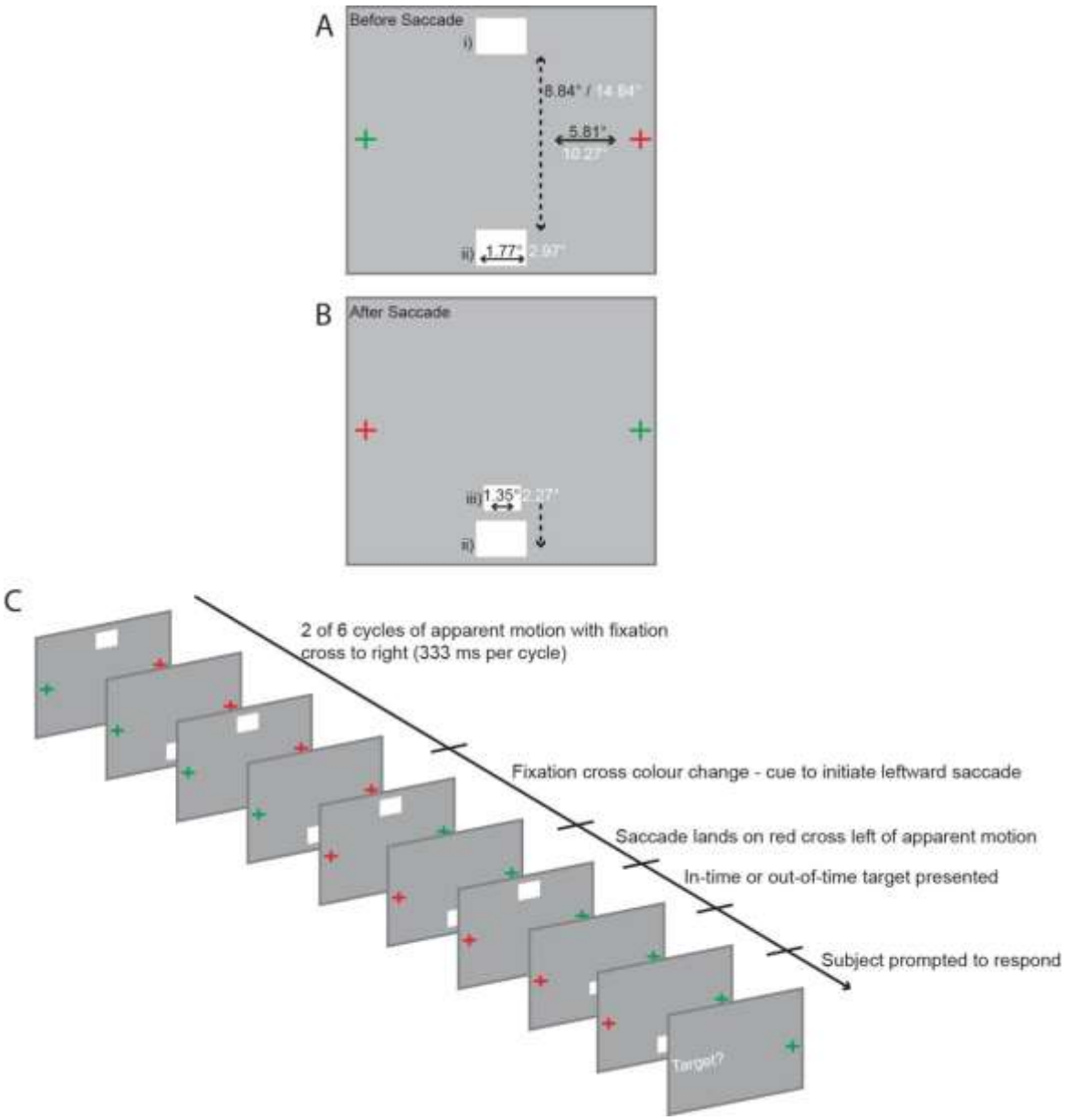

Figure 3.1 - Apparent Motion Stimuli
A: Stimulus before saccade: Subjects fixate on red cross. Apparent motion inducing stimuli i) & ii) flash in alternating rhythm. **B**: Red fixation cross moves to position of green cross to cue subjects to saccade. In the final cycle of apparent motion after saccade, the target iii) is presented along the trace either in-time (congruently) or out-of-time (incongruently) with the illusion. Visual angles for experiment 1 in white, and for experiment 2 in black. **C**: One apparent motion trial. Red fixation cross to the right of apparent motion stimulus for 6 cycles. Fixation cross moves to the left of the apparent motion cuing saccade. Saccade lands left of apparent motion during 8th cycle just prior to target presentation. Subjects prompted by 'target?' screen to indicate if they detect target.

3.3.2 Stimulus

3.3.2.1 Apparent Motion Stimulus

Apparent motion was presented in the centre of a grey screen (RBG: 153,153,153; Figure 3.1). The illusion of vertical motion was induced by two white rectangles flashing in alternating rhythm at a frequency of 3.75 Hz (Figure 3.1A – i) & ii)). These two white

rectangles were: 14.84° (exp. 2: 8.84°) apart and were each presented for 5 frames (66.67ms), followed by an inter-stimulus interval of 5 frames. A cross (2.1° (exp. 2: 0.7°) in size, one red, one green) was presented at 10.27° (exp. 2: 5.81°) either side of the centre of the apparent motion. The subjects were instructed to always focus on the red cross. The red cross alternated horizontally with the green cross prior to the 7th cycle of apparent motion, approximately 2 s after the apparent motion onset, cuing subjects to saccade across the illusion (Figure 3.1A & 3.1C). Shortly after the subjects' saccade had landed a target appeared in the 8th cycle and the illusion ceased. The design ensured the illusion was processed in the right hemisphere and the target in the left. To study predictive coding transfer across saccade, the targets were presented on the apparent motion trace either in-time or out-of-time with the illusion (Figure 3.1A – iii)). There were three apparent motion conditions: 1) with in-time target, 2) with out-of-time target, and 3) with no target. Our previous research indicated that subjects take approximately 300ms between saccade cue and saccade completion (Vetter, Edwards, & Muckli, 2012), hence the target was presented approximately 450ms after the red fixation cross has shifted location in the 8th cycle. After the 8th cycle, subjects were presented with the question 'target?' indicating that they should respond 'yes' or 'no' via button-press.

3.3.2.2 Mapping Stimulus

Lower inducing stimulus and target stimulus mapping conditions were presented in all runs. A still image of either the lower apparent motion inducer or target was presented for 4 s with the fixation cross to the left (Figure 3.1B – ii) or iii)). These conditions enabled mapping the exact spatial locations in the left hemisphere V1 (Figure 3.2E) and V2 that respond to the inducing stimuli and the target separately.

3.3.3 Procedure

Each subject completed one practice run in an fMRI simulation suite prior to scanning. Subjects completed four functional runs of 15 minutes. In experiment 1, stimuli were viewed through NordicNeuroLab goggles (screen res: 600 x 800). In experiment 2, stimuli were viewed on an fMRI compatible screen positioned in the bore of the magnet at a distance of 110 cm (screen res: 1024 x 768). The paradigm was presented using Neurobehavioral systems' Presentation® (Version 14.9) with a refresh rate of 60Hz. The three apparent motion conditions and a baseline were presented 25 times per run and 100 times across the whole experiment. The two mapping conditions were presented 12 times

each per run, 48 times across the experiment. Trials were presented in a random sequence using a randomization scheme to ensure that no triplets of conditions were repeated.

3.3.4 Data Acquisition

3.3.4.1 MRI Data Acquisition

Functional and anatomical MRI data was acquired using a 3 Tesla MRI system (Siemens Tim Trio) with a 12-channel head coil. For the functional scans an echo-planar imaging sequence was used with the following parameters: 17 slices, TR-1, TE-30, 860 volumes per run, an FOV of 205 mm, and a resolution of 2.5 x 2.5 x 2.5 mm. The 17 slices were orientated perpendicular to the calcarine sulcus to capture the early visual cortex. The anatomical MRI sequence used had a TR of 1.9, 192 volumes, and a resolution of 1 x 1 x 1 mm.

3.3.4.2 Eye-tracking Acquisition

In experiment two, subjects' eye-movements were recorded using an Eyelink 1000 (SR Research) mounted on the fMRI compatible projector screen with a sampling rate of 500Hz (calibrated at the start of each run). The data was recorded by Eyelink software and downloaded for analysis using Eyelink Data Viewer.

3.3.5 Data Analysis

3.3.5.1 Saccade Criterion

The saccade criterion denoted that subjects had to complete a saccade 400 ms after cue, and the saccade must cover at least 200 pixels horizontally across the apparent motion between onset and offset (Supplementary Figure 3.1A). The criteria ensured that subjects processed the apparent motion in the right hemisphere and the target in the left. Trials where a saccade did not meet the criterion were excluded along with one subject and one run from two other subjects who showed less than 20 trials per run with a correct saccade (Supplementary Figure 3.1B).

3.3.5.2 MRI Analysis

The functional and anatomical data were analysed using Brainvoyager QX® software (Version 2.4). The first two volumes of each functional run were discarded to preclude

saturation effects. To remove low-frequency noise and drift, high-pass filtering at 6 sines/cosines was performed during the 3D-motion correction for each run. After preprocessing, the functional data were aligned with the high resolution anatomical and transformed into talairach space (applying each subject's brain into a common space along the AC-PC plane). 3D aligned time courses were created for each run after the intra-session anatomical was aligned with the high resolution anatomical. Each subject's cortex was inflated into a surface model using the manually inhomogeneity corrected high resolution anatomical.

Once invalid eye-tracking trials were removed, single subject and group deconvolution analysis was performed. Betaweight values were contrasted over 3-7 seconds after stimulus onset in left V1 which corresponded to the time when the targets were presented in the apparent motion trials compensating for BOLD lag. The same analysis was performed on right V1, left V2, right V5, and left V5. The contrasts performed between in-time and out-of-time target trials were conducted using a serial correlation corrected comparison to determine activation difference. Deconvolution analysis was chosen due to the rapid event-related design, enabling analysis without overlap of BOLD signal across trials.

3.3.5.3 Retinotopically defining regions of interest

The primary region of interest in left hemispheric V1 was defined by the highest activation in response to the retinotopically mapped target position found within the calcarine sulcus, which was also adjacent to activation for the mapped lower inducing stimulus position (mean (SD) Talairach co-ordinates for left V1: x = -11.33 (4.4), y = -89.67 (2.7), z = -6.3 (7.5); FDR = 0.05; Figure 3.2). A GLM contrast of target>lower inducing stimulus was used to produce these activations (Figure 3.2A - 3.2D).

In experiment 2 further analyses was performed on right V1, left V2, right and left V5. Left hemisphere V2 was also defined using the target>lower GLM contrast (mean (SD) Talairach co-ordinates for left V2: x = -18.11 (5.6), y = -94 (3.9), z = 1.89 (6.4); FDR = 0.05). The ROIs for right V1, right V5 and left V5 were defined using apparent motion without target condition > baseline GLM contrast as no mapping data were collected for these regions (mean (SD) Talairach co-ordinates for right V1: x = 7.78 (3.3), y = -80.89 (6.9), z = -1.78 (7.0); right V5: x = 43.22 (4.4), y = -65.78 (4.1), z = 0.89(5.3); left V5: x = -45.22 (6.0), y = -70.44 (3.2), z = -0.89 (4.2); FDR = 0.05).

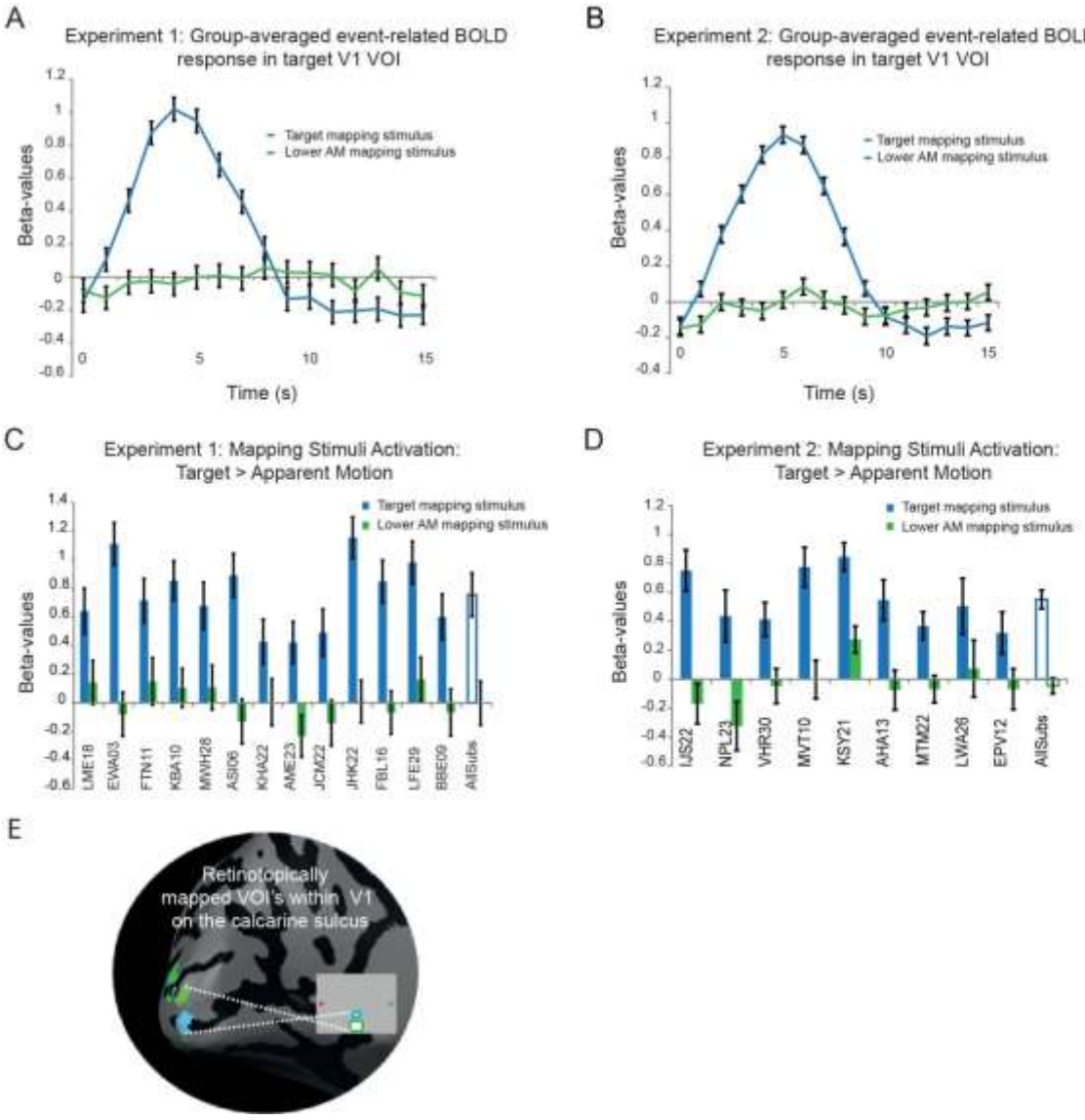

Figure 3.2 - Retinotopically Defined Region of Interest
A (Experiment 1) & **B** (Experiment 2): Group-average event-related BOLD response for mapping conditions. Target mapping stimuli > apparent motion mapping stimuli GLM contrast used to define target region of interest in V1. **C** (Experiment 1) & **D** (Experiment 2): Single subject and group BOLD beta-values for mapping stimuli in target region averaged over peak BOLD activation (*p<0.05). Empty blue and green bars illustrate pooled group data for target mapping > apparent motion mapping stimuli for peak BOLD activation. **E**: Mapped region of interest in left V1 for target (blue) and apparent motion stimuli (green) on inflated surface.

3.3.5.4 Behavioural Analysis

The behavioral data was recorded using Neurobehavioral System's Presentation® during the fMRI runs. Three subjects were excluded from data analysis in experiment 1 and one subject in experiment 2 due to data recording issues. The analysis was conducted after the saccade criteria were applied. The binomial data was then bootstrapped to determine if subjects accurately detected more in-time or out-of-time targets.

3.3.6 Psychophysical control experiment

In the fMRI experiments, short baselines between each trial were incorporated to minimize adaptation in V1 (Grill-Spector, Henson, & Martin, 2006). This design was necessary to study different activation responses between in-time and out-of-time target presentation, but was not optimal for collecting behavioural data. One concern from the fMRI experiments was that targets were behaviorally predictable regardless of in-time or out-of-time presentation as they were always presented post-saccade. A continuous apparent motion paradigm was incorporated for the extra-session experiment to enabled target presentation both after saccade and during fixation. Targets presented during fixation reduced the predictability of target presentation directly after saccade.

3.3.6.1 Subjects

Nine subjects (6 male; 19-28 years) who participated in fMRI experiment also completed a psychophysical counterpart. One of these subjects was excluded from analysis using the same saccade criterion employed for fMRI trial exclusion (Supplementary Figure 3.1). The experiment was approved by the ethics committee of the College of Science and Engineering, University of Glasgow.

3.3.6.2 Stimuli

The paradigm was presented using Neurobehavioural Systems‘ Presentation® (Version 14.9) with the exact same parameters for the three apparent motion conditions as in fMRI *Apparent Motion Stimulus*. However, the apparent motion stimulation was continuous (onset and offset of each trial were not detectable) and no mapping conditions were presented. Subjects were cued to saccade across the apparent motion illusion every 2.66 s. Trials consisted of 10 cycles of apparent motion, and targets were presented in the cycle directly after saccade (at the same time as in the fMRI experiment) or during fixation.

3.3.6.3 Protocol

The three apparent motion conditions were presented at random within 5 runs of the experiment. In 60% of the 152 trials per run, targets were presented directly after saccade in the same time-period as was used for the fMRI experiment. Targets were also presented mid trial during fixation in 20% of trials and in the remaining 20% no target was presented, this decreased the probability of targets always appearing after saccade. Every 25 trials the

apparent motion was interrupted for 20 s with a natural scene to allow subjects to rest their eyes and prevent apparent motion breakdown (Anstis et al., 1985).

3.3.6.4 Task & Procedure

For the psychophysical version of the experiment the subjects were seated 70 cm from a 16 inch Sony Trinitron CRT Monitor (1024 x 768; 60Hz), upon which the stimuli was presented. Subjects' heads were supported using a chin and forehead rest. Subjects' eye-movements were recorded continuously throughout the experiment (EyeLink 1000, SR Research; acquisition as fMRI method). The subjects were instructed to always focus on the red fixation cross and move their eyes across the illusion when the red cross alternates with the green. Subjects were asked to detect the targets and indicate this with a button press.

3.3.6.5 Analysis

The behavioral data was recorded using Presentation® software. The same eye-tracking criterion for the fMRI data analysis was applied to each trial of the psychophysical. Detection of targets was only included if the button press occurred within 150 and 1200 ms after target onset. The binomial data was then bootstrapped to determine if subjects accurately detected more in-time or out-of-time targets. Analysis focused on accurate detection difference of in-time versus out-of-time targets in the cycle directly after saccade.

3.4 Results

We ran two identical functional magnetic resonance imaging (fMRI) experiments; eye-tracking data was used for trial exclusion in the second experiment. In both experiments, we induced an apparent motion illusion in the left visual field processed by right hemisphere V1. The illusion generates (i) a spatiotemporal predictive model of apparent motion prior to the saccade projected to the right V1 (Figure 3.1), (ii) triggered an interhemifield saccade transferring the prediction to new retinotopic coordinates in left V1, (iii) tested for prediction-related BOLD activity in left V1 using in-time and out-of-time targets, in a test region on the apparent motion trace (Figure 3.2). This test region corresponds to the position at which the target stimulus was processed after saccade. We examined this test 'target' regions in three apparent motion conditions: with no target, with in-time target, and with out-of-time target.

3.4.1 Retinotopic mapping of test 'target' region

During the apparent motion illusion, alternating flashing stimuli were presented in upper and lower positions (Figure 3.1). We tested for prediction-related activity on the non-stimulated illusory motion trace between these upper and lower inducing stimuli, by mapping a test region on this illusory path. Mapping conditions for the test region consisted of static presentations of the "target" and the "lower apparent motion inducing stimulus" (Figure 3.2). The "target" region of interest (ROI) in V1 (Figure 3.2 A-D) has beta weights for the contrast Target > Lower of a mean 0.76 (SE 0.153, $p<0.0001$ in experiment 1 and 0.55, SE 0.145, $p<0.0001$ in experiment 2 across subjects). In experiment 2 we also mapped right V1, left V2, and right and left V5 for comparison (left V2 beta-weights for Target > Lower were 0.53, SE 0.14, $p<0.02$ across subjects). Right V1 and right/left V5 were mapped using a contrast of apparent motion with no target trials > baseline, with the respective beta-weights: 0.17 (SE 0.07, $p<0.026$) 0.2 (SE 0.08; $p<0.03$) and 0.17 (SE 0.06, $p<0.01$).

3.4.2 Apparent motion activity in the target region of left V1 post-saccade

After identifying the target ROI in left V1, we compared activation patterns here for the three apparent motion conditions. In the first condition, no target was presented along the apparent motion trace, therefore activity in this condition relates to illusory motion perception (Muckli et al., 2002; Muckli et al., 2005). Significant BOLD activation in the target ROI during no-target trials was observed in 11/13 subjects (single subject: $*p<0.05$; group mean(SD)=0.6(0.12)β $p<0.0001$, Figure 3.3A & 3.3C) in experiment 1, and in 5/9 (single subject: $*p<0.05$; group mean(SD)=0.2(0.02)β $p<0.0001$, Figure 3.3B & 3.3D) in experiment 2. This confirms previous evidence of illusory activity on the apparent motion trace (Muckli et al., 2005; Sterzer, Haynes, & Rees, 2006; Larsen et al., 2006; Ahmed et al., 2008; Akselrod, Herzog, & Öğmen, 2014) and provides new evidence that this phenomenon transfers across saccades.

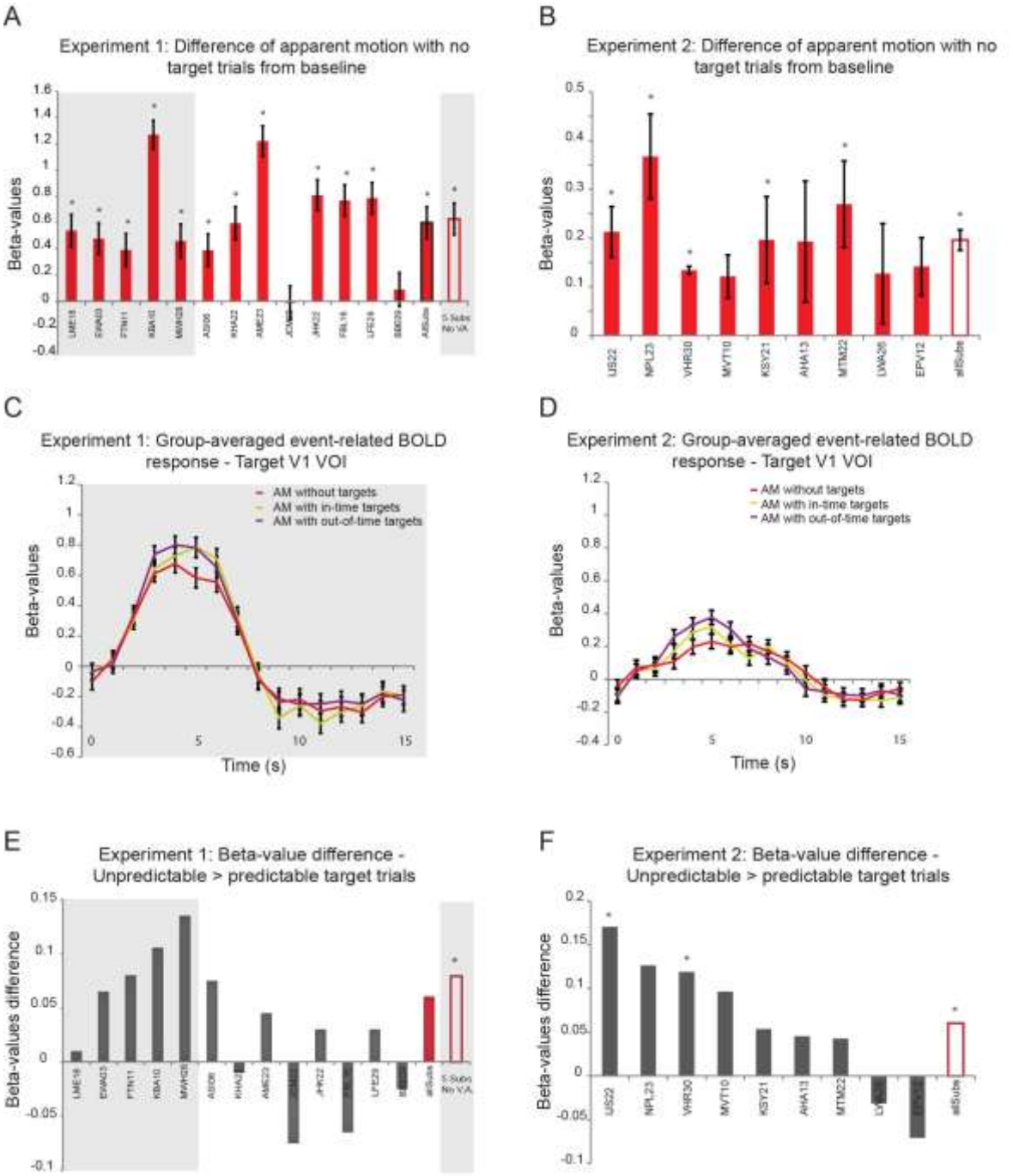

Figure 3.3 - BOLD Response to Apparent Motion in Left Hemisphere V1
A (Experiment 1) & **B** (Experiment 2): Individual and group activation for apparent motion with no target from baseline. Beta-values averaged over peak activation (*p<0.05). **A** (Experiment 1): Grey background indicates subjects without ventral activation, and therefore precise saccades. Group averaged data for all subjects (n=13; red bar, black boundary) and for all subjects without ventral activation (n=5; empty red bar). **B** (Experiment 2): Group-averaged for all subjects (n=9; empty red bar) after eye-tracking criterion applied. **C** (Experiment 1) & **D** (Experiment 2): Group-averaged event-related BOLD response for all three apparent motion conditions in left hemisphere ROI conditions onsets. **C** (Experiment 1): Group-average BOLD of subjects without ventral activation (grey background signifies subjects without ventral activation). **D** (Experiment 2): Group-average of all subjects after eye-tracking criterion applied to data (c.f. online methods). **E** (Experiment 1) & **F** (Experiment 2): Difference between in-time and out-of-time trials for individual and grouped subjects. **E** (Experiment 1): Red bar indicates grouped average for all subjects, empty red bar for subjects without ventral activation (n=5). **F** (Experiment 2): Individual subjects with significant activation difference indicated with. Group data (n=9) average in empty red bar.

We then tested whether the trace activity in left V1 after saccade confirms predictive coding feedback (Figure 3.3C – 3.3F). If predictive codes update to new retinotopic positions in left V1, in-time targets should lead to lower activation than out-of-time targets (Alink et al., 2010) post-saccade. Indeed, in experiment 1, in-time targets caused less BOLD activation than out-of-time targets in the left V1 ROI after the saccades (mean (SD): in-time target trials: 0.67(0.29)β; out-of-time target trials: 0.78(0.34)β; t(14)2.226, p=0.043, Figure 3.3E & Supplementary Figure 3.2A grey shading). However, data from 8/13 subjects were excluded due to imprecise eye-movements. We observed ventral V1 activation suggesting that saccades were landing below the horizontal meridian of the screen where the stimuli were presented. To validate this lower BOLD response to in-time targets found in 5/13 subjects, we ran a second fMRI experiment in which we obtained high quality eye-movement data. Eye-tracking data enabled trial-by-trial rejection due to imprecise saccades (Supplementary Figure 3.1 & Online Methods).

In the second fMRI experiment, decreased BOLD in the target ROI to in-time versus out-of-time targets was also observed in 7/9 subjects (mean(SD): in-time target trials: 0.23(0.13)β; out-of-time target trials: 0.29(0.17)β; t(8)=2.388,p=0.044, Figure 3.3F & Supplementary figure 3.2B). Activation difference between experiment 1 and 2 for apparent motion conditions (Figure 3.3A - 3.3D) can be attributed to the viewing distance and visual angle difference (Online Methods).

3.4.3 Predictions update to post-saccadic left V1

Significant activation for apparent motion with in-time and out-of-time target trials was found in right V1, with no activation difference (mean (SD): in-time target trials: 0.47(0.08)β; out-of-time target trials: 0.52(0.07)β; t(8)1.595, p=0.149; Figure 3.4A & Supplementary Figure 3.3A). A small, but significant activation increase was found above baseline for all apparent motion conditions in left V2 (in-time target trials $p<0.05$; out-of-time target trials $p<0.05$; no target trials $p<0.003$; Figure 3.4B & Supplementary Figure 3.3B). This activation was lower than left V1 ($p<0.0001$), and showed no activation difference for in-time and out-of-time target trials (mean (SD): in-time target trials: 0.07(0.03)β; out-of-time target trials: 0.08(0.02)β; t(8)0.587, p=0.573). Activation difference between left V1 and V2 indicates that feedback after saccade is directed to left hemisphere V1, and residually also to V2.

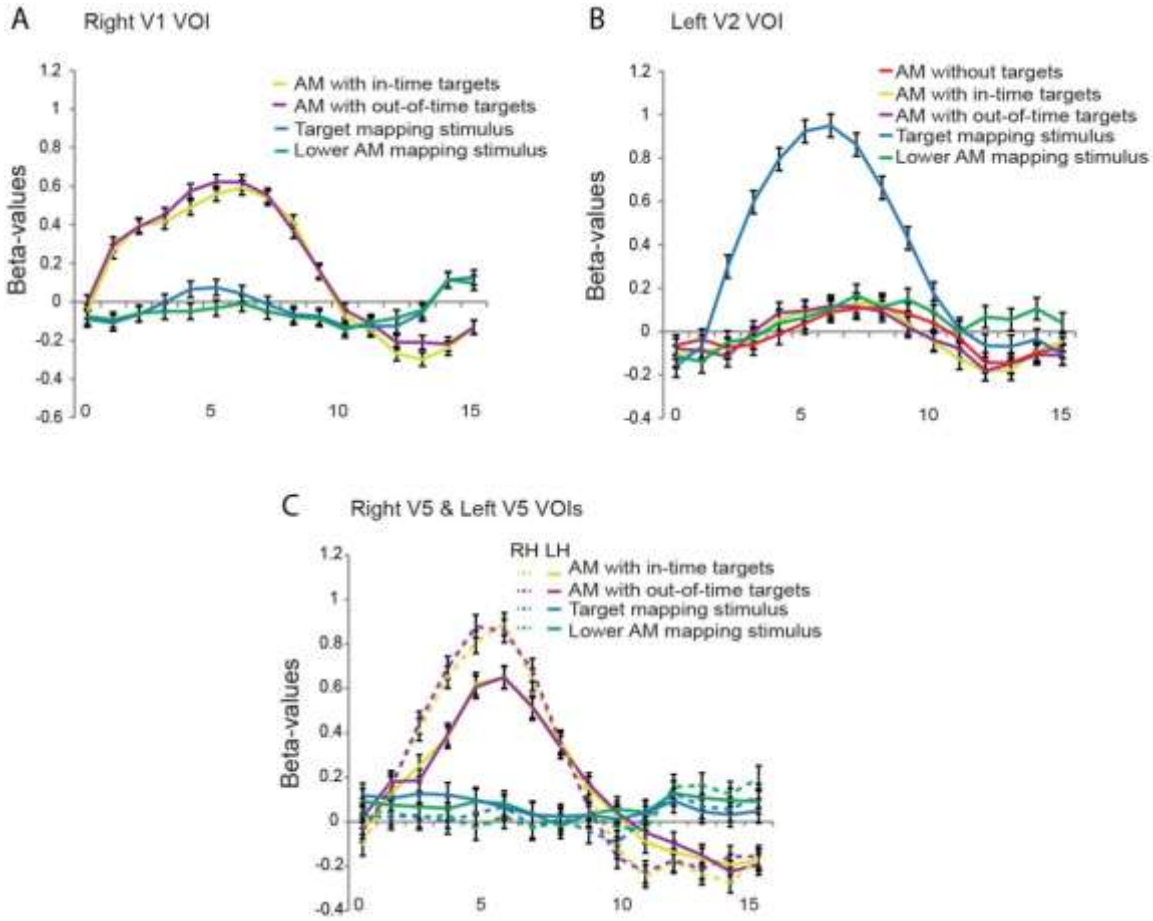

Figure 3.4 - BOLD Response to Apparent Motion Trials in Experiment 2 – Right V1, Left V2, Right V5, Left V5
A: Group-averaged event related BOLD response in right V1 ROI. **B**: Group-average event related BOLD response in left V2 ROI. All apparent motion conditions activated above baseline, and no activation difference found between in-time and out-of-time target conditions at peak. **C**: Group-averaged event related BOLD response at right and left V5 ROIs superimposed onto one graph. No activation difference between in-time and out-of-time target trials for right V5 or left V5. Activation difference for in-time and out-of-time targets was also analyzed during later activation in left V5 resulting in a non-significant result.

3.4.4 Predictive feedback from V5

Right and left V5 were analysed to ensure the motion sensitive regions were active during apparent motion processing (Sterzer, Haynes, & Rees, 2006; Vetter, Grosbras, & Muckli, 2013). Both regions were identified in all subjects using the no target apparent motion condition as a localiser (Figure 3.4C & Supplementary Figure 3.3C & 3.3D). Large activation was found in right V5 for in-time and out-of-time target trials (group deconvolution averaged peak: mean (SD): in-time target trials: 0.67(0.09) β; out-of-time target trials: 0.69(0.09) β; Figure 3.4C & Supplementary figure 3.3C) (Muckli et al., 2002; Muckli et al., 2005; Wibral et al., 2009; Alink et al., 2010; Vetter, Grosbras, & Muckli,

2013). Reduced and slightly later activation was found in left V5 for the in-time and out-of-time target trials (group deconvolution averaged peak: mean (SD): in-time target trials: 0.50(0.06) β; out-of-time target trials: 0.50(0.06) β). Right V5 has an increased activation above left V5 as the apparent motion is mainly presented in the left visual field. The later activation in left V5 may relate to the processing of the final cycle of apparent motion across saccade. There was no activation difference between in-time and out-of-time target trials in right or left V5 (right hemisphere V5: t(8)1.152, p=0.282, left hemisphere V5: t(8)0.547, p=0.599; Figure 3.4C & Supplementary figure 3.3C & 3.3D).

3.4.5 Predictable and unpredictable target detection

At the end of each trial subjects were required to respond if they detected a target presented within the apparent motion trace after saccade. Previous research has indicated that subjects are better at detecting more predictable in-time targets both during steady fixation (Schwiedrzik et al., 2007; Vetter, Grosbras, & Muckli, 2013) and after saccade (Vetter, Edwards, & Muckli, 2012). In experiment 1 three subjects showed significant differences between in-time and out-of-time target detection (alpha = 0.05), only two of which with the in-time target detection advantage (Figure 3.5A). Group data demonstrated there was no difference in target detection between target types for all subjects. The probability of subjects detecting in-time targets is 61.62% with a 95% confidence interval (CI) of (3.09,-3.02) versus a 58% (CI(3.13,-3.08)) out-of-time target detection. Furthermore, no detection difference was found for the four remaining subjects (in-time detection accuracy 61.86% (CI (4.98,-4.80)); out-of-time detection accuracy 61.86% (CI (4.98,-4.80)); Figure 3.5A). The lack of predictable target detection advantage was also found in the eye-tracking controlled experiment 2 (in-time detection accuracy 51.31% (CI (5.43,-5.40)); out-of-time detection accuracy 49.40% (CI (5.45,-5.48)); Figure 3.5B).

3.4.6 Extra-session psychophysical control experiment

The fMRI experiments revealed no behavioral detection advantage for either in-time or out-of-time targets, likely related to the design of the fMRI apparent motion paradigm. Targets were always displayed directly after saccade so may have become more predictable regardless of whether they are presented in-time or out-of-time with the illusion. An indication of this is seen in the percentage detection rates which show that targets were generally better detected in fMRI experiments 1 and 2 (Supplementary Figure 3.4). However, early visual processing may be more sensitive to the predictability of the

incoming stimuli even though behavioral results might be insensitive (Vandenbroucke et al., 2014). Design changes were undertaken for an extra-session psychophysical version to combat target predictability after saccade (See Online Methods). We found that subjects were more accurate at detecting predictable in-time targets after saccade (Figure 3.5C), probability of detection(CI): in-time target trials: 32.50% (2.34,-2.41); out-of-time target trials: 22.0%(2.07,-2.18)) replicating previous work with steady fixation (Schwiedrzik et al., 2007; Vetter et al., 2013) and after eye-movement (Vetter et al., 2012). The difference between in-time and out-of-time target detection was significant for four subjects (Figure 3.5C, *alpha = 0.05). This demonstration of an increased detection rate for predictable in-time targets provides behavioral evidence of prediction transfer with saccade.

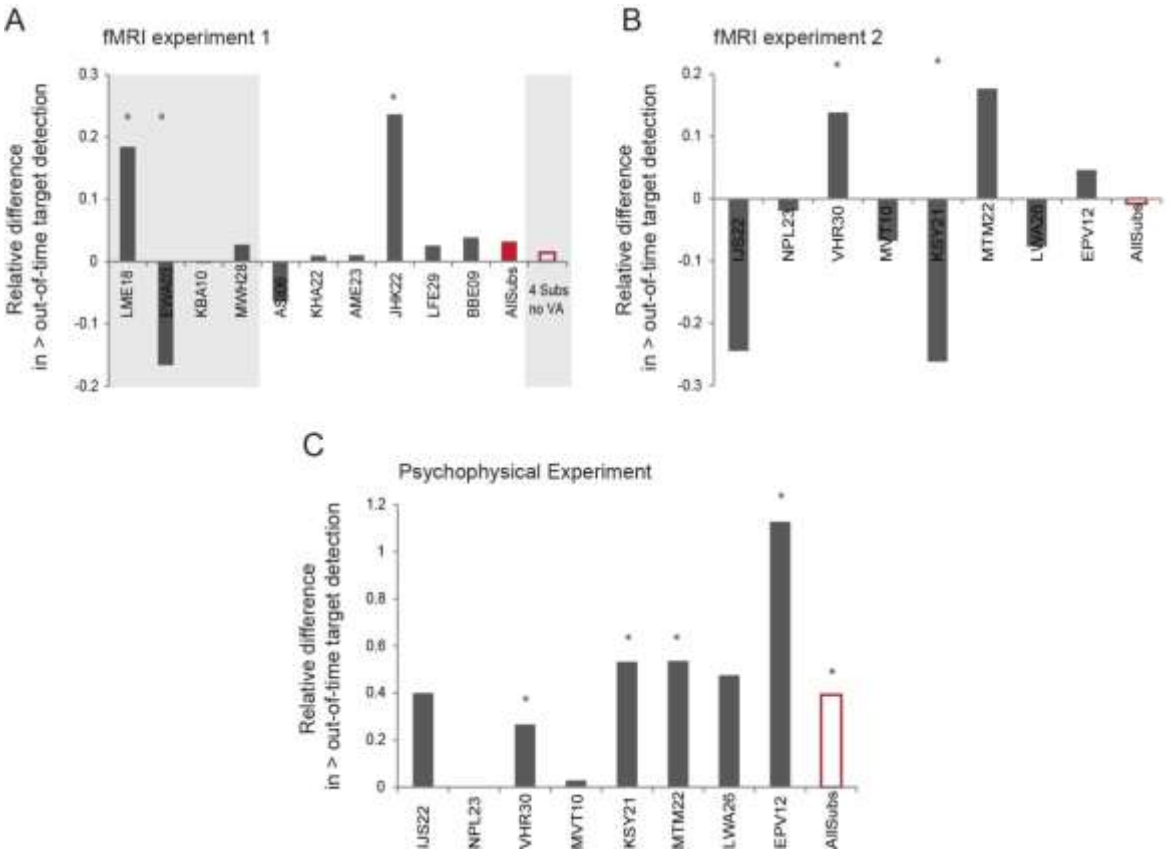

Figure 3.5 - Bootstrapped Behavioural Data – Target Detection Accuracy
Once trials removed using saccade criterion, in-time and out-of-time target detection accuracy difference was determined by bootstrapping the data to ensure observations are assumed from an identically distributed population. Single subject and group data presented. **A**: Experiment 1(in fMRI): Two subjects showed a significantly different binomial fit in favor of in-time targets to the alpha of 0.05 indicated by a *. The data was averaged across all subjects (black outlined bars) and across the four who showed no ventral activation (grey background, empty bars). No significant difference was found in detection accuracy. **B**: Experiment 2 (in fMRI): No significant difference between in-time and out-of-time target detection for single subjects (filled bars) or group data (empty bars). **C**: Extra-session psychophysical data: Two subjects were significantly better at detecting in-time targets (*alpha = 0.05), and the group data also showed a significantly different binomial fit in favor of in-time targets to the alpha 0.05 (empty bars).

3.5 Discussion

We provide evidence for predictive coding as a viable theory of perception by demonstrating the ability of predictions to relocate to new retinotopic regions in V1 with saccade. Using saccades across an illusion of motion, we find predictions of the illusory token project to new retinotopic regions in V1 with saccade. Additionally, we find evidence of a post-saccadic error signal in V1 when the post-saccadic stimulus did not match the relocated prediction of the illusory moving token. Finally, we show evidence that these predictions originated from the motion sensitive higher cortical area hMT/V5+. The evidence for neural relocation of feedback predictions was supported by the extra-session behavioural experiment which demonstrated a detection advantage for predictable targets directly after saccade. Evidence of motion related predictions in V1 directly after saccade indicate that predictive feedback relocates to new regions of V1 with saccade, thereby indicating predictive coding is relevant during naturalistic viewing conditions.

Prediction relocation in V1 of a moving token with saccade was demonstrated by post-saccadic activity along the illusory motion trace. Without feedforward sensory input along the trace, we suggest the illusory motion activity was created by feedback predictive signals from higher cortical areas and lateral interactions in V1 (Muckli et al., 2005; Sterzer et al., 2006). Others have previously demonstrate that the illusion of motion causes feedback activity to V1 during steady fixation (Muckli et al., 2005; Sterzer et al., 2006; Alink et al., 2010; Akselrod et al., 2014). Chong et al., (2012) and Familiar et al. (2014) also found that the expected representation of the moving token (i.e. the tilt of the illusory moving grating) could be decoded along the apparent motion trace. The expected representation of the illusory token provides evidence of predictive models projecting feedback to V1 (Chong, Yu, & Shim, 2012 VSS; Familiar, Chong, & Shim, 2014 VSS). We found further evidence of prediction relocation with post-saccadic prediction error production in V1. Targets presented out-of-time with the illusion directly after saccade caused increased activity in the new retinotopic location. The error signal was produced due to the inability of relocated apparent motion predictions to predict out-of-time targets presented post-saccade. Alink and colleagues (2010) also demonstrated an increased activity for targets presented out-of-time with the illusory moving token during fixation. Therefore, our data support the feedback of spatiotemporally predictive signals to V1 and further demonstrate that these feedback signals can relocate in V1 during saccadic eye-movements.

Our data supports predictive feedback signals relocating with saccade in V1; however some V1 activity may be explained by neural effects of saccadic eye-movements. Integration of information across saccades occurs via multiple processes, such as saccadic suppression which affords visual stability across saccades by reduced sensory input processing during saccade (Wurtz, 2008). Saccadic suppression causes approximately 1% signal decrease in V1 during saccades (Sylvester, Haynes, & Rees, 2005) and this suppression may last up to 50 ms post-saccade (Duhamel, Colby, & Goldberg, 1992). We focus on a time-window after saccadic suppression release, during a period of post-saccadic enhancement (MacEvoy, Hanks, & Paradiso, 2008; Ibbotson & Krekelburg, 2011; Ruiz & Paradiso, 2011). Remnants of receptive field mapping will still be available in the BOLD signal during this period of enhancement (Merriam, Genovese, & Colby, 2007). Receptive field remapping is the activation of receptive fields which are about to receive sensory input after saccade (Melcher & Colby, 2008). Therefore, our finding of post-saccadic activity related to the illusory motion trace may also reflect receptive field remapping with eye-movement (Merriam, Genovese, Colby, 2007). The error signal indicated by an increased activity for out-of-time targets still suggests the activity in V1 is predictive of the location of the illusory moving target, which aligns with predictive coding rather than activation of receptive fields. Nonetheless, there are error signals related to receptive field remapping. A disparity between the remapped receptive fields and the sensory input can cause an error signal in the frontal eye fields (FEF; Crapse & Sommer, 2008). Even if these error signals propagate to V1, the error signal is relevant to the predicted saccade landing location, not the presentation of stimuli after the saccadic event. Importantly, the activity difference related to target presentation has been found without saccade (Alink et al., 2010) suggesting saccades are not necessary to provide this activation in V1.

Attention to a specific stimulus does not seem to be a prerequisite for cognitive predictive feedback signals biasing perception (Summerfield & de Lange, 2014). Specifically, previous studies have found that attention has little effect on the activation of the AM path in V1 (Muckli et al., 2005). Nevertheless, attention may play a role in the activity created by the unpredicted targets through weighting the error signal communicated back to higher cortical regions (Friston, 2009; Feldman & Friston, 2010; den Ouden, Kok, & de Lange, 2012; Hohwy, 2012; Summerfield & de Lange, 2014). Attention handles the precision of errors based on the reliability of the sensory input (i.e. the weight of the error increases as the reliability of the sensory information increases; den Ouden, Kok, & de Lange, 2012).

Therefore, attention may affect the weight of prediction errors for out-of-time targets presented post-saccade, however an internal model predicting sensory input is still necessary to produce the prediction error.

Although V1 is highlighted as the region integrating feedback predictions and feedforward sensory information, V2 was also active during apparent motion trials. Activation difference for predictable and unpredictable targets in V2 was not detected, however V2 was active during processing of the illusion indicating a possible involvement in the propagation of the feedback predictive signal (Mckeefry et al., 1997; Girard, Húpe, & Bullier, 2001; Sincich & Horton, 2005).

The signal propagated back to V1 is likely a prediction of motion demonstrated by an increased activity for the post-saccadic target presented out-of-time with the illusion. The increased activity is indicative of an interaction of motion prediction with unpredictable out-of-time feedforward input resulting in error signal production (Alink et al., 2010). Importantly, these findings depend on predictive feedback relocating from right V1 to left V1 with saccade. As V1 is acallosal (van Essen et al., 1982; Dumoulin & Wandell, 2008; Saenz & Fine, 2010) predictive feedback must relocate via higher cortical areas. hMT/V5+ is a motion sensitive region (Chawla et al., 1998; Goebel et al., 1998) known to integrate long-range apparent motion (Muckli et al., 2002; Muckli et al., 2005; Sterzer, Haynes, & Rees, 2006; Wibral et al., 2009; Vetter, Grosbras, & Muckli, 2013). Our data demonstrated that both right and left hMT+/V5 were active during apparent motion presentation, indicating involvement in creating the internal model and percept of the illusory moving token. The role of hMT/V5+ in creating an internal predictive motion model is supported by a dynamic causal modelling study which illustrated hMT/V5+ modulating V1 during apparent motion stimulation (Sterzer, Haynes, & Rees 2006). Saccade related noise in the BOLD signal could account for the lack of error detected in hMT/V5+ when unpredicted stimuli were presented. Saccade-related modulation of MT has been shown in monkeys (Bakola, et al., 2007) and a weak reduction caused by saccadic suppression in humans (Sylvester, Haynes, & Rees, 2005). Alternatively, the weight of the error created in response to the short presentation of an unpredicted target was not large enough to cause activity in hMT/V5+.

Our extra-session psychophysical study demonstrated that our MRI subjects were better at detecting in-time targets directly after saccade. The detection advantage for in-time targets replicates previous finding during steady fixation (Schwiedrzik et al., 2007; Vetter,

Grosbras, & Muckli, 2013) and during saccades (Vetter, Edwards, & Muckli, 2012), thereby further supporting predictive signals transferring with saccade. Vetter and colleagues (2013) found that transcranial magnetic stimulation (TMS) to hMT/V5+ decreased the target detection difference between in-time and out-of-time targets. This further highlights the importance of hMT/V5+ in perception of predictable stationary targets within illusory motion. Attention has been used to explain predictable target detection along the apparent motion trace. Shioiri and colleagues (2002) suggested that better detection for predictable targets within apparent motion was related to moving visuo-spatial attention. However, Shioiri and colleagues' apparent motion paradigm incorporated a larger number of feedforward inducing stimuli (12 discs) to cause the illusion of a rotating circle. Synaptic gain, controlled by attention to feedforward stimuli, could account for in-time target detection (Desimone & Duncan, 1995). Gain control is less likely to account for our psychophysical findings as our apparent motion paradigm was induced with significantly less feedforward information (2 inducers). Szinte & Cavanagh (2011) found that subjects perceive apparent motion tilt across saccade. This tilt is a mislocalisation of sensory input caused by saccadic eye-movement which is thought to facilitate trans-saccadic perception (Cicchini et al., 2013; Zimmermann, Morrone, & Burr, 2014). Mislocalisation was not examined within our study, but due it is likely that mislocalisation would occur between 50 ms prior to saccade and 50 ms post-saccade (Cicchini et al., 2013; Zimmermann, Morrone, & Burr, 2014). Nevertheless, our targets were presented after the period of saccadic mislocalisation, therefore the predictability of the in-time and out-of-time target within the predicted illusory motion would not be affected (Vetter, Edwards, & Muckli, 2012).

Our data give way to fascinating empirical challenges such as differentiating the activity of error-encoding and prediction units (Friston, 2005), determining if predictable neural representations are amplified (Carpenter & Grossberg, 1987) or suppressed (as seems to be the case with our data; Rao & Ballard, 1999), understanding driving and modulatory processes in contextual connections (Kay & Philips, 2011), and investigating the bidirectionality of prediction and error signalling in the cortex (Spratling, 2008). The predictive nature of this signal found in our data and its updating to new retinotopic locations indicates that predictive coding is relevant in natural viewing conditions. To our knowledge, this is the first evidence to demonstrate that predictive coding tolerates the rapidly changing visual inputs as a result of saccades.

4 Contextually relevant predictive feedback interacts with post-saccadic input to V1

4.1 Abstract

Sensory input and internal models combine to generate perception of the world. In vision, internal models can influence processing of feedforward sensory input in the primary visual cortex (V1) through cortical feedback. Whether such cortical feedback is retinotopically specific is still a matter of debate. Here we simultaneously recorded BOLD signal and eye-movements to study the spatial precision of cortical feedback in V1 during saccades. Subjects were shown images of natural scenes and instructed to execute a saccade across visual hemi-fields. During the saccade, the scene stimuli remained the same, changed, or disappeared. Retinotopic localizers were used to identify the processing region in V1 following the saccade. We trained support vector machines (SVM) on one-second time-windows at the post-saccade processing region to assess the extent of feedback related to the pre-saccadic scene. Integration of the relocated feedback and the post-saccadic feedforward signals was expected to affect SVM performance. After eye-movement, we observed lower SVM accuracy to scenes that changed across saccades in comparison to scenes that remained the same. These results suggest an interference of the feedback for the expected post-saccadic content with the processing of the newly presented scene. The decrease in SVM accuracy co-occurred with a univariate increase in BOLD activity at the post-saccadic region, indicative of a predictive coding error signal (Alink et al., 2010; Kok et al., 2012). Classification analysis did not reveal feedback to new retinotopic regions when the scene disappeared with the saccade. We suggest that a post-saccadic reference frame is necessary to support the remapped feedback in V1 across saccades. Our results demonstrate that with each saccade cortical feedback projects to the new relevant retinotopic regions to integrate the expected content with new sensory information. An interaction of predictive coding, saccadic remapping, and visual attention is likely to account for feedback relocation.

4.2 Introduction

Visual perception is actively constructed using sensory input and cortical feedback (Budd, 1998; Bastos et al., 2012). Sensory input and cortical feedback have been found to integrate early in the visual system at the level of the primary visual cortex (V1; Muckli et al., 2005; Sterzer, Haynes, & Rees, 2006; Alink et al., 2010; Bannert & Bartels, 2013; Ban

et al., 2013; Akselrod, Herzog, & Öğmen, 2014). Cognitive processes which project feedback signals to V1 include attentional control (Gilbert & Sigman, 2007; Chalk et al., 2010; Harris & Thiele, 2011), prior expectation (Muckli et al., 2005; Kok & de Lange, 2014), and saccadic updating (Merriam, Genovese, Colby, 2007). The significance of feedback to our perception of the visual world is indicated by the proportions of input connections to V1 (Douglas & Martin, 2007; Larkum, 2013). Only 20% of V1 activity variance can be attributed to feedforward projections (Carandini et al., 2005). Ten times more axons arrive from V2 than from the lateral geniculate nucleus (LGN). In relation to V2 input, twice as many excitatory synapses feed to the upper layer pyramidal V1 cells from other higher cortical regions (Budd, 1998; Muckli & Petro, 2013).

A neurobiologically plausible account of cortical feedback is provided by inference model theorists, an example of which is hierarchical predictive coding (Rao & Ballard, 1999). In vision, the predictive coding framework theorises that models of the visual environment are created in high cortical areas. Predictions created by these models are then communicated to early cortical areas (such as V1) which cause inhibition. However if the sensory input violates the model, an excitatory error signal is created in lower cortical areas which update the internal model (Mumford, 1992; Rao & Ballard, 1999). Currently, little is known about the effect of saccades on cortical feedback to V1. Humans saccade several times per second in natural viewing (Melcher, 2011). Saccades are known to alter V1 activity through saccadic suppression just prior to saccade followed by an excitation which begins 50 ms after saccade offset (MacEvoy, Hanks, & Paradiso, 2008; Ibbotson & Krekelburg, 2011; Ruiz & Paradiso, 2012). However, how saccades effect predictive cortical feedback to V1 has had little investigation.

Input from the retina to V1 remains spatially preserved, meaning V1 is retinotopically organised (Sereno et al., 1995; Hadjikhani et al., 1998). If sensory input is retinotopically relocated due to a saccadic eye-movement, sensory specific feedback should also be redirected to new retinotopic positions in V1. The spatial specificity of predictive feedback has been demonstrated by retinotopic specific filling-in of an illusory moving token dependent on the illusion path (Akselrod, Herzog, & Öğmen, 2014). Neural evidence for retinotopic relocation of spatiotemporally predictive feedback with eye-movements has been demonstrated (Edwards et al., submitted. **Chapter 3**). This prediction transfer across eye-movements has been found to occur within 50 – 100 ms of saccade offset (Vetter, Edwards, & Muckli, 2012; **Chapter 2**).

The objective of the current study was to increase the wealth of neural evidence for predictive feedback transfer across eye-movements by using complex visual stimuli with rich contextual associations (Bar, 2004) and a combination of univariate and multivariate analysis methods. The relationship between saccadic eye-movements and natural scene stimuli has been demonstrated as functionally unique. An enhancement in activity was found for natural stimuli brought onto receptive fields in V1 in comparison to when stimuli was flashed onto the receptive field or when the an optimal bar stimulus was used (MacEvoy, Hanks, & Paradiso, 2008). The unique interaction between saccades and natural stimuli found in V1 further motivates the investigation of predictive feedback relocation across saccades using natural scenes in V1. Moreover, by using natural scenes the ventral stream is incorporated into stimulus processing (Grill-Spector et al., 1999; Koutzi & Kanwisher, 2001; Ewbank et al., 2005; Reddy & Kanwisher, 2006; Cant, Arnott, & Goodale, 2009). Previous evidence for predictive feedback relocation in V1 involved spatiotemporal feedback, which engaged more dorsal stream processing (Milner & Goodale, 1995; Braddick, Atkinson, & Wattam-Bell, 2003). Using natural scene stimuli would demonstrate predictive feedback relocation to V1 is not motion specific.

In the current study we designed an fMRI experiment which investigates predictive feedback to new retinotopic positions in V1 with interhemifield saccades. To address this question we first use multivariate pattern analysis (MVPA) to determine if the contextual content of the feedback updates to new locations with or without saccade initiation. Secondly we study predictive feedback by changing the contextual information of the image during saccade. We hypothesise that predictive feedback associated with the pre-saccadic original image will relocate with saccade and interfere with the internal representation of the unpredicted new stimulus post-saccade. Therefore post-saccadic classification performance of the changed image will decrease. We found that feedback signals generated by pre-saccadic stimulation interfere with pattern classification of the image which changed trans-saccade, supporting our hypothesis. However, predictive feedback was only detected across saccade when interacting with feedforward information after saccade; predictive feedback was not detected at the new retinotopic coordinates by saccade execution alone.

4.3 Materials & Method

Two fMRI experiments were conducted on two separate groups of subjects. The second experiment included a control condition. The control condition was included to ensure that the feedback projected to the post-saccadic region of V1 was related to pre-saccadic processing of the natural scene.

4.3.1 Subjects

Twelve healthy subjects (6 male; 19-28 years) were recruited for experiment 1 and three (all female; 20-27 years) for experiment 2 from the University of Glasgow, School of Psychology subject pool website. All subjects had normal or corrected-to-normal vision. Each subject signed written consent forms and was paid for their participation in the experiment. The experiment was conducted with approval of the School of Psychology internal ethics committee.

4.3.2 Stimuli & Task

The stimuli for each condition were presented on a grey screen (RBG: 128, 128, 128, Figure 4.1 A). The contextually rich scenes used in both experiments were a people scene and a car scene. Basic low-level stimulus features of the images (i.e. global luminance, contrast, energy at differing spatial frequencies, orientations) were controlled by spectral normalisation (Smith & Muckli, 2010). Each condition began with one of two scenes presented centrally with one red cross presented right of the image and one green cross presented left. Subjects were to fixate the red cross and use the green cross as a reference for potential saccade target. The scenes were 6.66° by 8.30°, and the crosses (0.7° in size) were presented along the meridian of the image 0.52°. In condition 1, subjects remain fixated on the red cross to the right of the image. In conditions 2, 3, 4, and control, a yellow arrow (0.7°) replaced the red cross which cued subjects to saccade left when the red cross reappeared in the green cross position. During the saccade the image either disappeared (condition 2), remained unchanged (condition 3), or the changed (condition 4 & control) contingent to eye-movement (Figure 4.1A). In condition 4 only the centre of the image changed for the centre of the other image, in the control the whole image changed. At the end of each trial subjects would report if the image had changed during saccade and the red cross returned to the original position right of the image before baseline began. As a slow event-related design, each trial lasted for 6666 ms with a baseline of approximately

9334 ms between each trial. Baseline time was dependent on saccade initiation time per trial, slower saccade reaction lead to shorter baselines as experiment was gaze contingent. In rare instances where the Eyelink eyetracker failed to detect a pupil, the experiment was programmed to override the gaze contingent programming.

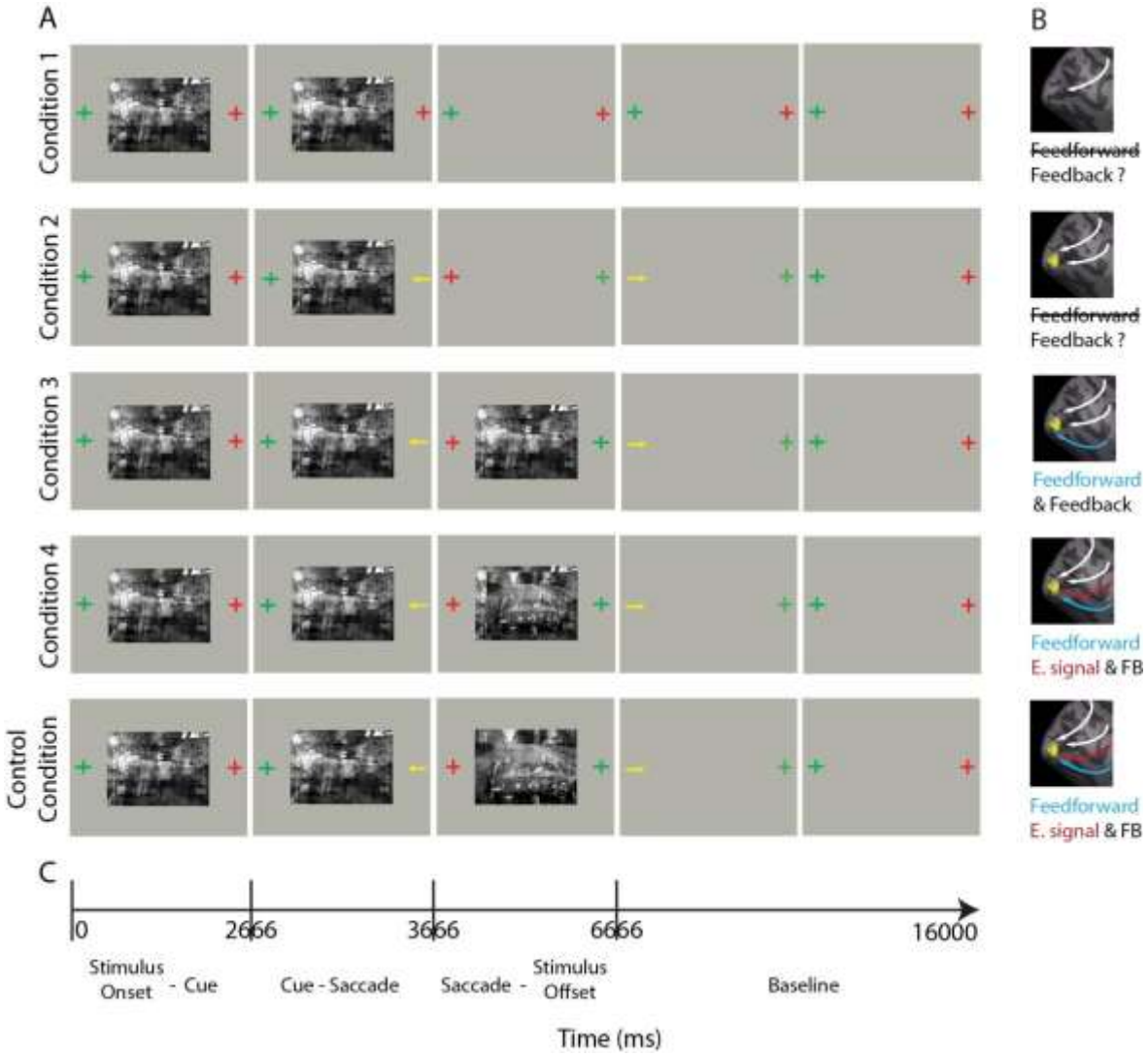

Figure 4.1 - Illustration of stimuli
A: Stimulus presented per condition. Subjects fixate on red cross, saccade cued by yellow arrow and performed when red cross alternated to left of image. Subjects reported if image was same or different after saccade. **B**: Illustrations of hypothesised predictive feedback to left V1 with saccade. **C**: Condition specific stimulus onsets (ms).

4.3.3 Mapping Stimulus

At the end of each run subjects were presented with mapping stimuli to define retinotopic processing regions in left and right hemisphere V1. Four regions of interest (ROI(s)) were identified for experiment 1 and 2, the whole image ROI in right and left hemispheres separately, the image boarder ROI, and the image centre ROI. The whole image ROI in left V1 was used for analysis of all conditions (Figure 4.2 A). Analysis was split into centre

and boarder ROIs to study activity effects for regions of the image that changed and remained the same. To map the left hemisphere ROIs, subjects were to fixate on the red cross presented to the left of the central checker boards (Figure 4.2). A checkerboard for each ROI was flashed on and off for 12000 ms to maximise activation of the processing region in V1, followed by a 12000 ms baseline. Subjects fixated to the right of the whole image checkerboard to map the whole image in the right hemisphere for both experiments.

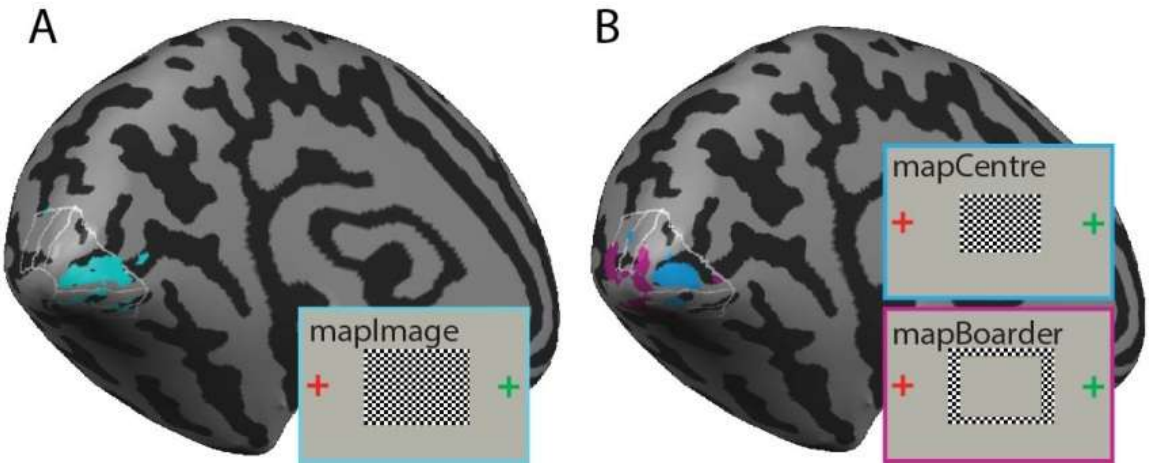

Figure 4.2 - Bowtie phase-encoded retinotopic mapping
A: Whole image ROI within left V1 - turquoise (GLM contrast: mapImage>baseline). **B**: Image centre ROI in left V1 – blue (GLM contrast: mapCentre>mapBoarder) and image boarder in left V1 – purple (GLM contrast: mapBoarder>mapCentre).

4.3.4 Procedure

A practice run was conducted by each subject prior to the experiment. Subjects completed four functional runs (approx. 13 m) with eye-tracking calibration at the beginning and mapping sequences at the end of each run (Experiment 1: 3 m, Experiment 2: 1.30 m). Subjects viewed the stimulus through a mirror attached to the head coil which reflected an MRI compatible screen placed in the bore of the magnet behind the subjects' head. The viewing distance was 110 cm and the screen resolution was 1024 x 768. Neurobehavioural system's Presentation® was used to programme and present the stimulation (Version 16.5) with a refresh rate of 60 Hz. In experiment 1, the conditions 1 to 4 were presented 6 times for each image (people or car scene) in each run with a 9334 ms baseline between each condition (12 trials per condition). Each of the four mapping conditions were presented twice interleaved with baseline conditions. In experiment 2, conditions 2, 3, and control were presented 8 times for each image (16 trials per condition). Condition 1 was excluded to increase the number of trials for the other 3 conditions per run and therefore increase statistical power. The two mapping conditions were presented twice interleaved with

baseline conditions. A randomisation scheme for each run was employed to create the trial sequence. Before every run subjects has a 10 second AHH scout for aid with functional run alignment on the anatomical data. Subjects also underwent a nine minute high resolution anatomical and a seven minute bowtie phase-encoded retinotopic mapping run to map the early visual areas.

4.3.5 Data Acquisition

4.3.5.1 MRI Data Acquisition

Functional and anatomical data was acquired on a 3 Tesla Siemens Tim Trio scanner using a 32-channel head coil. An echo-planar imaging sequence was used for the functional runs with the following parameters: 17 slices, TR: 1, TE: 30, 875 volumes per run, field of view of 205 mm, and a resolution of 2.5 x 2.5 x 2.5 mm. The slices were aligned to the calcarine sulcus in order to capture the whole of the early visual cortex. The parameters of the anatomical sequence were TR: 1.9, 192 volumes, and a resolution of 1 x 1 x 1 mm.

4.3.5.2 Eye-tracking Acquisition

Eye-movements were recorded using an Eyelink 1000 (SR Research®) with a sampling rate of 500 Hz. The hardware was mounted on the MRI compatible projector screen and the data was recorded by Eyelink software which was programmed into the Neurobehavioural System's Presentation® script. Data analysis was performed using Eyelink Data Viewer and MatLab®.

4.3.6 Data Analysis

4.3.6.1MRI Analysis

The following analysis was performed on each subject separately. The functional (experimental runs and retinotopic mapping run) and anatomical runs were analysed in BrainVoyager QX® (Version 2.8). The first two volumes were removed to preclude saturation effects. A high-pass filtering at 6 sines/cosines was performed during the 3D-motion correction to remove low-frequency noise and drift for each run. Once the functional data was preprocessed, alignment to the high-resolution anatomical and AHH scout were performed. Each subject's brain was transformed to talairach space resulting in a common brain space along the AC-PC plane. 3D aligned time courses were created using

either standard alignment of functional data onto the high resolution anatomical scan or alignment using functional data onto each run's AHH scout and high resolution anatomical scan (Supplementary Figure 4.1). Inflations of cortical surfaces were created using manual inhomogeneity corrected anatomical data.

Early visual areas of both the right and left hemispheres were identified using linear correlation maps of the bowtie phase-encoded retinotopic mapping data projected onto the cortical surfaces (Supplementary Figure 4.2). The ROIs within left V1 were then defined for further analysis using a standard general linear model (GLM). To define the whole image ROI, a univariate contrast of whole image > baseline was performed (left hemisphere whole image Talairach co-ordinates for experiment 1: mean (SD): x = -9.67(3.31), y = -82.75(2.49), z = -3.75(2.60); FDR = 0.05; Figure 4.2 A. Left hemisphere whole image Talairach co-ordinates for experiment 2: mean (SD): x = -9.33(1.53), y = -85(8.89), z = -2.33(2.09); FDR = 0.05). Contrasts between boarder and central checkerboards were also conducted to locate their retinotopic processing region in V1 (left hemisphere boarder > centre Talairach co-ordinates for experiment 1: mean (SD): x = -12.83(6.03), y = -87.42(7.55), z = -10.58(5.11); left hemisphere boarder > centre Talairach co-ordinates for experiment 2: mean (SD): x = -14.33(3.78), y = -93(2), z = -9.33(3.06); left hemisphere centre > boarder Talairach co-ordinates for experiment 1: mean (SD): x = -10.58(4.32), y = -84.75(2.73), z = -6.83(3.38); FDR = 0.05; left hemisphere centre > boarder Talairach co-ordinates for experiment 2: mean (SD): x = -8(3.61), y = -85.67(7.09), z = -3.67(5.69); FDR = 0.05; Figure 4.2 B). A univariate contrast of condition 1 > baseline was also conducted to define the image processing ROI of the right hemisphere V1 (right hemisphere whole image Talairach co-ordinates for experiment 1: mean (SD): x = 6.67(2.71), y = -85.42(3.85), z = -7.25(6.27); FDR = 0.05. Right hemisphere whole image Talairach co-ordinates for experiment 2: mean (SD): x = 10.67(3.05), y = -84.67(3.05), z = 1.67(5.15); FDR = 0.05).

4.3.6.2 Multivariate Pattern Analysis – Sliding window

To determine when predictive feedback relocates across saccade the multivariate pattern analysis (MVPA) was be performed as a sliding time-window across the trial.

One second time-period classification was performed every 500 ms from onset of stimulation for all ROIs in both experiments. Single trial beta-weights were estimated for all the voxels in each ROI during each time-period using a 2-gamma hemodynamic response function and were fed into a linear support vector machine (LIBSVM toolbox, Chang & Lin, 2001). Here, the classifier learns to associate multivariate brain activity to

one of two scenes presented (people or car) using a pattern of activity created voxels in a region of interest (Kriegeskorte & Bandettini, 2007) at the different time-periods. Then the classifier can be tested on an independent data set to show if a one second time-period of brain activity is indicative of people scene or car scene processing activity. The MVPA performed for the current experiment was a leave-one-run-out classification where the classifier was trained on three runs, and tested on one run. The sliding window classifications across the trials were also concatenated into larger time-periods to determine if correct classification was significantly different between conditions at specific time-points during the trial.

To control for statistical significance, all classifications were permutation tested which enabled a robust test of classification performance against chance. During permutation testing, random labels are applied to each condition 1000 times and then classifier is trained and tested. The output p-value indicates the difference of classification performance between the correctly labelled conditions versus the randomly labelled conditions classifications. These permutation tests were performed for each subject, in each ROI, at each time-point. The group data was produced by averaging the permutated performance classifications and randomisation distributions.

4.3.6.3 Univariate Analysis

To determine activation amplitude difference between conditions, group analysis was performed in the left V1 centre and boarder ROIs in experiments 1 and 2 during the time-period from saccade offset until left fixation offset. A simple GLM was performed with a contrast of condition 4 > condition 3 to investigate activation differences in the two regions related to the image change during eye-movement. The same time-period was analysed in experiment 2 with a contrast of control condition > condition 3 in the left hemisphere whole image ROI.

4.4 Results

4.4.1 Experiment 1

4.4.1.1 One Second Sliding Classification

We built a one second sliding decoder to reveal information feedback prior, during and after saccade. Firstly, we ran a control sliding classification between images in the right

hemisphere whole image processing region (Figure 4.3 A). This analysis ensured that the classifier was able to decode between images during feedforward stimulation prior to saccade. Classification between the two images in all four conditions was significantly above chance (50%) until after saccade when all conditions dropped to chance by 5.5 seconds after stimulation onset (*$p<0.05$; Figure 4.3 A). The persistent classification performance after saccade could be due to temporal smoothing. This pre-saccade classification performance was further demonstrated by collapsing across the first 4 time-points (Figure 4.3 C; $p<0.0001$)). No classification performance difference was found across conditions ($F(3,56)=0.368$, $p=0.777$).

To determine if predictive feedback relocates with eye-movement we performed a sliding classification in the left V1 whole image ROI. Conditions 1 and 2 in experiment 1 did not classify above chance at any time-window from stimulus onset (Figure 4.3 B). This indicated that feedback signals to left V1 was not detected when a saccade was not initiated (Condition 1) or when saccade was initiated and image disappeared (Condition 2) during any time-period. The classifier performed significantly above chance when classifying between images in conditions 3 and 4 just prior to saccade cue and throughout the rest of the trial (*$p<0.05$; Figure 4.3 B). Temporal smoothing would also account for some of the pre-saccadic classification. Averaged post-saccadic time-points demonstrates that conditions 3 and 4 significantly classify above conditions 1 and 2 post-saccade (Figure 4.3 D; ($t(11)=3.144$; $p<0.01$).

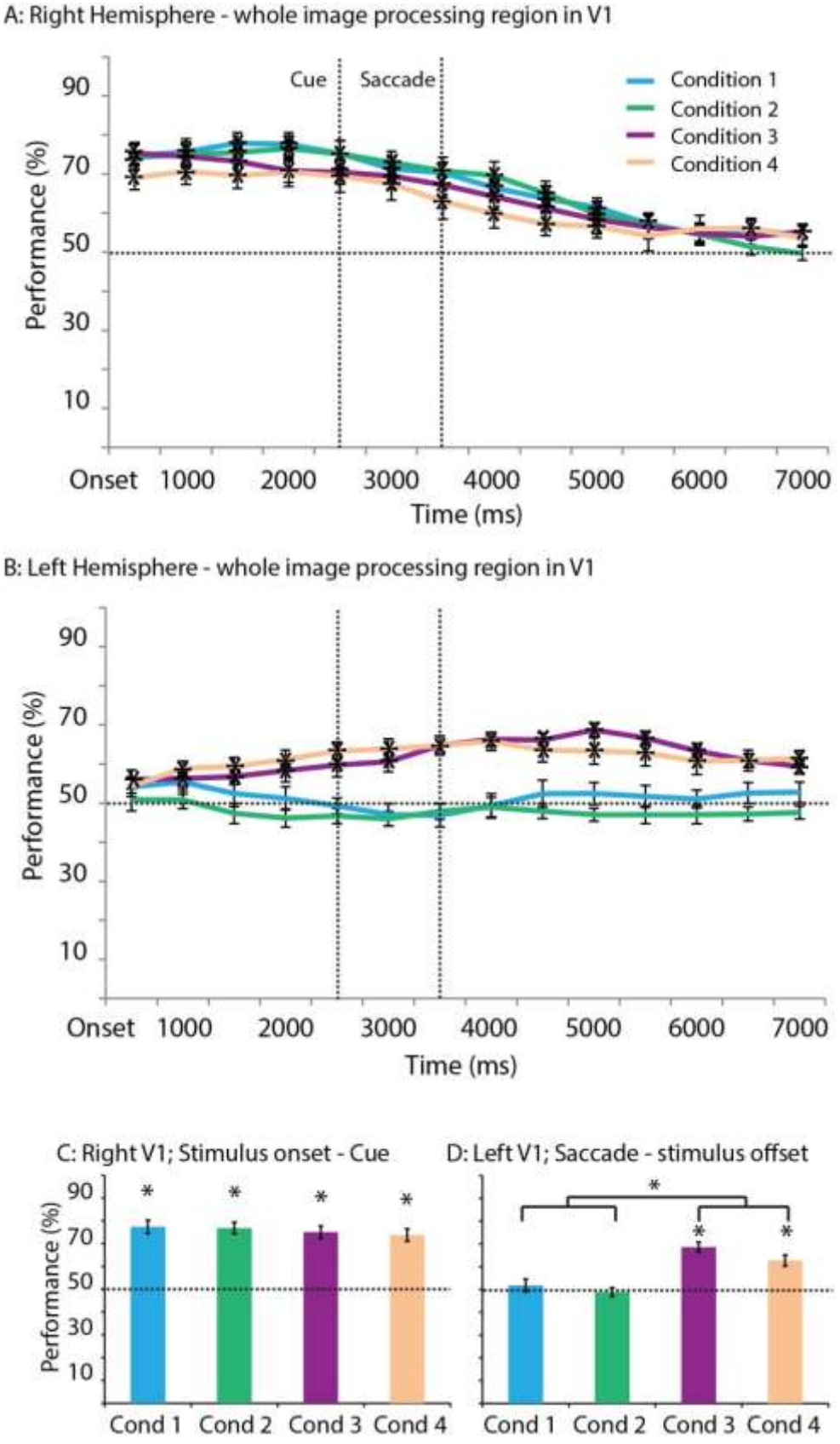

Figure 4.3 - Experiment 1: Pattern classification in right and left V1: whole image processing region

A: Group one-second sliding decoder in right hemisphere whole image processing region of V1. **B**: Group one-second sliding decoder in left hemisphere whole image processing region in V1. **C**: Control classification between images in right hemisphere whole image ROI between stimulation onset and cue to saccade. **D**: Classification between images in left hemisphere whole image ROI between saccade and stimulus offset.

Classification performance difference in the centre and boarder ROIs was conducted to determine if feedback signals from the right hemisphere interacts with feedforward input post-saccade. Importantly the feedforward input remained the same across saccade in the boarder ROI, but changed in the centre ROI for condition 4. As with the whole image ROI, neither condition 1 or 2 classifier above chance in the boarder or the centre ROI. The boarder ROI classification performance was similar between conditions 3 and 4 (*$p<0.05$; Figure 4.4 A). Classification performance between the two images in the image centre ROI was significant for conditions 3 and 4 just prior to saccade cue until the end of the trial (*$p<0.05$; Figure 4.4 B). Again, it should be mentioned that temporal smoothing may cause some pre-saccadic classification. Moreover, the sliding classifier indicated a classification performance difference between conditions 3 and 4 in the centre ROI. This classification difference was clarified by collapsing across the post-saccadic time-points (Figure 4.4 C & D). In the collapsed time-period classification, only Condition 4 classified above chance in the boarder ROI ($p<0.05$), and no difference was found in classification discrimination between Condition 3 and 4 ($t(11)=1.82$, $p=0.1$; Figure 4.4 C). Classification performance was above chance for both conditions 3 and 4 in the centre ROI ($p<0.02$), and performance for condition 3 classification was significantly above condition 4 ($t(11)=3.144$; $p<0.01$, Figure 4.4 D).

Classifying scene specific feedback in the three left V1 ROIs (centre, boarder, and whole image) after saccade demonstrated that saccade initiation was not sufficient to cause predictive feedback relocation (Condition 2). However, predictive feedback was evident at the post-saccade ROIs when feedforward information was present for the feedback to interact with in V1 (Conditions 3 and 4). In comparison to when the image remained the same across saccade (Condition 3), if the image changed mid-saccade (Condition 4) classification performance decreased. This decrease could be due to post-saccadic input not matching the pre-saccadic feedback signals which relocated with saccade, therefore feedback signals interfere with classification.

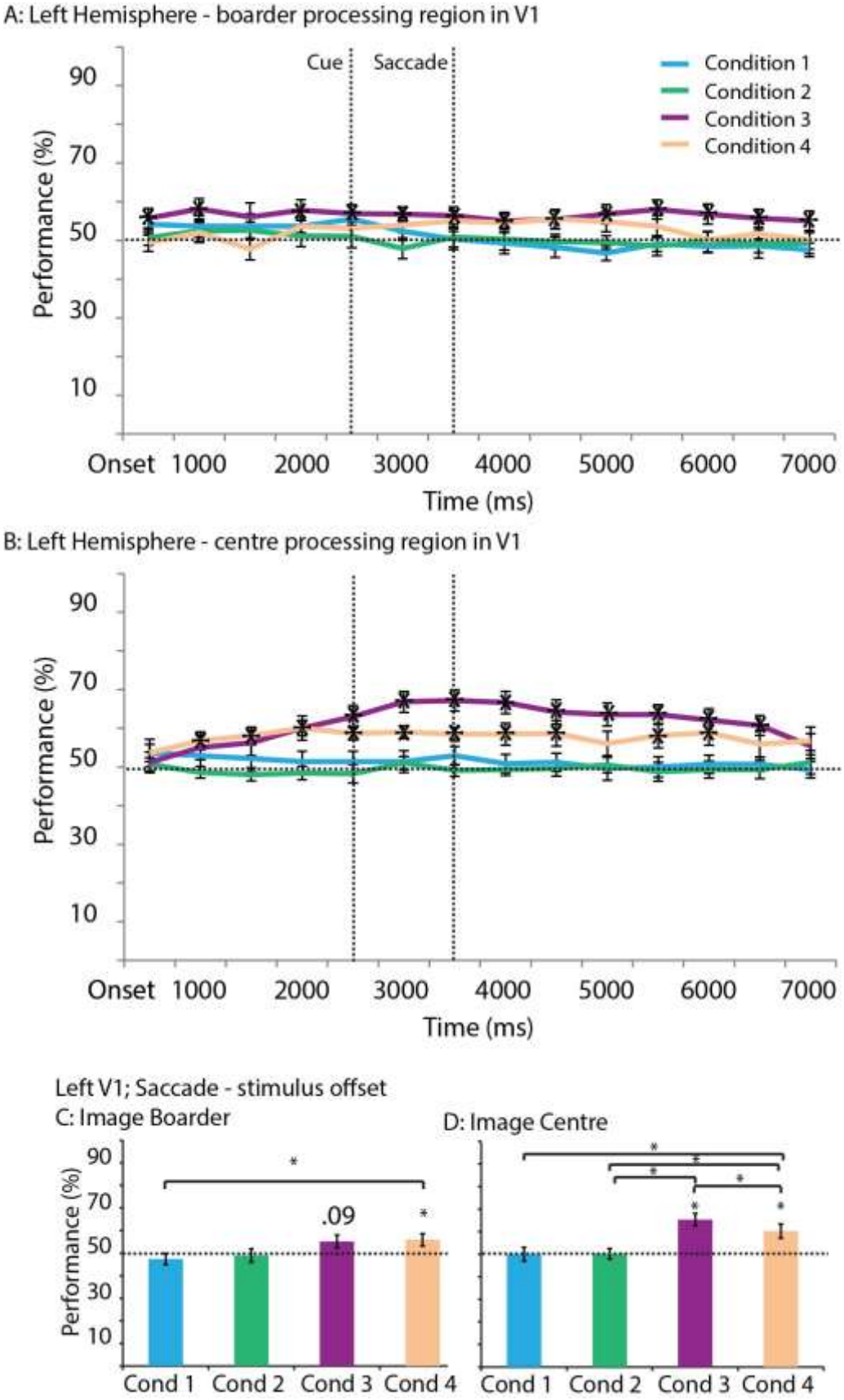

Figure 4.4 - Experiment 1: Pattern classification in left hemisphere V1 boarder and centre processing regions
A: Group one-second sliding decoder in left hemisphere image boarder processing region of V1. **B**: Group one-second sliding decoder in left hemisphere image centre processing region in V1. **C**: Classification between images in left hemisphere image boarder ROI between saccade and stimulus offset. **D**: Classification between images in left hemisphere image centre ROI between saccade and stimulus offset.

4.4.1.2 Univariate Analysis

Univariate analysis was performed to further investigate predictive feedback signal relocation with saccade. An activation difference between Conditions 3 and 4 was only found in the centre ROI, with Condition 4 causing more activation than Condition 3 after saccade ($t(11)3.472$, $p<0.006$). No activation difference was found for the boarder ROI ($t(11)0.153$,$p=0.881$; Figure 4.5 A & B). The activation difference found in the centre ROI where information changed over saccade further supports a mismatch between feedback signals and feedforward input in condition 4. An increased activity for an unpredicted stimulus indicates error signal production according to inference model frameworks (Mumford, 1992; Rao & Ballard, 1999).

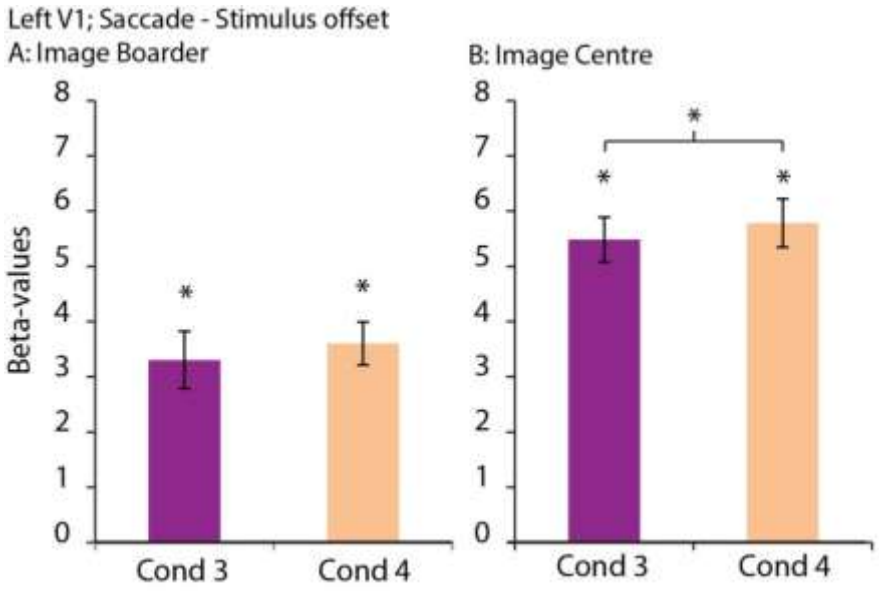

Figure 4.5 - Experiment 1: Univariate analysis between saccade and stimulus onset
A: Beta-value difference between conditions 3 and 4 in image boarder ROI. **B**: Beta-value difference between conditions 3 and 4 in image centre ROI.

Event-related averages were performed for each region of interest to show BOLD response from 2 s prior to trial onset til the end of trial duration. In the right hemisphere ROI BOLD response began 3 seconds after stimulation onset and peaked at 8-9 seconds (Figure 4.6 A). Conditions 2, 3, and 4 showed a similar profile, whereas activity for condition 1 declined one second before the other conditions. Adaptation may cause activity decrease in condition 1 as subjects remain fixated, whereas in conditions 2, 3, and 4, subjects are preparing to saccade. The BOLD profiles for the left hemisphere regions of interest (figure 4.6 B: whole image, 4.6 C: boarder, 4.6 D: centre) are temporally similar. BOLD response

begins 7 seconds after stimulation onset and peaks at 11 seconds. The whole image ROI has the highest BOLD response, followed by the centre ROI and then the boarder ROI. In all ROIs condition 1 does not rise above baseline activity. Condition 2 shows a slight increase above baseline which is most prevalent in the whole processing region of left hemisphere V1. From univariate analysis, we can interpret the activity as saccade related. Both conditions 3 and 4 peak significantly above baseline in all three left hemisphere ROIs, with condition 4 causing the most activity.

Importantly, the profiles of the multivariate analysis do not mirror the hemodynamic response demonstrated by the event-related averages. The event-related averages show that there is a delay in the hemodynamic response of approximately 3 seconds after stimulation onset. The multivariate analysis is performed using a 2-gamma hemodynamic response function, therefore the single subject design matrix files fed into the classifier are sampling beyond the onset, accounting for the delay in BOLD response. Therefore the profile of the multivariate does not match the temporal profile of the event-related averages.

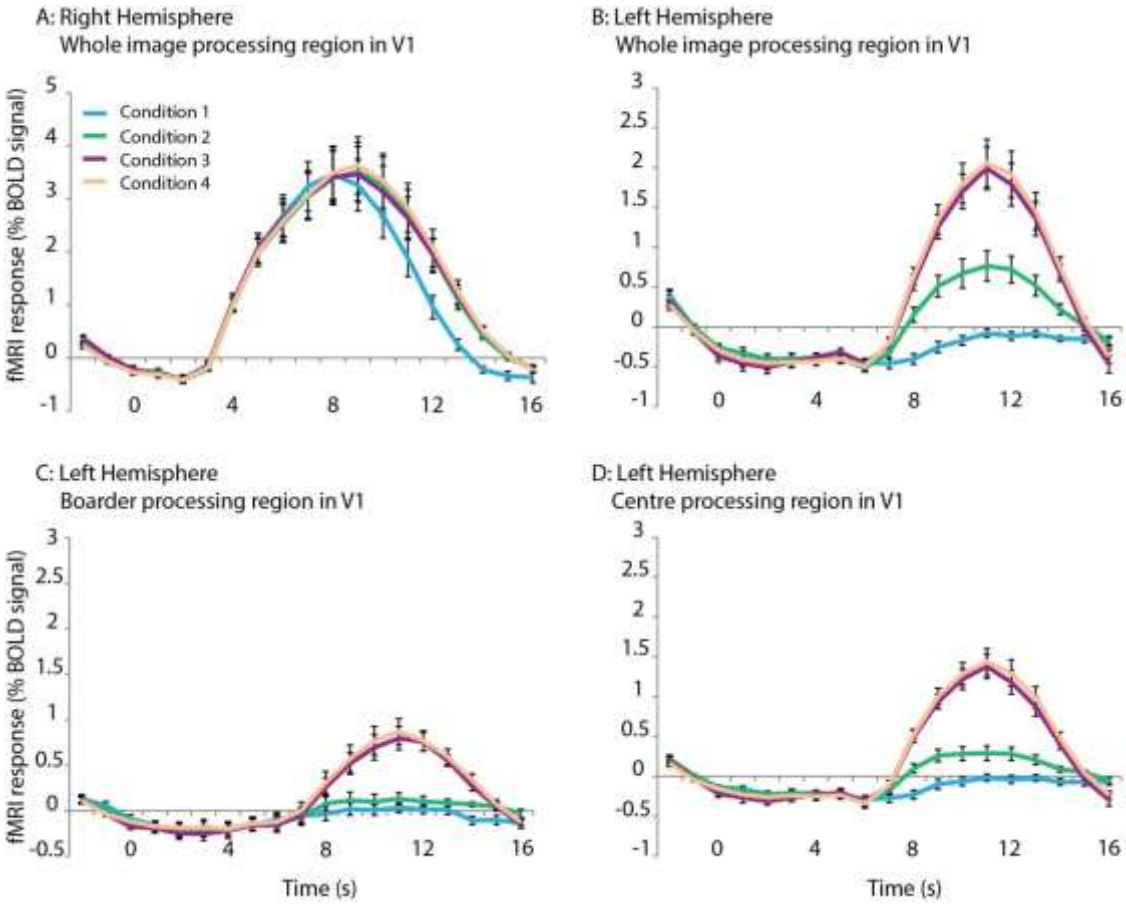

Figure 4.6 - Experiment 1: Group event-related averages
Event-related average from -2 s til 16 s post-onset in **A**: right hemisphere whole processing region of V1, **B**: left hemisphere whole processing region of V1, **C**: left hemisphere image boarder processing region of V1, **D**: left hemisphere image centre processing region of V1.

4.4.2 Experiment 2

Experiment 1 provides evidence for predictive feedback interfering with the processing of an unpredicted feedforward stimulus. However, this predictive feedback could be transferred across saccade (as hypothesised), or could be related to contextual inconsistency provoked by merging two scenes in condition 4. Experiment 2 was designed to ensure that the feedback signals were relevant to pre-saccade processing by changing the whole image across saccade (control condition), therefore removing contextual inconsistency. It should be noted that the data present is an average of 3 subjects and no inferential statistics were performed at a group level.

4.4.2.1 One second sliding decoder

The sliding pattern classification and collapsed classification performed on the right hemisphere whole image ROI demonstrated discrimination between the two images prior to saccade for all conditions (Figure 4.7 A & C; • = individual subject data). Classification performance decreased down to chance by 5.5 seconds (*$p<0.05$; Supplementary Figure 4.3 A). The right hemisphere V1 classification performance replicated the findings from experiment 1. Although a there was a large amount of variation between subjects ($p<0.05$; Supplementary figure 4.3 A).

As with experiment 1, in left V1 whole image ROI no classification discrimination between images was also found for condition 2 after saccade (Figure 4.7 B & D; • = individual subject data), indicating predictive feedback did not relocate by saccade alone. Both condition 3 and the control condition classified above 60% once saccade landed, with a slightly higher classification in condition 3 with subject variability (Figure 4.7 B & D; *$p<0.05$ - Supplementary figure 4.3 B). The increased classification performance for condition 3 above the control condition was similar to the findings of experiment 1 between condition 3 and condition 4. The similarity of experiments 1 and 2 in left hemisphere V1 whole image ROI motivated centre and boarder specific analysis. Importantly, the whole image changed across saccade in the control condition therefore no classification difference was expected between centre and boarder. Both the boarder and centre ROIs indicated an increased classification for condition 3 above classification in the control condition (Figure 4.8 A-D; • = individual subject data) supporting the findings in experiment 1. No significant classification for condition 2 was identified. The better classification performance for condition 3 was more pronounced in the boarder ROI

(Figure. 4.8 A & C; • = individual subjects data). However a large amount of between subject variance was present (* $p<0.05$ - Supplementary figure 4.3 C & D).

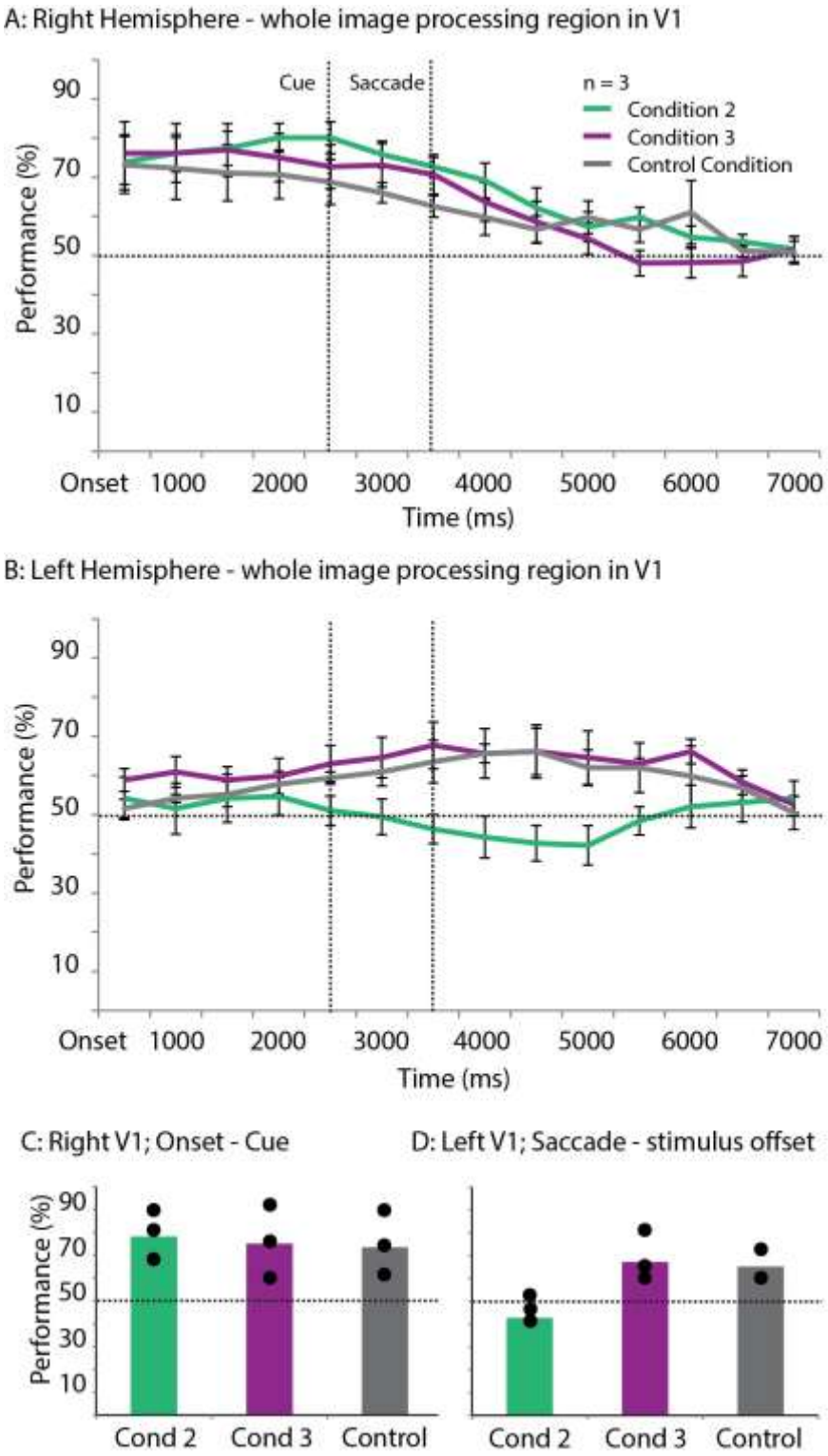

Figure 4.7 - Experiment 2: Pattern classification in right and left V1 whole image processing region

A: Group one-second sliding decoder in right hemisphere whole image processing region of V1. **B**: Group one-second sliding decoder in left hemisphere whole image processing region in V1. **C**: Control classification between images in right hemisphere whole image ROI between stimulation onset and cue to saccade. **D**: Classification between images in left hemisphere whole image ROI between saccade and stimulus offset.

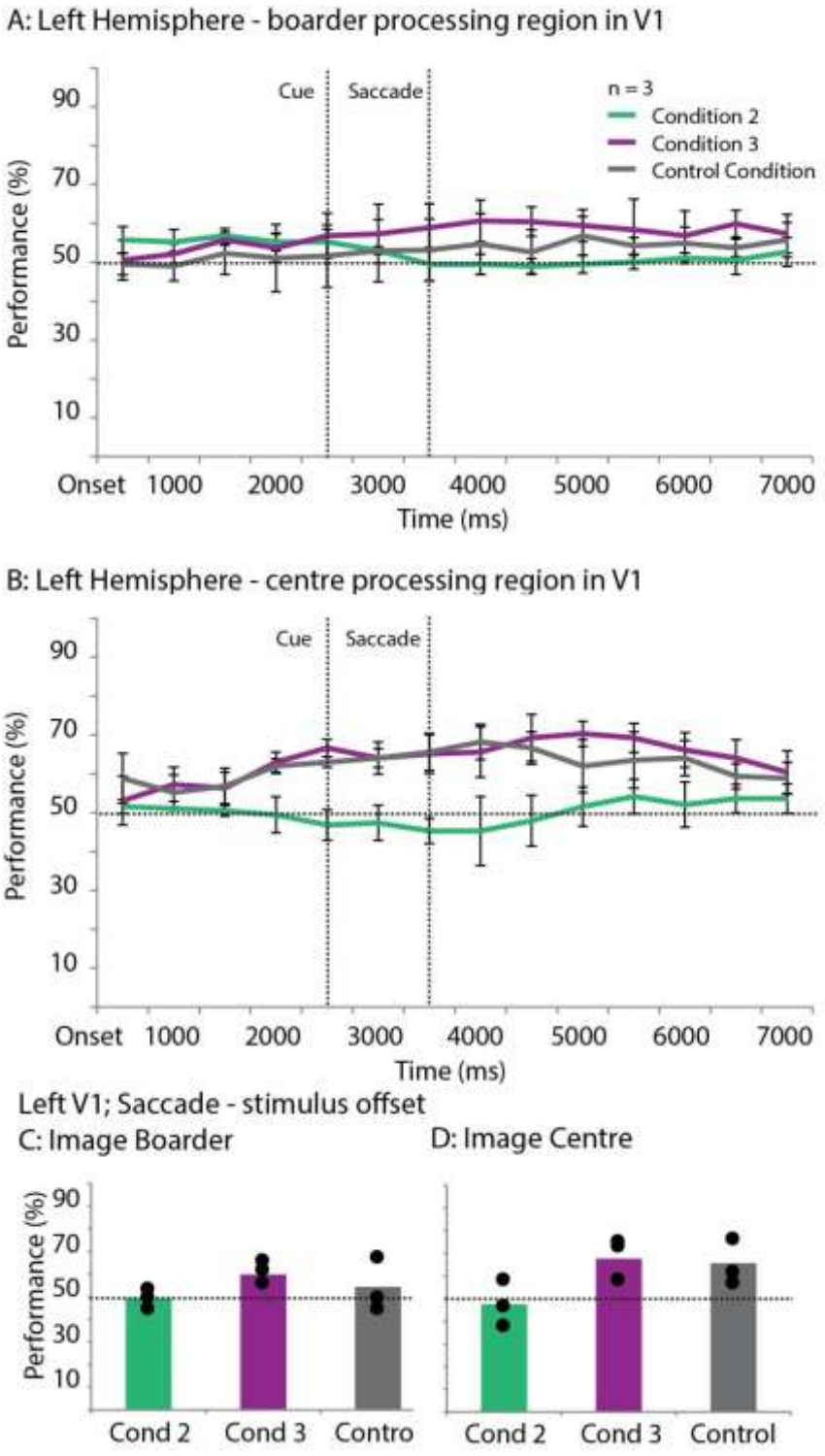

Figure 4.8 - Experiment 2: Pattern classification in left hemisphere V1 boarder and centre processing regions

A: Group one-second sliding decoder from saccade offset in left hemisphere image boarder processing region of V1. **B**: Group one-second sliding decoder from saccade offset in left hemisphere image centre processing region in V1. **C**: Classification between images in left hemisphere image boarder ROI between saccade and stimulus offset. **D**: Classification between images in left hemisphere image centre ROI between saccade and stimulus offset

4.4.2.2 Univariate Analysis

Univariate analysis was also performed on the centre and boarder ROIs for experiment 2. The boarder ROI demonstrated an activation decrease for condition 3 in comparison to the control (Figure 4.9 A & B). The activity for condition 3 and the control was more similar in the image centre.

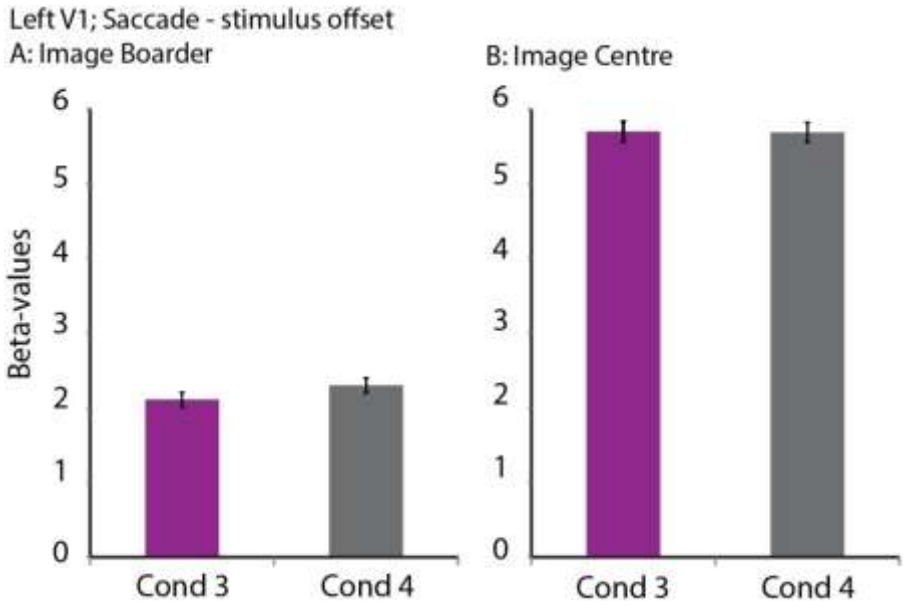

Figure 4.9 - Experiment 2: Univariate analysis between saccade and stimulus onset
A: Beta-value difference between conditions 3 and 4 in image boarder ROI. **B**: Beta-value difference between conditions 3 and 4 in image centre ROI.

In the centre ROI there was no activation difference between condition 3 and control, however there was a noticeable difference in the boarder ROI. In the boarder ROI there was a classification decrease and activation increase for the image that changed. This supports the hypothesis that predictive feedback relocated from right V1 to left V1 with saccade. When the image changes the feedback no longer predicts the sensory input resulting in error signal and decreased classification performance, supporting the results of experiment 1.

Event-related averages performed for all four regions of interest indicate the BOLD signal profile through the trial (Figure 4.10). The event-related averages mirror the BOLD profile found in experiment 1. The BOLD peaked at 8 seconds post-saccade onset for all conditions in the right hemisphere ROI (Figure 4.10 A). In the left hemisphere ROIs both condition 3 and the control condition peaked at 11 seconds (Figure 4.10 B-D). Condition 2 caused less activity in the left ROIs than found in experiment 1. Activity for condition 3

and the control is most likely related to processing the scenes post-saccade. A slight increase in activity for the control condition is shown in the centre processing region, indicating error signal production due to mid-saccade image change, however this was not reflected in the boarder ROI. The activity produced by condition 2 is likely saccade related activity projected to V1. These results replicate those found in experiment 1. It is important to note that the multivariate classification profile is does not reflect the profile of the event-related averages. This difference is due to the hemodynamic response function used for the single subject design matrix file, which is described in more detail in experiment 1 univariate results section.

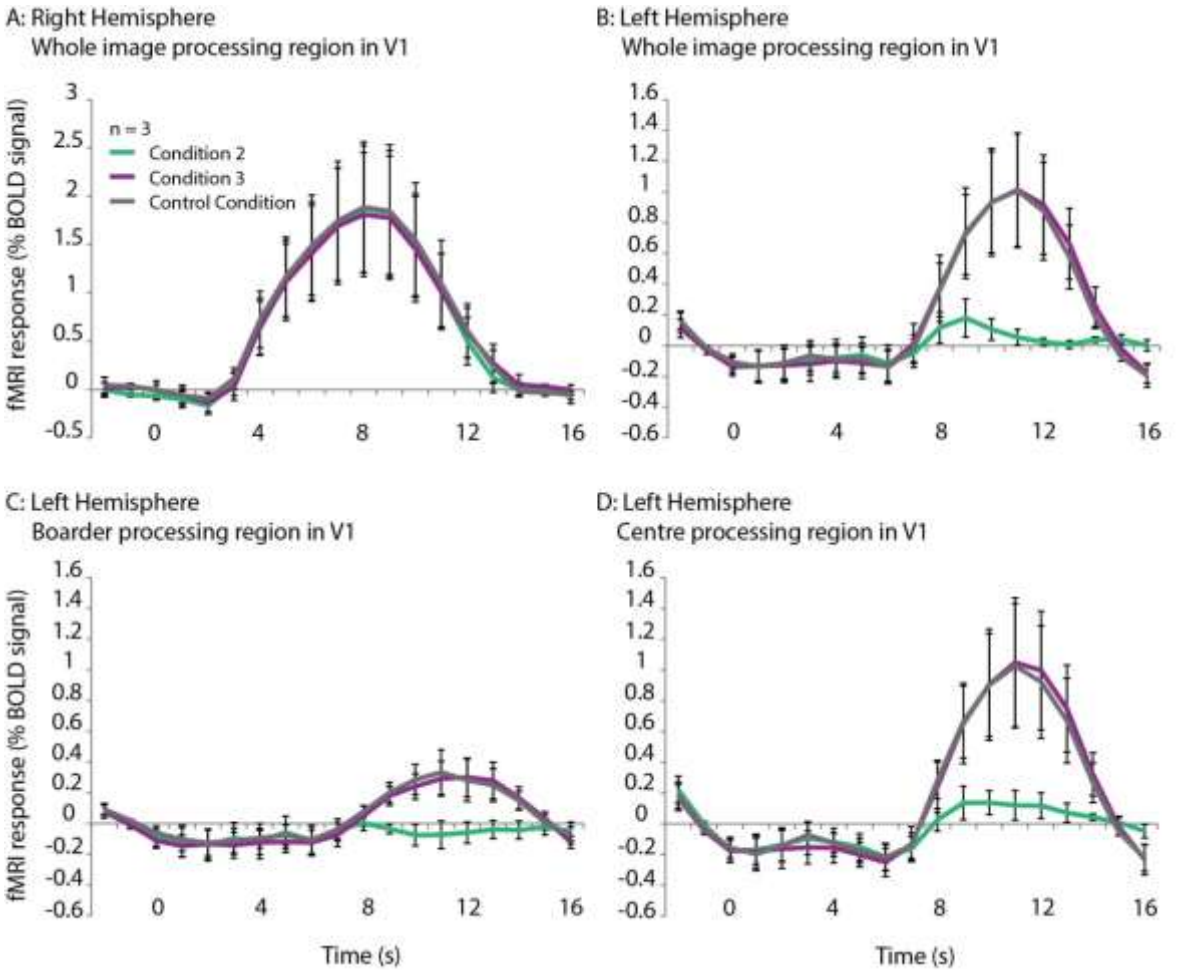

Figure 4.10 - Experiment 2: Group event-related averages
Event-related average from -2 s til 16 s post-onset in **A**: right hemisphere whole processing region of V1, **B**: left hemisphere whole processing region of V1, **C**: left hemisphere image boarder processing region of V1, **D**: left hemisphere image centre processing region of V1.

4.5 Discussion

We provide evidence for contextually relevant predictive feedback relocating to new retinotopic regions of V1 with saccade. Feedback signal relocation was demonstrated by weaker image classification performance at the new retinotopic region when the image was changed during saccades. The weaker classification for the trans-saccadic image change condition was likely due to the mismatch of predictive feedback generated by pre-saccadic stimulation and new feedforward stimulation. The mismatch proposed to explain the decreased classification for the image change was supported by an increase in BOLD activity in the new retinotopic region, above the activity associated with processing the image that remained the same across saccade. The increased activation for the changed image can be attributed to an error signal that is produced when feedback signals were not met with predicted stimuli post-saccade (Edwards, et al., submitted). Below we discuss the support for predictive feedback relocation with saccade alongside our conflicting result, which demonstrated feedback signal relocation did not occur with saccade initiation alone.

Previously, using an illusion paradigm, we found that prediction signals from a model which predicted the spatiotemporal position of an illusory moving token can be projected to new retinotopic regions with saccade (Edwards, et al., submitted). Other studies have discovered that the perception of objects after saccade is influenced by the object presentation prior to saccade through trans-saccadic integration (Prime, Niemeier, & Crawford, 2006; Van Eccelpoel et al., 2008; Wittenburg, Bremmer, & Wachtler, 2008; Pertzov, Avidan, & Zohary, 2009; Demeyer et al., 2009). Our data support this finding and develops the literature by providing evidence of predictive feedback transfer using naturalistic scene images. However, it could be postulated that the predictive feedback interaction with the image post-saccade was due to contextual inconsistency within the image, rather than predictive feedback from the pre-saccade image relocating with saccade. A predictive prior for a contextually inconsistent image would be unlikely, therefore errors may occur. To ensure predictive feedback was related to the pre-saccade image, a control was conducted using a whole image change across saccade, thereby controlling for post-saccadic contextual inconsistency. The control provided further evidence for predictive feedback relocating in V1 with saccade. A similar decrease in classification was found post-saccade along with increased activity for the changed image in the control. Therefore, these findings support the notion that the transferred information is contextually relevant to the scene processed prior to saccade.

The relocation of predictive feedback was demonstrated using both multi voxel pattern analysis and analysis of activation amplitude at the new retinotopic location after the saccade. Inference model theorists indicate that sensory stimuli which are not predicted through probabilistic inference result in an error signal, which causes an increased activation in comparison to predicted stimuli (Murray et al., 2002; Harrison et al., 2007; den Ouden et al., 2009; Alink et al., 2010; Edwards, et al., submitted). Therefore our data supports inference models, when the stimulus was predicted after saccade, activity was reduced and an improved internal representation was found. The combination of improved stimulus representation using MVPA and decreased activity amplitude for predicted sensory input has been demonstrated in a steady fixation paradigm (Kok, Jehee, & de Lange, 2012).

Although we have found evidence for predictive feedback signal relocation in V1, we also produced a potentially confounding result. Feedback signals were not detected in the new retinotopic region when a saccade was initiated and the image disappeared contingent to the eye-movement. The lack of feedback signal relocation may be a result of no feedforward stimulation for predictive feedback to interact with at the new retinotopic region. Previous studies on face after-effect use an outline of the face to facilitate after-effect (Afraz & Cavanagh, 2009). Therefore if an outline remains when the image disappears, feedback signals to the new cortical region of V1 may be detected. Moreover, our previous psychophysical experiment indicated that the transfer of predictive feedback across saccades can be as rapid as 50 – 100 ms post-saccade offset (Edwards, Vetter, & Muckli, 2012). MRI does not have the temporal resolution to investigate that particular time-window (Amaro & Barker, 2006; Logothetis, 2008; Parks & Corballis, 2010). To resolve the temporal resolution issue an experiment could be designed using magnetoencephalography (MEG) and a sliding window decoder to determine how visual representations change in relation to saccade in the new target region (Carlson et al., 2013). Specifically, by acquiring MEG and fMRI data, a time-course of feedback relocation using multivariate pattern classification may be enabled, providing both spatial and temporal information (Cichy, Pantazis, & Oliva, 2014).

Our findings are consistent with saccadic updating, specifically dynamic receptive field remapping in early visual areas. Receptive field remapping is the activation of receptive fields at the post-saccadic location for visual processing just prior to saccade initiation (Colby & Goldberg, 1999). Previous research has demonstrated that 22% of V1 voxels

activate at new retinotopic target regions in V1 during saccade (Merriam, Genovese, & Colby, 2007). Remapping in early visual areas was also found in primates, but to a lesser extent (Nakamura & Colby, 2002). Therefore receptive field remapping may have effected BOLD activation or activation patterns in the new retinotopic location in our study. Remapped receptive fields may cause a pattern of activity which enables the pattern classifier to dissociate between the images presented. However, the increased activity found in relation to an image change across saccades provides evidence for the influence of a generative model in the processing of the post-saccadic input.

Attentional factors may also contribute to some of our findings. When separating the centre and boarder ROIs, we find that activation between images for the feedforward conditions (when the image remains, regardless of whether the image centre changes or not) in the boarder ROI is lower than the centre ROI. This may be because subjects are attending to the centre of the image which is relevant to their task (i.e. is the image same or different after saccade; Egner & Hirsch, 2005). The centre ROI for experiment 2 also showed increased activity, even when the task was relevant to a *whole* image change. Therefore attention may be drawn to the most categorical information which is central in both scenes and important for the task (the people or the car). Although attention remains constant across conditions, it has been suggested that attended elements of a scene could cause differing activation patterns (Smith & Muckli, 2010). If this spatial attention relocates with saccade (Burr & Morrone, 2011), the remapped attended objects could also interfere with the internal representation of the post-saccade image, thereby interfere with classification. However, an internal representation of predicted sensory input is still necessary to attain the pattern classification differences. Therefore, although attention may contribute to the activation patterns, it is unlikely that attention could account for the activity amplitude difference found for expected and unexpected stimuli. An element of predictive feedback is still ascertained from the reported findings.

Lateral interactions have been suggested for propagating feedback signals in V1 (Gilbert & Li, 2013; Piëch et al., 2013). However, the classification difference found in the left hemisphere after saccade is not likely the result of lateral interactions filtering information from right hemisphere. Communication between right and left hemisphere V1 must travel through higher cortical areas as there is no direct connection in the medial portion of the primary visual cortices (van Essen, Newsome, & Bixby, 1982; Dumoulin & Wandell, 2008; Saenz & Fine, 2010). Direct connections across hemispheres in the early visual

cortex only begin along the V1-V2 boarder; therefore it is unlikely that lateral interactions can project contextual information across hemispheres.

Predictive feedback origination is dependent on the content of the feedback signals, such as hMT+/V5 for activity found in V1 related to the perception of illusory motion (Muckli et al., 2005; Sterzer, Haynes, & Rees, 2006; Alink et al., 2010), and V4 which showed that memory-colour representation was similar to that in V1 for grey-scale images (Bannert & Bartels, 2013). It is conceivable that the content of the predictive feedback transferred across the saccade in this study is contextually relevant to the scene processed prior to saccade. The location of origin for contextual feedback across saccade is difficult to determine. If receptive field remapping is involved, then the frontal eye fields would produce feedback signals to V1 (Felleman & van Essen, 1991). If object recognition within the scene is involved, then lateral occipital cortex would feedback information to V1 (Malach et al., 1995; Kanwisher et al., 1996). Other examples of regions involved in processing scene information and potentially projecting information across saccade include the posterior parietal cortex with space representation (Andersen et al., 1997), the inferior parietal sulcus with working memory (Friedman & Goldman-Rakic, 1994), and V3a through contrast sensitivity (Tootell et al., 1997).

Future research in the relocation of feedback signals across hemispheres should focus on the type of feedback received (Smith & Muckli, 2010) and further investigation to predictive feedback transfer with saccade initiation. By focusing on the type of information fed-back across hemispheres we would have a more conclusive idea of where the predictive feedback originates, and which mechanism controls information relocation across saccades. The likelihood is that multiple mechanisms work in cohort (predictive coding, saccadic remapping, and attention), meaning that future research should study how the mechanisms work together (Friston, 2010). Future research should also focus on saccade initiated predictive feedback relocation which was not detected in this study. Interactions between feedforward and feedback information may be important for information to transfer across saccade which could be combated through incorporating a feedforward frame (Afraz & Cavanagh, 2009). Predictive feedback initiated by saccade could also be better studied using a high temporal brain imaging technique, such as MEG, to detect the rapid relocation of feedback signals across saccade. Furthermore, due to the hemodynamic response function applied to the data which was fed into the one-second sliding window multivariate analysis, the temporal profile of feedback relocation does not

coincide with the BOLD activation profile. By utilising an MEG and fMRI approach (Cichy, Pantazis, Oliva, 2014), a more specific temporal profile of feedback relocation in V1 could be discerned.

To conclude, our data provides evidence for contextually relevant predictive feedback relocating to new retinotopic regions in V1 with saccades. Predictive feedback relocation was demonstrated by cortical feedback signals interacting with post-saccadic input. This finding supports inference models in active perception through demonstrating the relevance of inference models in processing naturalistic sensory input across saccade.

5 Chapter 5 – General Discussion

The main objective of this thesis was to determine if internal generative models could project predictions to new retinotopic locations in V1 with eye-movements. Frameworks which have previously focused on internal generative models in the visual domain have done so under the assumption that predictions fed-back from higher cortical areas to V1 can update with saccade. Within the inference model frameworks there is little to no mention of this complex task, except for Mumford (1991) who noted that continuously changing input to the LGN would be a challenge for feedback predictions. Therefore frameworks for generative models have concentrated on modelling and paradigms based on steady fixation, without saccades. Regardless, inference models in visual perception have been widely accepted. This thesis aims to support the hypothesis of active visual perception by showing that inference models are relevant in more naturalistic viewing conditions (i.e. with saccades).

Three studies were undertaken in order to investigate predictive feedback transfer with saccade. In **Chapter 2** a psychophysical paradigm was programmed to determine if spatiotemporally specific feedback could transfer with saccade, and the speed at which the transference would occur. **Chapter 3** incorporated the **Chapter 2** paradigm into an fMRI design to investigate neural evidence for the spatiotemporal feedback in V1 directly after saccade. Stemming from **Chapter 3,** another fMRI experiment was conducted in **Chapter 4** which studied contextual feedback across saccades in V1 using natural scenes. Accordingly, this general discussion will firstly focus on each chapter in turn, highlighting main findings. These findings are then incorporated into the main message of the thesis and discussed with respect to the current literature and challenges of the field.

5.1 Chapter 2 – Conclusions

In this chapter we performed two psychophysical experiments which focused on spatiotemporal prediction transference across saccade. An internal generative model was created using the apparent motion illusion which has previously been shown to produce spatiotemporally specific filling-in of the apparent motion trace in V1 (Alink et al., 2010). The subjects' task was to detect targets which were presented along this apparent motion trace. The targets were presented either in-time or out-of-time with the illusory motion. In-time targets are spatiotemporally predictable within the apparent motion (Schwiedrzik et al., 2007; Alink et al., 2010). Importantly, subjects had to perform an interhemifield

saccade across the illusion approximately every 3 seconds and the targets were presented contingent upon saccade.

Firstly we find that there was a main effect of target detection; in-time targets were better detected than out-of-time targets, which replicate previous findings (Schwiedrzik et al., 2007). An in-time target detection advantage supports the theory that predictable input is processed more efficiently. This efficient processing is most likely the result of a prediction created by an internal spatiotemporally specific generative model of the apparent motion percept. Secondly, subjects' detection advantage for in-time targets was dependent on when the target was presented with respect to saccade. During fixation in-time targets are better detected, however just prior to and during the saccade there was little target detection difference between in-time and out-of-time targets. The In-time target detection advantage returned 50 – 100 ms after saccade offset. Importantly, this rapid reappearance of the in-time detection advantage is indicative of prediction transference across saccade. Feedback predictions from the internal model of the illusory moving token would have had to transfer in order to facilitate in-time target detection as the internal model of the illusion would not have had time to build in the new hemisphere within 50 – 100 ms.

The 50 – 100 ms time-window after saccade has been found to be crucial in saccade literature. Saccadic suppression has been found to begin at 75 ms prior to saccade (Vallines & Greenlee, 2006) and release at 50 ms after saccade offset (Deubel, Schneider, & Bridgeman, 1996; Royal et al., 2006; Wurtz, 2008; Ibbotson & Krekelburg, 2011). Moreover, an ERP component indicative of visual integration has been found to follow 50 ms after saccade offset (Bellebaum & Daum, 2006). This activity accompanying saccades is consistent with our findings which show detection rate decreased prior to saccade and returned 50 ms post-saccade. These results provide the first evidence of predictive feedback relocating across saccade, thereby supporting inference models in visual perception under more naturalistic viewing conditions.

5.2 Chapter 3 – Conclusions

Following the psychophysical evidence to support the projection of predictive feedback across saccades, an fMRI study was performed in **Chapter 3** to collect neural evidence for prediction signal transfer. Previously, predictive feedback in vision has been found to project down to the primary visual cortex (V1; Mckeefry et al., 1997; Murray et al., 2002; Harrison et al., 2007; Bartels, Zeki, & Logothetis, 2008; den Ouden et al., 2009; Alink et al., 2010; Kok, Jehee, & de Lange, 2012). The apparent motion paradigm used in **Chapter**

2 is known to cause activation in V1 in the region retinotopically associated with the illusory trace which is thought to represent a filling-in of the illusory moving token (Muckli et al., 2005; Sterzer, Haynes, & Rees, 2006; Alink et al. 2010; Akselrod, Herzog, & Öğmen, 2014). The spatiotemporal specificity of the filling-in has been determined by analysing BOLD activation related to in-time and out-of-time targets. Out-of-time targets cause increased activation in V1 (Alink et al., 2010), thought to signify error signal production as the stimulus is spatiotemporally unpredictable (den Ouden et al., 2009; Alink et al., 2010; Kok, Jehee, & de Lange, 2012). In **Chapter 3**, fMRI was employed to determine if spatiotemporally specific feedback pertaining to apparent motion relocates to new retinotopic positions with saccade. Importantly, the predictions of the generative model were originally projected to right V1 and the relocation of the spatiotemporal predictions was tested in left V1 directly after saccade.

The region where targets were processed after saccade (in left V1) was located to study BOLD activation differences between apparent motion trials. In apparent motion conditions where no target was presented directly after saccade an increase in activity was found in the test region of left V1. This finding replicates Muckli and colleagues (2005) who suggested that the activity was a feedback signal filling-in the perceived motion provided by internal generative models of the illusory token. The activation found in **Chapter 3** relates to the illusory moving token after saccade, suggesting a retinotopic relocation of predictive feedback with eye-movement. Furthermore, to investigate the spatiotemporal specificity of the relocated predictive feedback, activation related to in-time and out-of-time target trials was analysed in the target region of left V1. An increased activation was found for out-of-time targets directly after saccade, demonstrating predictive feedback relocation. Analysis of the right V1 and left V2 indicated that the feedback signals were specific to left V1. Right and left V5 were active throughout apparent motion presentation indicating that these areas are relevant in the creation of the apparent motion percept, and likely involved in the generative internal model of apparent motion (Muckli et al., 2005; Wibral et al., 2009; Alink et al., 2010; Vetter, Grosbras, & Muckli, 2013).

5.3 Chapter 4 – Conclusions

Chapters 2 and **3** provided behavioural and neural evidence for the transfer of spatiotemporal predictive feedback across hemispheres. Subsequently, **Chapter 4** focused on the neural relocation of contextual feedback pertaining to the processing of natural scenes. Natural scene stimuli were used to demonstrate that predictions fed-back to V1

across saccade were not just specific to the dorsal processing stream (i.e. motion specific). The importance of naturalistic experimental paradigms has also recently been highlighted, this includes the incorporation of naturalistic sensory input (i.e. with saccades; MacEvoy, Hanks, Paradiso, 2008; Temereanca et al., 2012) and naturalistic sensory stimuli (e.g. natural scenes; MacEvoy, Hanks, Paradiso, 2008; Ayzenshtat et al., 2012; Ruiz & Paradiso, 2012) into experiments. MacEvoy and colleagues (2008) found that the difference in activation between a stimulus flashed or brought into fixation by saccade was more pronounced with natural scenes than with an optimal bar stimulus on grey background. That is, when a natural stimulus was brought into the receptive field via saccade, there was an enhancement in activity. MacEvoy and colleagues (2008) infer that the physical interaction between saccades and natural stimuli is highly significant, supporting the motivation of the experiments performed in **Chapter 4**. Confirmation of predictive feedback relocation using complex natural stimuli motivated the use of multivariate statistics. Multivoxel patterns illustrating an increased internal representation in V1 whilst collective activity in the region is reduced would support for prediction projection relocation of generative models across saccade. In **Chapter 4** the saccade execution across a natural scene was controlled to determine if saccade execution was sufficient to produce predictive feedback relocation. Image content was also manipulated contingent to saccade. The aim was to investigate if an error signal was produced with image content change and if multivariate analysis techniques could demonstrate interference between feedback of expected context and changed contextual feedforward input. Image specific processing was decoded using a one second sliding window multivariate pattern classifier.

Scene information could be decoded just prior to saccade in trials where the natural scene remained after saccade (regardless of whether it was same or different). This reflects saccade literature which indicates receptive field remapping just before saccade (Vallines & Greenlee, 2006; Wurtz, 2008; Wurtz et al., 2011). However, saccade execution alone was not sufficient to transfer predictive contextual feedback as demonstrated by the lack of contextual information in the new location when the image disappeared contingent to eye-movement. When the image changed contingent to saccade, a decrease in classification performance in the new processing region was found after saccade. This indicates that internal representation was distorted by non-matching feedforward and feedback information. Therefore classification of the changed image implied that feedback signals pertaining to the original image (pre-saccade) were transferred with saccade. Further support was found in the univariate analysis which demonstrated an increased activation

for the changed image. The increased activation may represent an error signal as the changed feedforward sensory input did not match the relocated predictive feedback. Previous research has also demonstrated that object perception after saccade has been shown to be influenced by the perceptual processing of the object prior to saccade through trans-saccadic integration (Prime, Niemeier, & Crawford, 2006; Van Eccelpoel et al., 2008; Wittenburg, Bremmer, & Wachtler, 2008; Pertzov, Avidan, & Zohary, 2009; Demeyer et al., 2009). The results of **Chapter 4** therefore further support the relevance of inference models in naturalistic viewing conditions by demonstrating contextual feedback relocation across saccade.

Chapter 4 concludes the experiments performed on the transference of predictive feedback in visual processing across saccades. Throughout the three chapters, evidence has built for the relocation of predictive feedback across hemispheres with eye-movements. During this research interesting themes have reoccurred. The following sections aim to encapsulate some of these themes and provoke thought on others.

5.4 Inferential perception and trans-saccadic perception

Investigating the transference of predictions across saccades motivated thought on the interaction between saccades and inferential perception. Classically, saccades are studied as a function of foveating critical scene elements for comprehension of sensory input. One of the main focuses of saccade research is how we combine sensory information across saccades. Merging information across saccades is thought to be achieved through five components which are collectively termed trans-saccadic perception (Melcher & Colby, 2008). In research on trans-saccadic perception, the influence of generative models only is suggested and rarely fully focused upon. A discussion on the relationship between generative models and trans-saccadic perception is presented in the following section. Generative feedback will be proposed as part of trans-saccadic perception (Harrison & Bex, 2014; Pickering & Clark, 2014) and the function of saccades is also considered from the perspective of inference models (Friston et al., 2012). The trans-saccadic perception mechanisms are also discussed along with the inference model frameworks of perception from the perspective of the free-energy principle.

5.4.1 Remapping internal generative models: the trans-saccadic perspective

To some extent, research on trans-saccadic perception touches on the internal generative models of the sensory environment, but not as explicitly as has been suggested within this thesis. Highlighting three of the components of trans-saccadic perception, it becomes clear that internal generative models must also be integrated into trans-saccadic perception, and therefore update across saccades. The three components with connection to generative models are dynamic receptive field remapping, the intermediate processing stages, and the perception of gist. These components, outlined by Melcher & Colby (2008), are presented in more detail in **Chapter 1**. Dynamic receptive field remapping (i.e. the activation of receptive fields in the new fixation location) is usually discussed in terms of receiving sensory input (Melcher & Colby, 2008; Parks & Corballis, 2008; Wurtz, 2008). However, receptive field remapping may also be conceived as preparation for receiving predictive feedback to a new retinotopic location. This is suggested by our data in **Chapters 3** and **4** where we find predictive feedback in new retinotopic locations of V1 indicating that the feedback signals relocate to the new receptive sight of sensory input. Although it is important to note that there is mixed evidence regarding the extent of receptive field remapping in V1 (Nakamura & Colby, 2002; Merriam, Genovese, & Colby, 2007).

The second trans-saccadic component, namely intermediate processing stages, are where low-level features are combined to create an entire percept (Melcher & Colby, 2008). This percept is then incorporated into the processing of the next fixation. A large number of cognitive processes are involved in the intermediate processing stages, as sensory representations are constructed during these stages. This is when processing transfers from retinotopic coordinates to a spatiotopic frame (Harrison & Bex, 2014). Generative models have been demonstrated in multiple experimental paradigms to be incorporated in the inferential perception of sensory input. One example is the ability to perform object completion using prior knowledge when an object is partially occluded (van Lier, van der Helm, & Leeuwenberg, 1994; Sugita, 1999; Erlhagen, 2003; Wyatte, Jilk, O'Reilly, 2014). There is an opportunity, therefore, for the use of prior expectations to play a role in perceptual inference in these processing stages across saccade (Harrison & Bex, 2014).

The final component of trans-saccadic perception to involve generative models is the gist component. It is suggested that gist is used to identify inconsistencies in perceptual experience across saccade (Melcher & Colby, 2008), which closely resonates with generative models of sensory input. Predictions and prediction errors in inferential perception have been found to have close ties with gist information (Bar, 2007; Kveraga,

Ghuman, & Bar, 2007; Hohwy, 2012). Previous findings have suggested that changes in a scene which violate the gist are more likely to be detected (Wolfe, 1998; O'Regan & Noë, 2001). Therefore, the use of gist to detect unexpected information across saccades in the trans-saccadic perception suggested by Melcher & Colby (2008) supports the thesis motivation for investigating prediction feedback transference with saccade.

This is the first research to empirically test relocation of predictive feedback in V1 with saccades; nonetheless research on trans-saccadic perception supports a role for generative models in naturalistic viewing. Generative models can be freely incorporated into, and complement, the trans-saccadic perception perspective.

5.4.2 Combining visual search and inferential perception: the inferential modelling perspective

The above section highlights elements of trans-saccadic perception which reflect inferential perception, indicating that inferential perception may be incorporated into trans-saccadic perception. As much as inferential perception is part of trans-saccadic perception, it has also been suggested that saccades may also be a tool in inferential perception. Itti and Baldi (2009) found that humans saccade towards unexpected items in the visual field. The finding that surprising stimuli attracts saccades indicates sensory information accumulation is directed by hypothesis driven saccadic eye-movements. Friston and colleagues (2012) have suggested that a plausible model for saccadic eye-movements is 'saccades as experiments'. Under this idea, the purpose of saccades is to collect evidence to fulfil predictions created by generative models. Therefore saccadic eye-movements can be viewed as hypothesis testing of predicted input (Gregory, 1980). In inference models the result of a prediction error is typically an alteration of the generative model to provide a better prediction of sensory information. However, as noted in Friston's (2010) article a change in sensory input may also fulfil the original hypothesis. This change in sensory input can be implemented in vision through saccade. For other sensory modalities, the ability to alter sensory input is less clear. It is likely that input alteration is achieved using location attention in hearing (Feldman & Friston, 2010) or a change in tactile stimulation, for example velvet fabric's most definitive feature are it's two textures (soft and coarse) which can only be extrapolated from a self-directed change in tactile input.

Saccades as a method of fulfilling generative models through active sampling demonstrate another tie between these active perception theories. It seems that one acts in tandem with the other in order to enable rapid perception of the visual environment.

5.4.3 The unifying theory of the brain

As discussed above, inferential perception and saccades can (theoretically) be placed under the common category of active vision. Visual searches enabled by saccades may be an instrument in inferential perception for fulfilling predictions (Friston et al., 2012) and generative models could facilitate the integration of information across saccades in three of the five main components of trans-saccadic perception.

Trans-saccadic perception and inferential perception can be unified in another way, under the free-energy principle. The free-energy principle is a mathematical framework created by Karl Friston et al. and built on work of physicists Geoffry Hinton and Terry Sejnowski (Huang, 2008). The principle limits the surprise of sensory input using generative models. Therefore sensory states remain at low entropy. The free-energy principle has been suggested as a unifying theory of the brain as the mathematical laws underlying the principle explain much of cognitive function (Huang, 2008; Friston, 2010). The Bayesian brain hypothesis and hierarchical predictive coding framework have been explained using the free-energy principle and describing trans-saccadic perception using this principle seems readily possible. In terms of the Bayesian brain hypothesis, reducing prediction errors through generative models based on probabilities from prior knowledge is the same as reducing free-energy (Friston, 2010). Such computations can also be used to describe the saccadic system (Crapse & Sommer, 2008). Specifically, the cognitive computations using the corollary discharge (CD) have been based on Bayesian principles (Bays & Wolpert, 2007; Pickering & Clark, 2014). The CD is a neural copy of saccadic eye-movements (Sperry, 1950), which enables receptive field remapping in vision (Crapse & Sommer, 2008). CD signals are employed to generate predictions about the post-movement sensory input which is common across all instances of the CD in different sensory domains (Eliades & Wang, 2008; Pickering & Clark, 2014). In vision, the physical eye-movement is compared with the CD and any residual movement detected within the scene is perceived as external environmental movement (i.e. perceiving a car as moving during saccade). Bayes-optimal modelling captures the principle function of CD as it uses probabilistic computations to create motor predictions. Crapse and Sommer (2008) suggest that a comparison between the predicted sensory input created by the CD and the actual sensory input can also result in prediction errors. Therefore, both mechanisms function by reducing error signal production which results in efficient coding and so enables proficient visual perception. The ability to determine when self-induced action occurs in sensory events using the CD may be impaired in those with schizophrenia, which leads to the inability to distinguish between self-produced or externally-produced events (Synofzik et al., 2010;

Picard & Friston, 2014). This has been shown to result in sensory hallucinations (Ford et al., 2001; Ford et al., 2008; Pynn & DeSouza, 2013).

As stated previously, the free-energy principle has been suggested as a brain wide coding strategy (Friston, 2005; Clark, 2013). Predictions from generative models and prediction errors can be found in relation to multiple cognitive processing including sensory input, motor action, higher cognitive control, and perceptual value (den Ouden, Kok, & de Lange, 2012). Although the idea of a brain wide coding strategy suggests simplicity, the complexity arises with the content of the predictions and prediction errors. The exact nature of this content is yet to be fully determined in many cognitive processes. The difference is clearly highlighted by predictions and prediction errors in saccades versus predictions and prediction errors in inference models. Predictions in saccades are based on the corollary discharge which gives a copy of the motor signal to aid saccadic suppression and trans-saccadic perception. If there is a mismatch between predicted sensory stimulus from receptive field remapping and actual sensory stimulus, an error signal is produced in the frontal eye field which informs the visual system (Crapse & Sommer, 2012). On the other hand, predictions in inference models of the visual environment are sent to lower cortical areas of the visual system to inhibit activity matching predicted sensory input. Any input not predicted by the generative model causes error signal production in the early cortical areas which are fed-forward to update the generative models in higher cortical areas. The nature of predictions and prediction errors seems to be universal, the content of the predictions and predictions errors are different and are indicative of the neural networks involved in certain processing (den Ouden, Kok, & de Lange, 2012).

Fortunately the type of information within these predictions and prediction errors enables dissociation among the mechanisms involved in the experiments presented within this thesis (i.e. inferential models and trans-saccadic perception). The activation difference for spatiotemporally predicted and unpredicted stimuli presented in **Chapter 3** and the contextual information found in **Chapter 4** at the level of V1 indicates that generative models of the visual input are being employed. Although receptive field remapping cannot be excluded as a cause of the activation in V1 (Merriam, Genovese, & Colby, 2007), any predictions or errors produced due to receptive field remapping are unlikely to consist of spatiotemporal dynamics and contextual information. Perhaps more importantly, prediction errors in receptive field remapping have been found to occur in the frontal eye fields rather than V1 (Crapse & Sommer, 2008).

5.5 The role of attention in inference models and saccades

Attention has been intertwined with inference models and saccades in multiple scenarios. Attention was classically in opposition to inference models (Koch & Poggio, 1999; Summerfield & Egner, 2009), however more recently attention has been proposed as the process of optimising the precision of predictions (Friston, 2009; Feldman & Friston, 2010; den Ouden, Kok, & de Lange, 2012; Hohwy, 2012). Attention has always been a consideration for the maintenance of visual stability through saccades (Cavanagh et al., 2010); especially as it is now accepted that attention drives saccadic eye-movements (Wurtz et al., 2011). Below, the role of attention is considered in the relocation of predictive feedback investigated in **Chapters 2, 3** and **4**, followed by the incorporation of attention into inference models and saccadic eye-movements.

Attention was not directly manipulated in the experiments of **Chapters 2**, **3**, and **4** however the effect of attention on the findings can be speculated upon. The detection advantage for predictable in-time targets compared to unpredictable out-of-time targets in **Chapters 2** and **3** is unlikely to be related to top-down attention alone. If attention was driving the target detection difference, out-of-time targets would have been more likely to be detected due to the pop-out effect (Alink et al., 2010). Pop-out refers to attention drawn to a stimulus in a bottom-up manner (Buschman & Miller, 2007; Hohwy, 2012). Out-of-time targets are more likely to produce a pop-out effect as they are unpredictable and are therefore likely to draw attention (Treisman, 1982), despite this, in-time targets were better detected. This demonstrates that the predictability of the target within the spatiotemporal generative model of apparent motion overrides any pop-out and shows that bottom-up attention does not cause the target detection difference. Also, attention cannot explain the decreased detection coupled with an increase in activation for out-of-time unpredicted targets. Attention has been shown to cause an activation *increase* for stimuli that are predicted (Doherty et al., 2005; Chaumon, Drouet, & Tallon-Baudry, 2008).

The evidence for spatiotemporal predictions in **Chapters 2** and **3** could also be explained by smoothly moving visuo-spatial attention (Shioiri et al., 2002). Shioiri and colleagues (2002) suggested that moving attention can predict the location of future stimulation in an apparent motion paradigm. This interpretation is of great interest, and should be highlighted in reference to our interpretation of predictive coding. Firstly, Shioiri and colleagues' (2002) results can be equally well explained with spatiotemporally generated models. The influence of generative models in spatiotemporal predictions, exemplified in

experiments similar to Shioiri and colleagues (2002), has gained increased support from functional brain imaging data (Alink et al., 2010). I would hypothesise that Shioiri and colleagues (2002) would find an increased activity for unpredictable out-of-time targets presented in their apparent motion paradigm as has been previously shown (Alink et al., 2010; **Chapter 3)**, which would favour inference models above moving visuo-spatial attention. Also, research provided by Muckli and colleagues (2005) found that when attention is diverted, activity can still be found along the apparent motion trace.

Moving attention may act upon the Shioiri and colleagues (2002) paradigm more than the **Chapter 2** and **3** paradigms. In the Shioiri and colleagues (2002) paradigm, apparent motion consisted of two sets of 6 disks, arranged in circular arrays, presented alternately causing the illusion of a single rotating array. Therefore the apparent motion was supported by 12 disks, which is a larger quantity of feedforward information than was present in the paradigms of **Chapter 2** and **3** of this thesis. An increased feedforward input enables an attentional shift to track one disk in the perceived rotating array through gain control of sensory input such as in biased competition. Gain control can readily occur under circumstances with feedforward input (Desimone & Duncan, 1995; Desimone, 1998) Attention through gain control is less likely to explain in-time and out-of-time target detection or processing for the apparent motion paradigm used in **Chapters 2** and **3** which was created using minimal feedforward information (two alternately flashing stimuli). Similarly, omission paradigms nicely dissociate stimulus-driven attention from inference models. Omission paradigms withhold the expected sensory stimulus and measure the neuronal response, which has been found to cause increased activity to surprising omissions (den Ouden et al., 2009; Todorovic et al., 2011; Wacongne et al., 2011; Kok et al., 2012). In omission paradigms there is no feedforward sensory information during a critical period when the level of activation is measured; therefore it is unlikely that stimulus-driven attention causes the activation difference through gain control.

Attention is also likely to have contributed to the neural activation patterns and amplitude findings of **Chapter 4** experiment 1. Activation differences were found for the regions processing the centre of the image and for the boarder of an image. The subject's response was determined by a task at the image centre; therefore the increased activity in the region processing the centre may have arisen from attention to the task-relevant part of the image (Egner & Hirsch, 2005). However, this task-related attention does not seem to be consistent in experiment 2. The whole image was important for the task, but there were still activity differences in the centre and boarder processing regions.

5.5.1 Attention in inference models

The proposal that attention is in opposition with inference models was supported by increased neural activity in response to expected stimuli which was attributed to spatial attention (Doherty et al., 2005; Chaumon, Drouet, & Tallon-Baudry, 2008). In inference models, predicted sensory input is usually accompanied by a suppression of neuronal response. Attention has recently been incorporated into inference model theories which accounts for the suggested attention related activation increase (Friston, 2009; Feldman & Friston, 2010; Bubic, Yves von Cramon, & Schubotz, 2010; den Ouden, Kok, & de Lange, 2012; Hohwy, 2012). Attention has been suggested to be the process that gates the precision of prediction errors. Precision of prediction errors is based on the reliability of the error which is in turn based on the reliability of the sensory input. This means that attention controls the weight carried by errors to effect change in generative models (Friston, 2009; Feldman & Friston, 2010; den Ouden, Kok, & de Lange, 2012; Hohwy, 2012). Therefore, attention increases the synaptic gain of sensory neurons according to more reliable sensory input. This is consistent with biased competition, where the dominant internal representation of sensory input is determined by top-down attention (Desimone & Duncan, 1995). As mentioned in **Chapter 1**, biased competition has been shown to arise from Bayes-optimal schemes like many inference model theories (Feldman & Friston, 2010). Support for attention acting on prediction error weighting was demonstrated by Kok and colleagues (2012). Kok et al. (2012) demonstrated that attention related activity was found to co-occur with expected sensory input indicating that attention increases activity based on input expectations. Therefore attention can reverse the inhibitory effect of predictions (Kok et al., 2012). Attention related enhancement of task-relevant stimuli has also been established in electroencephalography (EEG) and magnetoencephalography (MEG) studies (Pourtois, Schettino, & Vuilleumier, 2013). Therefore, the incorporation of attention into weighting prediction errors fits previous data which initially was thought to oppose inference models (den Ouden, Kok, & de Lange, 2012; Kok et al., 2012; Hohwy, 2012).

The current hypothesis for attention working within inference models suggests that attention plays a role in the neural activation found for **Chapter 3**. Specifically, attention causes an increased weighting of prediction errors for out-of-time target processing. The predictive feedback demonstrated through neural activation patterns and amplitude in **Chapter 4** is also expected to incorporate attention in the form of weightings for predictions errors. However, the effect of attention still necessitates inference modelling in

target processing. The other possible effects of attention on these paradigms must include the role of attention in saccades, especially for the findings of **Chapter 4**.

5.5.2 Attention in saccadic eye-movements

There is little doubt that attention guides saccadic eye-movements. It has been demonstrated that it is not possible to saccade to one location whilst attention is directed to another (Deubel & Schneider, 1996), which demonstrates the strength of the relationship between attention and saccades. The problem of an overwhelming sensory input is lessened by attentional control (Mazer, 2011). In this thesis, it is important to consider that elements can be held in attention across saccade. It has been found that the features of objects which are attended prior to saccade can be remapped to the new retinotopic position post-saccade through trans-saccadic perception (Melcher, 2009). Rolfs and colleagues (2011) found that attention to targets prior to saccade is shifted to new retinal locations that the target would be processed within after saccade. This suggests that attention is relocated to improve visual processing at the post-saccadic location (Cavanagh et al., 2010; Rolfs et al. 2011). These findings fit well with post-saccadic excitation which has been found in V1 (Kagan, Gur, & Snodderly, 2008; MacEvoy, Hanks, & Paradiso, 2008; Hass & Horowitz, 2011; Ibbotson & Krekelburg, 2011; Ruiz & Paradiso, 2012).

How did attention in saccadic eye-movements contribute to **Chapters 2**, **3**, and **4**? As the saccades performed in each of the experiments were controlled, attention would not have been as influential as it is in visual search. Nonetheless, attention in the remapping of visual information across saccades would still have been an important to our findings. Across all experiments in the three chapters, subjects were instructed to attend to central visual stimulation throughout the trials which included horizontal saccades over the stimulus, therefore features would have been held across saccade (Melcher, 2009; Cavanagh et al., 2010; Burr & Morrone, 2011; Irwin & Robinson, 2014). For experiments in **Chapters 2** and **3**, this feature remap has little bearing on the in-time and out-of-time detection or activation difference, however the remapping could account for some findings in **Chapter 4**. Attention is focused on specific features of the scenes when presented to the right hemisphere, therefore these attended features are likely to remap with saccade. In the condition where the image changes mid-saccade, the decreased classification post-saccade could be due to mixed patterns of activation caused by remapping of expected features and new attended features in the changed scene. Non-stimulated regions of V1 have previously been shown to contain information using multivariate pattern analysis (Serences &

Boynton, 2007; Smith & Muckli, 2010) and this contextual information was thought to be either a spread of feature-based attention (Serences & Boynton, 2007) or predictive feedback from generative models (Smith & Muckli, 2010). Importantly, in **Chapter 4**, the increased activity associated with the condition where the image changed during saccade indicates that an error signal was produced in the region that was processing the sensory input after saccade. This demonstrates that there was a violation of the predicted input, indicating that generative models were incorporated into the processing of the scene. Therefore, neither attention nor inferential models can be discounted in the processing of contextual information across saccades.

It is clear that attention has a significant role in processing sensory input. The findings of this thesis have also supported the role of attention in processing information across saccades in V1. Current theories of inference models incorporate attention into the weighting of prediction errors. This thesis does not attempt to dissociate attention from the inferential processing of sensory input across saccade. Most likely, attention enables the remapping of sensory stimuli across saccade in V1 and generative models project predictions of sensory input to the new location where attention weights any prediction errors.

5.6 Lateral interactions

Inference model theories consider the influence of feedback connections on the processing of stimuli in early cortical areas (Markov & Kennedy, 2013). However it has been suggested that the feedback signals affect intrinsic cortical connections (i.e. lateral interactions) to cause intra-cortical associations (Gilbert & Li, 2013). Piëch and colleagues (2009) modelled the effect of feedback signals on lateral connections and found that the gain produced by feedback signals onto lateral connections resulted in selectively expressed neuronal input (Piëch et al., 2009). More specifically, simulations of V1 neuron populations suggest that cortical feedback signals and lateral interactions lead to increased precision of spatial predictions (Erlhagen, 2003; Muckli & Petro, 2013; Clark, 2013). Therefore, lateral interactions are important for implementing predictive feedback from generative models in higher cortical areas. However, lateral interactions without feedback influence are unlikely to account for any neuronal findings within this thesis. In **Chapter 3**, activation along the apparent motion path was found without direct sensory input. The spread of the activation along this path maybe mediated by lateral interaction, but it seems only under the influence of feedback signals. This was demonstrated by Muckli and

colleagues (2005) who found that activation did not spread between the apparent motion inducing stimulus when the inducers were flickered randomly (i.e. not inducing an apparent motion percept). In all experiments performed within this thesis, interhemifield saccades were performed. This meant that predictive feedback originally projected to one hemisphere had to be relocated to influence processing in the other. Lateral interactions are highly unlikely to have transferred the information across hemispheres as V1 is acallosal (i.e. no direct connections between right and left V1; van Essen, Newsome, & Bixby, 1982; Dumoulin & Wandell, 2008; Saenz & Fine, 2010). Therefore, incorporation of feedback signals to influence the function of the lateral interactions certainly seems necessary when studying the relocation of information between right and left V1.

5.7 Microsaccades

The paradigms designed for the purpose of studying predictive feedback relocation with saccade within this thesis also allow speculation on the effect of microsaccades on our data. Microsaccades are very small saccades (smaller than 12 arc min) which occur when an individual is actively fixating (Martinez-Conde, Otero-Millan, & Macknik, 2013). Microsaccades have been suggested as an optimal visual sampling strategy as they ward off perceptual fading and adaptation (Martinez-Conde, Otero-Millan, & Macknik, 2013). In some paradigms, the transient burst firing which microsaccades cause has been associated with visibility (Macknik & Livingstone, 1998). Between each saccade within our paradigms, subjects are required to remain fixated which is when microsaccades are likely to affect activity in V1 (Martinez-Conde, Macknik, & Hubel, 2000). In fact, microsaccades have been shown to cause similar BOLD signal activity in early visual areas as a voluntary saccade (Tse, Baumgartner, & Greenlee, 2010). Peripheral attention has also been demonstrated to effect the direction of fixational microsaccade (Engbert & Kliegl, 2003). Across the fMRI experiments in **Chapters 3** and **4**, some of the activity we find prior to and post the transsaccadic period may be related to microsaccades. All our conditions across the experiments presented in the experimental chapters cause peripheral attention, however the occurrence of microsaccades would not be different across conditions, so is unlikely to account for the activity differences found between conditions. It could be theorised that the microsaccades performed between saccades were facilitating the processing of the pre-saccadic stimulus. For example in **Chapter 4**, microsaccades could have increased the sampling of the natural scene stimuli prior to saccade to support processing during fixation. According to our data, the feedback involved in the processing of stimuli consequently relocates to new cortical regions in V1 with saccade. With the

view that microsaccades are intrinsic to sampling information during fixation, microsaccades are therefore important in the mechanism which results in feedback relocation across saccade. Interestingly, microsaccades are thought to rarely occur in natural viewing as fixational periods are so short (Kagan, Gur, & Snodderly, 2008). Although the experiments of this thesis aim to determine the reaction of feedback to V1 under saccadic conditions, the long fixational periods in our paradigm highlight a non-realistic limitation to our experimental paradigms.

5.8 Future Directions

In support of inference models in visual perception this thesis aimed to provide evidence of predictive feedback relocation with saccades. In conducting this research, future directions for research on predictive feedback relocation have become apparent. The section below highlights potential research avenues following the findings of this thesis.

5.8.1 The timing of predictive feedback relocation

All three results Chapters provide an idea of how swiftly predictive feedback relocates to a new location with an interhemifield saccade. **Chapter 2** especially focuses on revealing the temporal aspects by design, and demonstrates that predictive feedback effects behaviour within 50 to 100 ms after saccade offset. However, as outlined in **Chapter 4**, the investigation of neural updating across saccade may benefit from a method with an increased temporal resolution, such as magnetoencephalography (MEG). Using a sliding time-window multivariate pattern classifier with MEG, as exemplified by Carlson and colleagues (2013), would enable temporally specific analysis on predictive feedback across saccade in V1. Furthermore, conducting an MEG and fMRI mixed methods experiment would provide a spatially and temporally rich profile of cortical feedback relocation which may also be able to identify active regions during the feedback relocation process (Cichy, Pantazis, & Oliva, 2014).

5.8.2 Predictive feedback relocation mechanism

The evidence for feedback from higher cortical areas to V1 has been thoroughly examined, as presented in the introduction. The psychophysical evidence and activity found in V1 (and V2 in **Chapter 3**) for all chapters has been interpreted as cortical feedback from higher cortical regions. This interpretation had been based on the theories of predictive

feedback created by inferential models, theories of attentional modulatory feedback, theories of saccadic remapping feedback and functional imaging paradigms which have tested the numerous theories. For example, Sterzer and colleagues (2006) used dynamic causal modelling (DCM) to demonstrate that activation in V1 for illusory motion was accompanied by enhanced feedback connections from hMT/V5+, a motion sensitive higher cortical region (Sterzer, Haynes, & Rees, 2006). However, further evidence could be provided to demonstrate that the activity found in V1 in **Chapters 3** and **4** are related to the relocation of cortical feedback with saccade. Using DCM, we would be able to demonstrate that the post-saccadic activity in V1 corresponds to connectivity with hMT/V5+ in **Chapter 3**. DCM would also be an informative addition to **Chapter 4** as the location of feedback has only been hypothesised. As suggested in **Chapter 4** a few regions which could be involved in feedback to V1 include the lateral occipital cortex which is involved in object recognition (Malach et al., 1995; Kanwisher et al., 1996), the posterior parietal cortex which is relevant for space representation (Andersen et al., 1997), and the frontal eye fields for receptive field remapping (Felleman & van Essen, 1991). Using connectivity analysis would enable a more encapsulating view on which of these regions feedback predictive signals of post-saccadic sensory input to V1.

In general, the relocation of predictive feedback should be further studied with a cortical layer specific approach. To date, many have explained the hierarchical nature of inference models using feedforward and feedback pathways, but recent research has found that there are at least two types of feedforward and feedback connections belonging to the supragranular and infragranular layers (Markov & Kennedy, 2013). The function of these two sets of neuronal pathways is still unknown (Markov & Kennedy, 2013), meaning that modelling the interaction between feedforward and feedback processes is challenging (Bubic, Yves von Cramon, & Schubotz, 2010). In order to further the understanding of the mechanisms behind predictive feedback relocation across hemispheres, experiments should be conducted using high-field high-resolution fMRI. Pioneering studies on generative perception are already producing revealing results of layer specific activation (Olsen et al., 2012; Muckli, HBM 2014). Furthermore, more precise tests of inference models could be achieved with more invasive techniques, such as optogenetic fMRI (ofMRI; Lee et al., 2010). ofMRI enables the simultaneous study of neuronal function and blood-oxygen-level-dependent (BOLD) activity, which should lead to a clearer understanding of how the BOLD signal is relevant at the neuronal level, and is therefore applicable to inference modelling (Larkum, 2013). Gavornik and Bear (2014) have also demonstrated that generative model creation may be studied in behaving mice using recordings from layer

specific visually evoked potentials. Recent tract tracing studies have revealed the neuroanatomy of feedforward and feedback projections at a laminar level (Markov et al., 2013) better informing structural models of the cortex.

Aside from modelling hierarchical inference frameworks within the neocortex, a structural framework of predictive feedback relocation should be considered. While the above methods would be highly informative in producing such a structural model, patient studies may also clarify prediction relocation at a neuronal level. One study located several patients with left frontal eye field (FEF) lesions which caused saccadic eye-movements disorders (Rivaud et al., 1994). Thus patients with FEF lesions may be useful in testing if trans-saccadic perception (e.g. through receptive field remapping) is necessary for the relocation of predictive feedback. Another study has investigated the updating of spatial representations in split-brain macaque monkeys (Berman et al., 2005). Even though an initial deficit in spatial representation was obvious, a rapid reorganisation indicating the employment of cortico-subcortical networks was demonstrated. This study indicates that direct cortical links were initially of high importance; however reorganisation resulted in regained ability (Berman et al., 2005). Finally, some studies have found impairments in people with schizophrenia related to the processing of the corollary discharge in distinguishing self-made movements or external environment movement (Synofzik et al., 2010; Picard & Friston, 2014). It has been suggested that the corollary discharge is not being properly processed due to a dysfunctional comparator between feedback of eye-movement and actual eye-movements (Leube et al., 2010; Pynn & de Souza, 2013). In light of these findings it would be informative to study predictive feedback relocation across eye-movement with schizophrenic patients to determine if the processing of the corollary discharge is involved in prediction relocation.

5.9 General conclusion

This thesis contributes to the rapidly growing knowledge of the role of inference models in visual perception. Specifically, the research conducted demonstrates that generative models in vision are able to project predictions to new retinotopic regions of V1 during saccades. Behavioural evidence was presented illustrating that spatiotemporal predictions transfer within 50 – 100 ms after saccade offset. Examination of neural activation demonstrated that spatiotemporal predictions relocated to new retinotopic regions of V1 directly after a saccade. Finally, the neural spatiotemporal feedback evidence was bolstered by decoding the relocation of contextual feedback in V1 with saccadic eye-movement. Therefore the obstacle of continuously changing sensory input highlighted by Mumford

(1991) has been addressed by this thesis: predictive feedback rapidly relocates projections to the early visual cortex to interact with post-saccadic sensory input. The support for prediction relocation with eye-movements enables further research into the structural mechanisms which maintain inference models during naturalistic viewing conditions.

Appendix A – Supplementary Figures Chapter 3

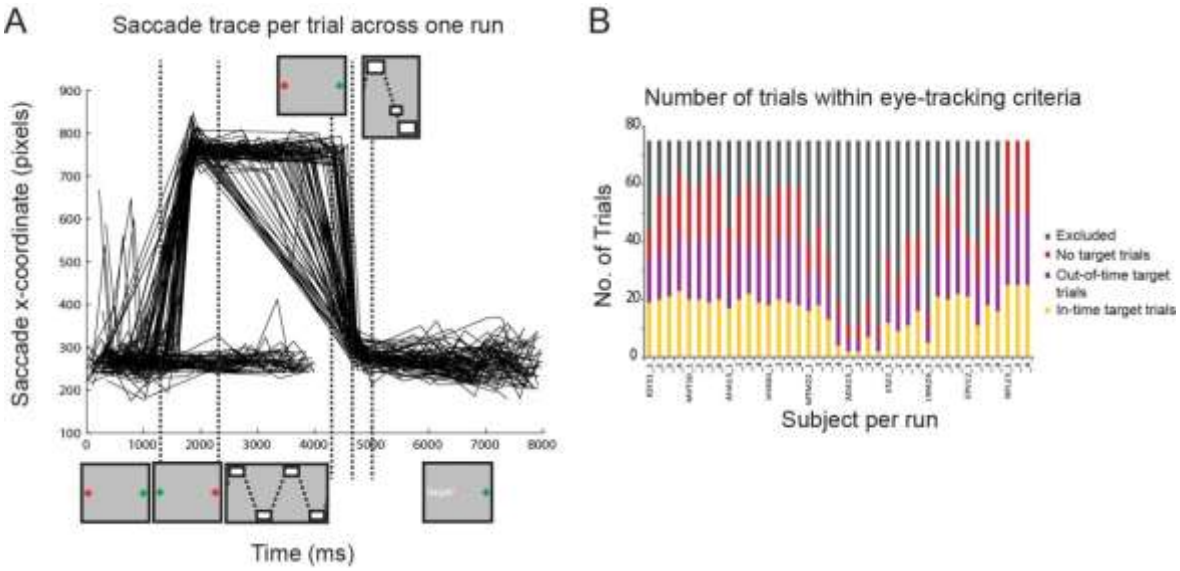

Supplementary Figure 3.1: Trial Exclusion Criterion
S1a: Saccade trace during trials for one run. Saccade criterion stipulates that saccade lands 400ms after cue and that the saccade should travel further than 200 pixels at a leftward trajectory. S1b: Number of trials excluded with eye-tracking criteria. Trial-by-trial exclusion per subject per run. One subject (ADA15) excluded due to a low number of trials in all runs. One run from two subjects (MTM22 & LWA26) also removed from analysis due to few successful trials remaining.

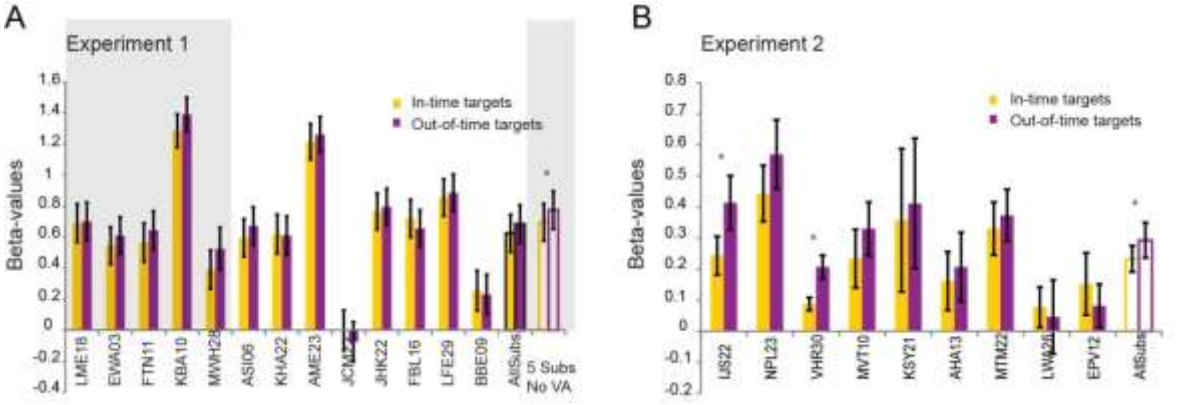

Supplementary Figure 3.2: BOLD Response for In- and Out-of-Time Target Trials in Left V1
S2a & S2b: Beta-values for in-time and out-of-time target trials per subject and whole group in left V1 ROI after saccade criterion applied. S2a: fMRI Experiment 1 - Grey background shows subjects without ventral activation, indicative of precise saccades. Group averaged data for all subjects (n=13; yellow and purple bars with black boundary) and for all subjects without ventral activation (n=5; empty yellow and purple bars). S2b - fMRI Experiment 2 – Individual subjects with significant activation difference indicated with *($p<0.05$) and group data (n=9) average in empty yellow and purple bars.

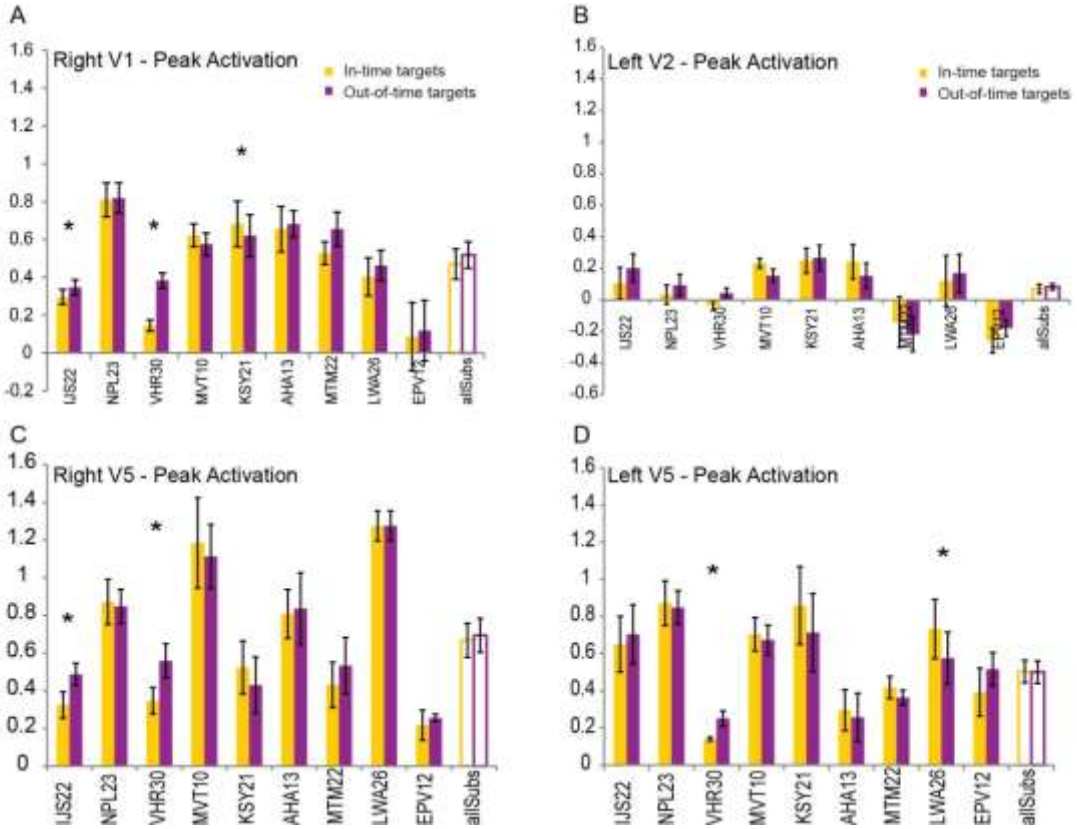

Supplementary figure 3.3: BOLD Response for In- and Out-of-Time Trials - Right V1, Left V2, Right V5, Left V5

S3a: Activation difference found in favor of out-of-time target conditions for 2 subjects (*p<0.046) and in favor of in-time targets for one subject (*p<0.049) in right V1 ROI. No activation difference was found across subjects. S3b: No activation difference was found between in-time and out-of-time target trials for any subject, or across group in left V2 ROI. S3c: Two subjects showed significant activation difference in favor of out-of-time targets in right V5 at peak activation (*p<0.005), no significant activation difference was found across group. S3d: Two subjects had an increased activation for out-of-time target trials (*p<0.04) in left V5 at peak, this was not found across subjects. S3e: A significant difference between in-time and out-of-time activation was found in one subject after peak activation in left V5 (*p<0.028), this was not reflected in the group analysis.

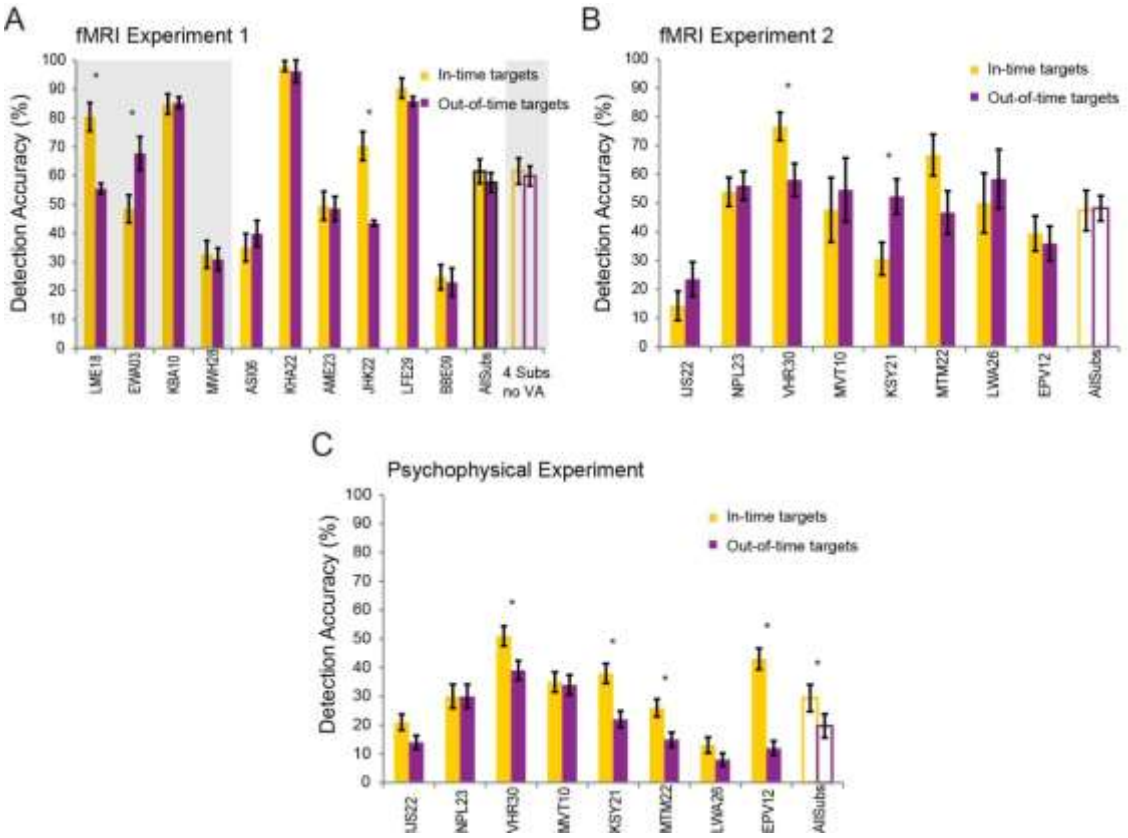

Supplementary figure 3.4: Percentage Detection Accuracy for Targets – Single Subject and Group Data

S4a, S4b, S4c: Yellow bars indicate in-time target detection accuracy and purple bars relate to out-of-time target detection accuracy. S4a: Behavioural data from fMRI experiment 1. Grey bars indicate subjects without ventral activation, yellow/purple bars with black boundary are the whole group mean, and yellow/purple empty bars are the non-ventral activation subjects group only. Single subject relative detection (*p<0.021), average data (whole group; n=10): t(9)0.898, p=0.392, group data for subjects with no ventral activation (grey background, n=4): t(3)0.192, p=0.860. S4b: Behavioural data from fMRI experiment 2. Single subjects relative detection (*p<0.018), average data (n=8): t(7)-0.115, p=0.881. S4c: Extra-session psychophysical data. Single subjects relative detection (*p<0.02), average data t(7)3.073, p=0.015.

Appendix B – Supplementary Figures Chapter 4

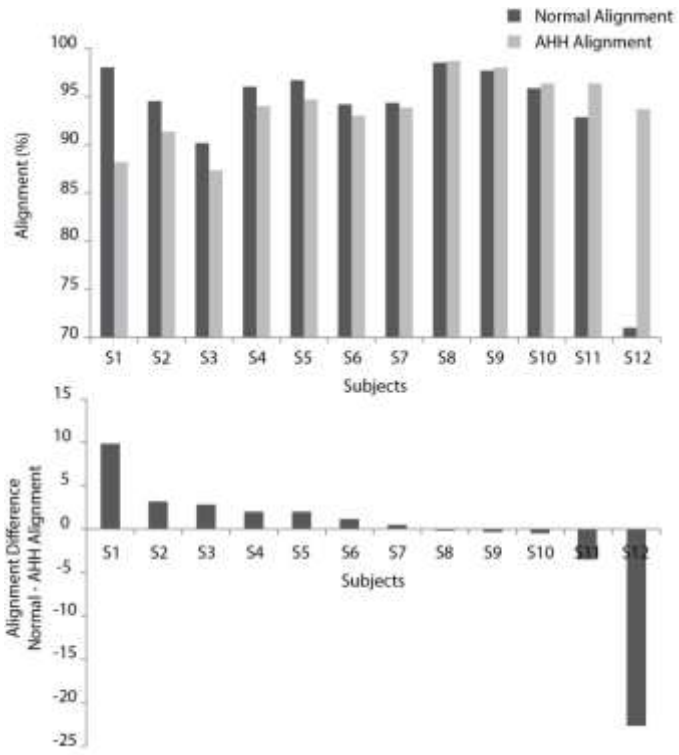

Supplementary Figure 4.1: Normal & AHH alignment per subject.
Alignment chosen for analysis completion (7 with normal anatomical, 5 with AHH scout anatomical).

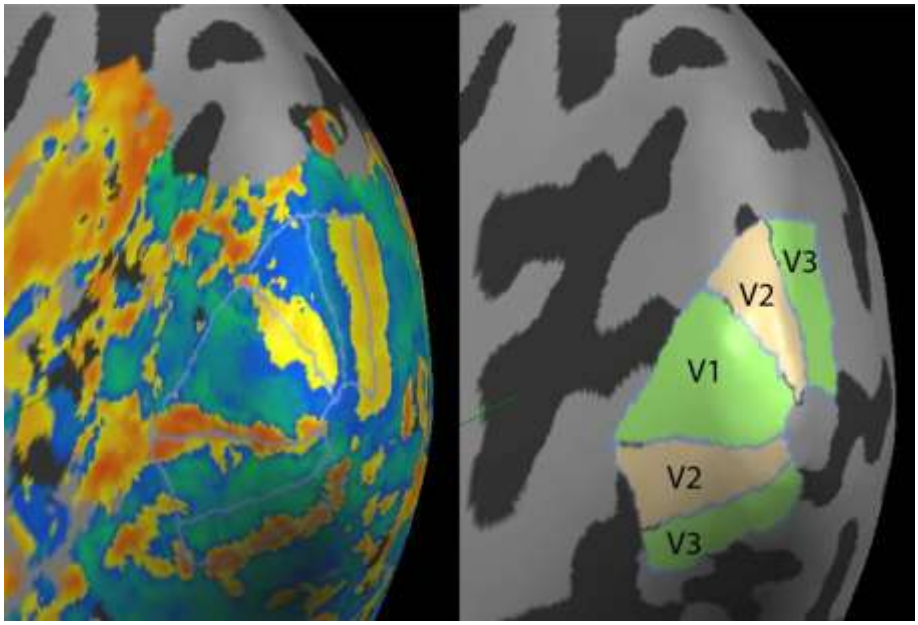

Supplementary Figure 4.2: Bowtie phase-encoded retinotopic mapping in the right hemisphere.
Left image: right hemisphere with linear correlation map; right image: right hemisphere with finished defined early cortical areas.

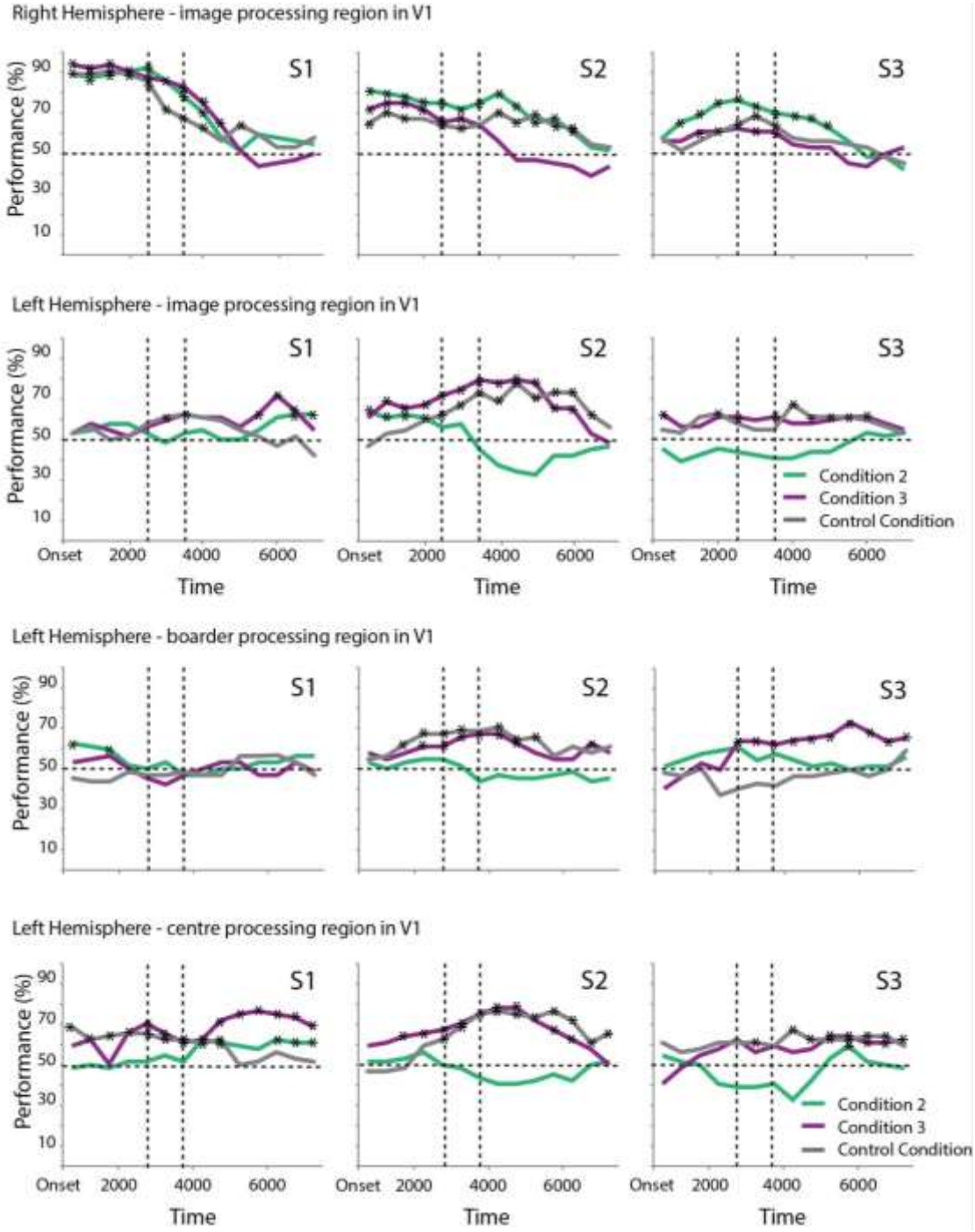

Supplementary figure 4.3 - Experiment 2: Single subject sliding pattern classification

References

Adams, D. L., Sincich, L. C., & Horton, J. C. (2007). Complete Pattern of Ocular Dominance Columns in Human Primary Visual Cortex. *The Journal of Neuroscience*, *27*(39), 10391–10403.

Afraz, A., & Cavanagh, P. (2009). The gender-specific face aftereffect is based in retinotopic not spatiotopic coordinates across several natural image transformations. *Journal of Vision*, *9*(10), 1-17.

Ahmed, B., Hanazawa, A., Undeman, C., Eriksson, D., Valentiniene, S., & Roland, P. E. (2008). Cortical Dynamics Subserving Visual Apparent Motion. *Cerebral Cortex*, *18*(12), 2796–2810.

Akselrod, M., Herzog, M. H., & Öğmen, H. (2014). Tracing path-guided apparent motion in human primary visual cortex V1. *Scientific Reports*, *4*, 1-5.

Albers, A. M., Kok, P., Toni, I., Dijkerman, H. C., & de Lange, F. P. (2013). Shared Representations for Working Memory and Mental Imagery in Early Visual Cortex. *Current Biology*, *23*(15), 1427–1431.

Alink, A., Schwiedrzik, C. M., Kohler, A., Singer, W., & Muckli, L. (2010). Stimulus Predictability Reduces Responses in Primary Visual Cortex. *The Journal of Neuroscience*, *30*(8), 2960–2966.

Amaro Jr., E., & Barker, G. J. (2006). Study design in fMRI: Basic principles. *Brain and Cognition*, *60*(3), 220–232.

Andersen, R. A., Snyder, L. H., Bradley, D. C., & Xing, J. (1997). Multimodal Representation of Space in the Posterior Parietal Cortex and Its Use in Planning Movements. *Annual Review of Neuroscience*, *20*(1), 303–330.

Anstis, S., Giaschi, D., & Cogan, A. I. (1985). Adaptation to apparent motion. *Vision Research*, *25*(8), 1051–1062.

Attneave, F., & Block, G. (1974). Absence of masking in the path of apparent movement. *Perception & Psychophysics*, *16*(2), 205-207.

Ayzenshtat, I., Gilad, A., Zurawel, G., & Slovin, H. (2012). Population Response to Natural Images in the Primary Visual Cortex Encodes Local Stimulus Attributes and Perceptual Processing. *The Journal of Neuroscience*, *32*(40), 13971–13986.

Bakola, S., Gregoriou, G. G., Moschovakis, A. K., Raos, V., & Savaki, H. E. (2007). Saccade-Related Information in the Superior Temporal Motion Complex: Quantitative Functional Mapping in the Monkey. *The Journal of Neuroscience*, *27*(9), 2224–2229.

Baloh, R. W., Sills, A. W., Kumley, W. E., & Honrubia, V. (1975). Quantitative measurement of saccade amplitude, duration, and velocity. *Neurology*, *25*(11), 1065–1065.

Ban, H., Yamamoto, H., Hanakawa, T., Urayama, S., Aso, T., Fukuyama, H., & Ejima, Y. (2013). Topographic Representation of an Occluded Object and the Effects of Spatiotemporal Context in Human Early Visual Areas. *The Journal of Neuroscience*, *33*(43), 16992–17007.

Bannert, M. M., & Bartels, A. (2013). Decoding the Yellow of a Gray Banana. *Current Biology*, *23*(22), 2268–2272.

Bar, M. (2004). Visual objects in context. *Nature Reviews Neuroscience*, *5*(8), 617–629.

Bar, M, Kassam, K. S., Ghuman, A S, Boshyan, J., Schmid, A. M., Schmidt, A. M., Dale, A. M., Hämäläinen, M.S., Marinkovic, K., Schacter, D.L., Rosen, B.R., & Halgren, E. (2006). Top-down facilitation of visual recognition. *Proceedings of the National Academy of Sciences of the United States of America*, *103*(2), 449-454.

Bar, M. (2007). The proactive brain: using analogies and associations to generate predictions. *Trends in Cognitive Sciences*, *11*(7), 280–289.

Bartels, A., Zeki, S., & Logothetis, N. K. (2008). Natural Vision Reveals Regional Specialization to Local Motion and to Contrast-Invariant, Global Flow in the Human Brain. *Cerebral Cortex*, *18*(3), 705–717.

Bastos, A. M., Usrey, W. M., Adams, R. A., Mangun, G. R., Fries, P., & Friston, K. J. (2012). Canonical Microcircuits for Predictive Coding. *Neuron*, *76*(4), 695–711.

Battaglini, P.P, Galletti, C., Aicardi, G., Squatrito, S. & Maioli, M.G. (1986). Effect of fast moving stimuli and saccadic eye movements on cell activity in visual areas V1 and V2 of behaving monkeys. *Archives Italiennes de Biologie*, *124*(2), 111–119.

Bays, P. M., & Wolpert, D. M. (2007). Computational principles of sensorimotor control that minimize uncertainty and variability. *The Journal of Physiology*, *578*(2), 387–396.

Bellebaum, C., & Daum, I. (2006). Time course of cross-hemispheric spatial updating in the human parietal cortex. *Behavioural Brain Research*, *169*(1), 150–161.

Bennett, D. J., Gorassini, M., & Prochazka, A. (1994). Catching a ball: contributions of intrinsic muscle stiffness, reflexes, and higher order responses. *Canadian Journal of Physiology and Pharmacology*, *72*(5), 525–534.

Berkes, P., Orbán, G., Lengyel, M., & Fiser, J. (2011). Spontaneous Cortical Activity Reveals Hallmarks of an Optimal Internal Model of the Environment. *Science*, *331*(6013), 83–87.

Berman, R. A., Heiser, L. M., Saunders, R. C., & Colby, C. L. (2005). Dynamic Circuitry for Updating Spatial Representations. I. Behavioral Evidence for Interhemispheric Transfer in the Split-Brain Macaque. *Journal of Neurophysiology*, *94*(5), 3228–3248.

Binzegger, T., Douglas, R. J., & Martin, K. A. C. (2004). A Quantitative Map of the Circuit of Cat Primary Visual Cortex. *The Journal of Neuroscience*, *24*(39), 8441–8453.

Braddick, O., Atkinson, J., & Wattam-Bell, J. (2003). Normal and anomalous development of visual motion processing: motion coherence and 'dorsal-stream vulnerability'. *Neuropsychologia*, *41*(13), 1769–1784.

Bremmer, F., Kubischik, M., Hoffmann, K.-P., & Krekelberg, B. (2009). Neural Dynamics of Saccadic Suppression. *The Journal of Neuroscience*, *29*(40), 12374–12383.

Brown H. & Friston, K.J. (2012) Free-Energy and illusions: the Cornsweet effect. *Frontiers in Psychology* 3, 43

Bubic, A., von Cramon, D. Y., & Schubotz, R. I. (2010). Prediction, Cognition and the Brain. *Frontiers in Human Neuroscience*, *4*:25

Budd, J. M. L. (1998). Extrastriate feedback to primary visual cortex in primates: a quantitative analysis of connectivity. *Proceedings of the Royal Society of London. Series B: Biological Sciences*, *265*(1400), 1037–1044.

Buffalo, E. A., Fries, P., Landman, R., Buschman, T. J., & Desimone, R. (2011). Laminar differences in gamma and alpha coherence in the ventral stream. *Proceedings of the National Academy of Sciences*, *108*(27), 11262–11267.

Bullier, J. (2001). Integrated model of visual processing. *Brain Research Reviews*, *36*(2–3), 96–107.

Burr, D. C., & Morrone, M. C. (2011). Spatiotopic coding and remapping in humans. *Philosophical Transactions of the Royal Society B: Biological Sciences*, *366*(1564), 504–515.

Buschman, T. J., & Miller, E. K. (2007). Top-Down Versus Bottom-Up Control of Attention in the Prefrontal and Posterior Parietal Cortices. *Science*, *315*(5820), 1860–1862.

Camprodon, J. A., Zohary, E., Brodbeck, V., & Pascual-Leone, A. (2009). Two Phases of V1 Activity for Visual Recognition of Natural Images. *Journal of Cognitive Neuroscience*, *22*(6), 1262–1269.

Cant, J. S., Arnott, S. R., & Goodale, M. A. (2009). fMR-adaptation reveals separate processing regions for the perception of form and texture in the human ventral

stream. *Experimental Brain Research*, *192*(3), 391–405.

Carlson, T., Tovar, D. A., Alink, A., & Kriegeskorte, N. (2013). Representational dynamics of object vision: The first 1000 ms. *Journal of Vision*, *13*(10), 1-19

Carpenter, G. A., & Grossberg, S. (1987). A massively parallel architecture for a self-organizing neural pattern recognition machine. *Computer Vision, Graphics, and Image Processing*, *37*(1), 54–115.

Carandini, M., Demb, J. B., Mante, V., Tolhurst, D. J., Dan, Y., Olshausen, B. A., Gallant, J.L., Rust, N. C. (2005). Do We Know What the Early Visual System Does? *The Journal of Neuroscience*, *25*(46), 10577–10597.

Cavanagh, P., Hunt, A. R., Afraz, A., & Rolfs, M. (2010). Visual stability based on remapping of attention pointers. *Trends in Cognitive Sciences*, *14*(4), 147–153.

Chalk, M., Herrero, J. L., Gieselmann, M. A., Delicato, L. S., Gotthardt, S., & Thiele, A. (2010). Attention Reduces Stimulus-Driven Gamma Frequency Oscillations and Spike Field Coherence in V1. *Neuron*, *66*(1), 114–125.

Chang C.-C., & Lin C.-J. (2006). LIBSVM: a Library for Support Vector Machines. *http://www.csie.ntu.edu.tw/~cjlin/papers/libsvm.pdf*. Retrieved from http://ntur.lib.ntu.edu.tw/handle/246246/200609271228473515 81#.VCK5oBaOrK0

Champion, R. A., & Adams, W. J. (2007). Modification of the convexity prior but not the light-from-above prior in visual search with shaded objects. *Journal of Vision*, *7*(13), 10.

Chaumon, M., Drouet, V., & Tallon-Baudry, C. (2008). Unconscious associative memory affects visual processing before 100 ms. *Journal of Vision*, *8*(3), 1-10.

Chawla, D., Phillips, J., Buechel, C., Edwards, R., & Friston, K. J. (1998). Speed-Dependent Motion-Sensitive Responses in V5: An fMRI Study. *NeuroImage*, *7*(2), 86–96.

Cicchini, G. M., Binda, P., Burr, D. C., & Morrone, M. C. (2013). Transient spatiotopic integration across saccadic eye movements mediates visual stability. *Journal of Neurophysiology*, *109*(4), 1117–1125.

Cichy, R. M., Pantazis, D., & Oliva, A. (2014). Resolving human object recognition in space and time. *Nature Neuroscience*, *17*(3), 455–462.

Clark, A. (2013). Whatever next? Predictive brains, situated agents, and the future of cognitive science. *Behavioral and Brain Sciences*, *36*(03), 181–204.

Colby, C. L., & Goldberg, M. E. (1999). Space and Attention in Parietal Cortex. *Annual Review of Neuroscience*, *22*(1), 319–349.

Coogan, T. A., & Burkhalter, A. (1990). Conserved patterns of cortico-cortical connections

define areal hierarchy in rat visual cortex. *Experimental Brain Research, 80*(1), 49–53.

Corthout, E., Uttl, B., Ziemann, U., Cowey, A., & Hallett, M. (1999). Two periods of processing in the (circum)striate visual cortex as revealed by transcranial magnetic stimulation. *Neuropsychologia, 37*(2), 137–145.

Crapse, T. B., & Sommer, M. A. (2008). Corollary discharge circuits in the primate brain. *Current Opinion in Neurobiology*, *18*(6), 552–557.

D' Avossa, G., Tosetti, M., Crespi, S., Biagi, L., Burr, D. C., & Morrone, M. C. (2007). Spatiotopic selectivity of BOLD responses to visual motion in human area MT. *Nature Neuroscience*, *10*(2), 249–255.

De Martino, F., Zimmermann, J., Muckli, L., Ugurbil, K., Yacoub, E., & Goebel, R. (2013). Cortical Depth Dependent Functional Responses in Humans at 7T: Improved Specificity with 3D GRASE. *PLoS ONE*, *8*(3), e60514.

de-Wit, L., Machilsen, B., & Putzeys, T. (2010). Predictive Coding and the Neural Response to Predictable Stimuli. *The Journal of Neuroscience*, *30*(26), 8702–8703.

Demeyer, M., Graef, P. D., Wagemans, J., & Verfaillie, K. (2009). Transsaccadic identification of highly similar artificial shapes. *Journal of Vision*, *9*(4), 28, 1-14

Den Ouden, H. E. M., Friston, K. J., Daw, N. D., McIntosh, A. R., & Stephan, K. E. (2009). A Dual Role for Prediction Error in Associative Learning. *Cerebral Cortex, 19*(5), 1175–1185.

Den Ouden, H. E. M., Daunizeau, J., Roiser, J., Friston, K. J., & Stephan, K. E. (2010). Striatal Prediction Error Modulates Cortical Coupling. *The Journal of Neuroscience*, *30*(9), 3210–3219.

Den Ouden, H. E. M., Kok, P., & de Lange, F. P. (2012). How Prediction Errors Shape Perception, Attention, and Motivation. *Frontiers in Psychology, 3*, 1-12.

Descartes, R., 1642 and 1648. Über den Menschen.Beschreibung des menschlichen Körpers. First published as 'De homine'. Transl. by K.E. Rothschuh, 1969. Heidelberg: Lambert Schneider.Descartes, R. (1972). *Treatise on man.* Hall, T. S. (Ed. And Trans.), Cambridge, Mass.: Harvard University Press (Originally published 1665).

Desimone, R. (1998). Visual attention mediated by biased competition in extrastriate visual cortex. *Philosophical Transactions of the Royal Society B: Biological Sciences, 353*(1373), 1245–1255.

Desimone, R., & Duncan, J. (1995). Neural mechanisms of selective visual attention. *Annual Review of Neuroscience, 18*, 193–222.

Deubel, H., & Schneider, W. X. (1996). Saccade target selection and object recognition: Evidence for a common attentional mechanism. *Vision Research*, *36*(12), 1827–1837.

Deubel, H., Schneider, W. X., & Bridgeman, B. (1996). Postsaccadic target blanking prevents saccadic suppression of image displacement. *Vision Research*, *36*(7), 985–996.

Diamond, M. R., Ross, J., & Morrone, M. C. (2000). Extraretinal Control of Saccadic Suppression. *The Journal of Neuroscience*, *20*(9), 3449–3455.

Doherty, J. R., Rao, A., Mesulam, M. M., & Nobre, A. C. (2005). Synergistic Effect of Combined Temporal and Spatial Expectations on Visual Attention. *The Journal of Neuroscience*, *25*(36), 8259–8266.

Douglas, R. J., & Martin, K. A. C. (2007). Mapping the Matrix: The Ways of Neocortex. *Neuron*, *56*(2), 226–238.

Duhamel, Colby, C., & Goldberg, M. (1992). The updating of the representation of visual space in parietal cortex by intended eye movements. *Science*, *255*(5040), 90 -92.

Duhamel, J.-R., Colby, C. L., & Goldberg, M. E. (1998). Ventral Intraparietal Area of the Macaque: Congruent Visual and Somatic Response Properties. *Journal of Neurophysiology*, *79*(1), 126–136.

Dumoulin, S. O., & Wandell, B. A. (2008). Population receptive field estimates in human visual cortex. *NeuroImage*, *39*(2), 647–660.

Dura-Bernal, S., Wennekers, T., & Denham, S. L. (2012). Top-Down Feedback in an HMAX-Like Cortical Model of Object Perception Based on Hierarchical Bayesian Networks and Belief Propagation. *PLoS ONE*, *7*(11), e48216.

Edwards, G., Vetter, P., Petro, L.S., & Muckli, L. (Sumitted). Predictive codes update to new retinotopic positions in human primary visual cortex.

Eccelpoel, C. V., Germeys, F., Graef, P. D., & Verfaillie, K. (2008). Coding of identity-diagnostic information in transsaccadic object perception. *Journal of Vision*, *8*(14), 29. 1-16.

Egner, T., & Hirsch, J. (2005). Cognitive control mechanisms resolve conflict through cortical amplification of task-relevant information. *Nature Neuroscience*, *8*(12), 1784–1790.

Eliades, S. J., & Wang, X. (2008b). Neural substrates of vocalization feedback monitoring in primate auditory cortex. *Nature*, *453*(7198), 1102–1106.

Engbert, R., & Kliegl, R. (2003). Microsaccades uncover the orientation of covert attention. *Vision Research*, *43*(9), 1035–1045.

Erlhagen, W. (2003). Internal models for visual perception. *Biological Cybernetics*, *88*(5), 409–417.

Ewbank, M. P., Schluppeck, D., & Andrews, T. J. (2005). fMR-adaptation reveals a distributed representation of inanimate objects and places in human visual cortex. *NeuroImage*, *28*(1), 268–279.

Feldman, H., & Friston, K. J. (2010). Attention, Uncertainty, and Free-Energy. *Frontiers in Human Neuroscience*, *4*:215

Felleman, D. J., & Van Essen, D. C. (1991). Distributed Hierarchical Processing in the Primate. *Cerebral Cortex*, *1*(1), 1–47.

Fischer, P. D. B., Boch, R., & Bach, M. (1981). Stimulus versus eye movements: Comparison of neural activity in the striate and prelunate visual cortex (A17 and A19) of trained rhesus monkey. *Experimental Brain Research*, *43*(1), 69–77.

Ford, J. M., Mathalon, D. H., Heinks, T., Kalba, S., Faustman, W. O., & Roth, W. T. (2001). Neurophysiological Evidence of Corollary Discharge Dysfunction in Schizophrenia. *American Journal of Psychiatry*, *158*(12), 2069–2071.

Ford, J. M., Roach, B. J., Faustman, W. O., & Mathalon, D. H. (2008). Out-of-Synch and Out-of-Sorts: Dysfunction of Motor-Sensory Communication in Schizophrenia. *Biological Psychiatry*, *63*(8), 736–743.

Fracasso, A., Caramazza, A., & Melcher, D. (2010). Continuous perception of motion and shape across saccadic eye movements. *Journal of Vision*, *10*(13), 14, 1-17

Friedman, H. R., & Goldman-Rakic, P. S. (1994). Coactivation of prefrontal cortex and inferior parietal cortex in working memory tasks revealed by 2DG functional mapping in the rhesus monkey. *The Journal of Neuroscience*, *14*(5), 2775–2788.

Friston, K. (2005). A theory of cortical responses. *Philosophical Transactions of the Royal Society B: Biological Sciences*, *360*(1456), 815–836.

Friston, K. (2009). The free-energy principle: a rough guide to the brain? *Trends in Cognitive Sciences*, *13*(7), 293–301.

Friston, K. (2010). The free-energy principle: a unified brain theory? *Nature Reviews Neuroscience*, *11*(2), 127–138.

Friston, K. J., Shiner, T., FitzGerald, T., Galea, J. M., Adams, R., Brown, H., Dolan, R.J., Moran, R., Stephan, K.E., & Bestmann, S. (2012). Dopamine, Affordance and Active Inference. *PLoS Computational Biology*, *8*(1), e1002327.

Friston, K., Adams, R. A., Perrinet, L., & Breakspear, M. (2012). Perceptions as Hypotheses: Saccades as Experiments. *Frontiers in Psychology*, *3*, 1-20.

Gallant, J. L., Connor, C. E., & Van Essen, D. C. (1998). Neural activity in areas V1, V2

and V4 during free viewing of natural scenes compared to controlled viewing. *Neuroreport*, *9*(1), 85–90.

Ganis, G., & Kutas, M. (2003). An electrophysiological study of scene effects on object identification. *Cognitive Brain Research*, *16*(2), 123–144.

Gavornik, J. P., & Bear, M. F. (2014). Learned spatiotemporal sequence recognition and prediction in primary visual cortex. *Nature Neuroscience*, *17*(5), 732–737.

Georges, S., Seriès, P., Frégnac, Y., & Lorenceau, J. (2002). Orientation dependent modulation of apparent speed: psychophysical evidence. *Vision Research*, *42*(25), 2757-2772.

Gilbert, C. D., & Sigman, M. (2007). Brain States: Top-Down Influences in Sensory Processing. *Neuron*, *54*(5), 677–696.

Gilbert, C. D., & Li, W. (2013). Top-down influences on visual processing. *Nature Reviews Neuroscience*, *14*(5), 350–363.

Girard, P., Hupé, J. M., & Bullier, J. (2001). Feedforward and Feedback Connections Between Areas V1 and V2 of the Monkey Have Similar Rapid Conduction Velocities. *Journal of Neurophysiology*, *85*(3), 1328–1331.

Goebel, R, Khorram-Sefat, D., Muckli, L, Hacker, H., & Singer, W. (1998). The constructive nature of vision: direct evidence from functional magnetic resonance imaging studies of apparent motion and motion imagery. *European Journal of Neuroscience*, *10*(5), 1563-1573.

Goldberg, M. E., & Bruce, C. J. (1990). Primate frontal eye fields. III. Maintenance of a spatially accurate saccade signal. *Journal of Neurophysiology*, *64*(2), 489–508.

Gombrich, E. (1979). *The sense of order: A study in the psychology of decorative art*. Oxford: Phaidon Press Limited.

Gregory, R. L. (1970). The Intelligent Eye. Retrieved from http://eric.ed.gov/?id=ED064889

Gregory, R. L. (1980). Perceptions as Hypotheses. *Philosophical Transactions of the Royal Society of London. B, Biological Sciences*, *290*(1038), 181–197.

Grill-Spector, K., Kushnir, T., Edelman, S., Avidan, G., Itzchak, Y., & Malach, R. (1999). Differential Processing of Objects under Various Viewing Conditions in the Human Lateral Occipital Complex. *Neuron*, *24*(1), 187–203.

Grill-Spector, K., Henson, R., & Martin, A. (2006). Repetition and the brain: neural models of stimulus-specific effects. *Trends in Cognitive Sciences*, *10*(1), 14–23.

Grossberg, S. (2013). Adaptive Resonance Theory: How a brain learns to consciously attend, learn, and recognize a changing world. *Neural Networks*, *37*, 1–47.

Hadjikhani, N., Liu, A. K., Dale, A. M., Cavanagh, P., & Tootell, R. B. H. (1998). Retinotopy and color sensitivity in human visual cortical area V8. *Nature Neuroscience*, *1*(3), 235–241.

Hall, N. J., & Colby, C. L. (2011). Remapping for visual stability. *Philosophical Transactions of the Royal Society B: Biological Sciences*, *366*(1564), 528–539.

Harris, K. D., & Thiele, A. (2011). Cortical state and attention. *Nature Reviews Neuroscience*, *12*(9), 509–523.

Harrison, L. M., Stephan, K. E., Rees, G., & Friston, K. J. (2007). Extra-classical receptive field effects measured in striate cortex with fMRI. *NeuroImage*, *34*(3), 1199–1208.

Harrison, W. J., & Bex, P. J. (2014). Integrating Retinotopic Features in Spatiotopic Coordinates. *The Journal of Neuroscience*, *34*(21), 7351–7360.

Hass, C. A., & Horwitz, G. D. (2011). Effects of microsaccades on contrast detection and V1 responses in macaques. *Journal of Vision*, *11*(3), 3, 1-17.

Helfrich, R. F., Becker, H. G., & Haarmeier, T. (2013). Processing of coherent visual motion in topographically organized visual areas in human cerebral cortex. *Brain topography*, *26*(2), 247-263.

Helmholtz, H. (1867). Handbuch der physiologischen Optik. Leipzig, Germany: Voss.

Hesselmann, G., Sadaghiani, S., Friston, K. J., & Kleinschmidt, A. (2010). Predictive Coding or Evidence Accumulation? False Inference and Neuronal Fluctuations. *PLoS ONE*, *5*(3), e9926.

Hidaka, S., Nagai, M., & Gyoba, J. (2009). Spatiotemporally coherent motion direction perception occurs even for spatiotemporal reversal of motion sequence. *Journal of Vision*, *9*(13), 6.1-12.

Hidaka, S., Nagai, M., Sekuler, A.B., Bennett, P.J., and Gyoba, J. (2011). Inhibition of target detection in apparent motion trajectory. *Journal of Vision*, *11*(10):2, 1-12.

Hohwy, J. (2012). Attention and Conscious Perception in the Hypothesis Testing Brain. *Frontiers in Psychology*, *3*, 1-14.

Holt, E. (1903). Eye movement and central anesthesia. Harvard Psychological Studies. 1, 3-45.

Huang, G. (2008). Is this a unified theory of the brain? *New Scientist.*2658, 30-33.

Hubel, D. H., & Wiesel, T. N. (1962). Receptive fields, binocular interaction and functional architecture in the cat's visual cortex. *The Journal of Physiology*, *160*(1), 106–154.2.

Hubel, D. H., & Wiesel, T. N. (1968). Receptive fields and functional architecture of monkey striate cortex. *The Journal of Physiology*, *195*(1), 215–243.

Hunt, A. R., & Cavanagh, P. (2009). Looking ahead: The perceived direction of gaze shifts before the eyes move. *Journal of Vision*, *9*(9), 1-7.

Hupé, J.-M., James, A. C., Girard, P., Lomber, S. G., Payne, B. R., & Bullier, J. (2001). Feedback Connections Act on the Early Part of the Responses in Monkey Visual Cortex. *Journal of Neurophysiology*, *85*(1), 134–145.

Ibbotson, M., & Krekelberg, B. (2011). Visual perception and saccadic eye movements. *Current Opinion in Neurobiology*, *21*(4), 553–558.

Ilg, U. J., & Hoffmann, K.-P. (1993). Motion perception during saccades. *Vision Research*, *33*(2), 211–220.

Irwin, D. E., & Robinson, M. M. (2014). Perceiving stimulus displacements across saccades. *Visual Cognition*, *22*(3-4), 548–575.

Itti, L., & Baldi, P. (2009). Bayesian surprise attracts human attention. *Vision Research*, *49*(10), 1295–1306.

Jehee, J. F. M., Rothkopf, C., Beck, J. M., & Ballard, D. H. (2006). Learning receptive fields using predictive feedback. *Journal of Physiology-Paris*, *100*(1–3), 125–132.

Jensen, O., Bonnefond, M., & VanRullen, R. (2012). An oscillatory mechanism for prioritizing salient unattended stimuli. *Trends in Cognitive Sciences*, *16*(4), 200–206.

Johnson, J. S., & Olshausen, B. A. (2005). The recognition of partially visible natural objects in the presence and absence of their occluders. *Vision Research*, *45*(25-26), 3262-3276.

Kagan, I., Gur, M., & Snodderly, D. M. (2008). Saccades and drifts differentially modulate neuronal activity in V1: Effects of retinal image motion, position, and extraretinal influences. *Journal of Vision*, *8*(14), 19, 1-25.

Kanwisher, N., Chun, M. M., McDermott, J., & Ledden, P. J. (1996). Functional imaging of human visual recognition. *Cognitive Brain Research*, *5*(1-2), 55–67.

Kastner, S., Pinsk, M. A., De Weerd, P., Desimone, R., & Ungerleider, L. G. (1999). Increased Activity in Human Visual Cortex during Directed Attention in the Absence of Visual Stimulation. *Neuron*, *22*(4), 751–761.

Kay, J. W., & Phillips, W. A. (2011). Coherent Infomax as a Computational Goal for Neural Systems. *Bulletin of Mathematical Biology*, *73*(2), 344–372.

Koch, C., & Poggio, T. (1999). Predicting the visual world: silence is golden. *Nature Neuroscience*, *2*(1), 9–10.

Koivisto, M., Railo, H., Revonsuo, A., Vanni, S., & Salminen-Vaparanta, N. (2011). Recurrent Processing in V1/V2 Contributes to Categorization of Natural Scenes.

The Journal of Neuroscience, *31*(7), 2488–2492.

Kok, P., Jehee, J. F. M., & de Lange, F. P. (2012). Less Is More: Expectation Sharpens Representations in the Primary Visual Cortex. *Neuron*, *75*(2), 265–270.

Kok, P., Brouwer, G. J., Gerven, M. A. J. van, & Lange, F. P. de. (2013). Prior Expectations Bias Sensory Representations in Visual Cortex. *The Journal of Neuroscience*, *33*(41), 16275–16284.

Kok, P., & de Lange, F. P. (2014). Shape Perception Simultaneously Up- and Downregulates Neural Activity in the Primary Visual Cortex. *Current Biology*, *24*(13), 1531–1535.

Kohler, A., Haddad, L., Singer, W. & Muckli, L. (2008). Deciding what to see: the role of intention and attention in the perception of apparent motion. *Vision Research*, *48*(8), 1096-1106.

Kolers, P. A. (1963). Some differences between real and apparent visual movement. *Vision Research*, *3*(5–6), 191–206.

Koopmans, P. J., Barth, M., & Norris, D. G. (2010). Layer-specific BOLD activation in human V1. *Human Brain Mapping*, *31*(9), 1297–1304.

Koopmans, P. J., Barth, M., Orzada, S., & Norris, D. G. (2011). Multi-echo fMRI of the cortical laminae in humans at 7 T. *NeuroImage*, *56*(3), 1276–1285.

Korte, A. (1915). Kinematoskopische untersuchungen. *Z. Psychol*, *72*, 193-296

Kourtzi, Z., & Kanwisher, N. (2001). Representation of Perceived Object Shape by the Human Lateral Occipital Complex. *Science*, *293*(5534), 1506–1509.

Kriegeskorte, N., & Bandettini, P. (2007). Combining the tools: activation- and information-based fMRI analysis. *NeuroImage*, *38*(4), 666–668.

Kveraga, K., Ghuman, A. S., & Bar, M. (2007). Top-down predictions in the cognitive brain. *Brain and Cognition*, *65*(2), 145–168.

Lamme V.A.F. (2006). Towards a true neural stance on consciousness. *Trends in Cognitive Sciences*, *10*(11), 494–501

Larkum, M. (2013). A cellular mechanism for cortical associations: an organizing principle for the cerebral cortex. *Trends in Neurosciences*, *36*(3), 141–151.

Larsen, A., Madsen, K. H., Lund, T. E., & Bundesen, C. (2006). Images of illusory motion in primary visual cortex. *Journal of Cognitive Neuroscience*, *18*(7), 1174–1180.

Latour, P. L. (1962). Visual Threshold During Eye Movements. *Vision Research*, *2*(3), 261–262.

Lee, J. H., Durand, R., Gradinaru, V., Zhang, F., Goshen, I., Kim, D.-S., Fenno, L.E., Ramakrishnan, C., & Deisseroth, K. (2010). Global and local fMRI signals driven

by neurons defined optogenetically by type and wiring. *Nature*, *465*(7299), 788–792.

Lee, T. S., & Mumford, D. (2003). Hierarchical Bayesian inference in the visual cortex. *Journal of the Optical Society of America A*, *20*(7), 1434–1448.

Liu, T., Slotnick, S. D., & Yantis, S. (2004). Human MT+ mediates perceptual filling-in during apparent motion. *NeuroImage*, *21*(4), 1772-1780.

Livingstone, M. S., Freeman, D. C., & Hubel, D. H. (1996). Visual Responses in V1 of Freely Viewing Monkeys. *Cold Spring Harbor Symposia on Quantitative Biology*, *61*, 27–37.

Logothetis, N. K., Pauls, J., & Poggio, T. (1995). Shape representation in the inferior temporal cortex of monkeys. *Current Biology*, *5*(5), 552–563.

Logothetis, N. K., Pauls, J., Augath, M., Trinath, T., & Oeltermann, A. (2001). Neurophysiological investigation of the basis of the fMRI signal. *Nature*, *412*(6843), 150–157.

Logothetis, N. K. (2008). What we can do and what we cannot do with fMRI. *Nature*, *453*(7197), 869–878.

Lomber, S. G., Payne, B. R., & Horel, J. A. (1999). The cryoloop: an adaptable reversible cooling deactivation method for behavioral or electrophysiological assessment of neural function. *Journal of Neuroscience Methods*, *86*(2), 179–194.

Leube, D. T., Knoblich, G., Erb, M., Schlotterbeck, P., & Kircher, T. T. J. (2010). The neural basis of disturbed efference copy mechanism in patients with schizophrenia. Cognitive Neuroscience, 1, 111–117.

MacEvoy, S. P., Hanks, T. D., & Paradiso, M. A. (2008). Macaque V1 Activity During Natural Vision: Effects of Natural Scenes and Saccades. *Journal of Neurophysiology*, *99*(2), 460–472.

Macknik, S. L., & Livingstone, M. S. (1998). Neuronal correlates of visibility and invisibility in the primate visual system. *Nature Neuroscience*, *1*(2), 144–149.

Malach, R., Reppas, J. B., Benson, R. R., Kwong, K. K., Jiang, H., Kennedy, W. A., Ledden, P.J., Rosen, B.R., & Tootell, R. B. (1995). Object-related activity revealed by functional magnetic resonance imaging in human occipital cortex. *Proceedings of the National Academy of Sciences*, *92*(18), 8135–8139.

Markov, N. T., Misery, P., Falchier, A., Lamy, C., Vezoli, J., Quilodran, R., Gariel, M.A., Giroud, P., Ercsey-Ravasz, M., Huissoud, C., Barone, P., Dehay, C., Toroczkai, Z., Van Essen, D.C., Kennedy, H. & Knoblauch, K. (2011). Weight Consistency Specifies Regularities of Macaque Cortical Networks. *Cerebral Cortex*, *21*(6),

1254–1272.

Markov, N. T., & Kennedy, H. (2013). The importance of being hierarchical. *Current Opinion in Neurobiology*, *23*(2), 187–194.

Markov, N. T., Ercsey-Ravasz, M., Lamy, C., Gomes, A. R. R., Magrou, L., Misery, P., Giroud, P., Barone, P., Dehay, C., Toroczkai, Z., Knoblauch, K., Van Essen, D.C. & Kennedy, H. (2013a). The role of long-range connections on the specificity of the macaque interareal cortical network. *Proceedings of the National Academy of Sciences*, *110*(13), 5187–5192.

Marr, D. (1982) *Vision.*W H. Freeman, San Francisco, CA.

Martinez-Conde, S., Macknik, S. L., & Hubel, D. H. (2000). Microsaccadic eye movements and firing of single cells in the striate cortex of macaque monkeys. *Nature Neuroscience*, *3*(3), 251–258.

Martinez-Conde, S., Otero-Millan, J., & Macknik, S. L. (2013). The impact of microsaccades on vision: towards a unified theory of saccadic function. *Nature Reviews Neuroscience*, *14*(2), 83–96.

Maus, G. W., & Nijhawan, R. (2008). Motion extrapolation into the blind spot. *Psychological Science*, *19*(11), 1087-1091.

Maus, G. W., Weigelt, S., Nijhawan, R., & Muckli, L. (2010). Does Area V3A Predict Positions of Moving Objects? *Frontiers in Psychology, 1* (186). 1-11.

Mazer, J. A. (2011). Spatial Attention, Feature-Based Attention, and Saccades: Three Sides of One Coin? *Biological Psychiatry*, *69*(12), 1147–1152.

McKeefry, D. J., Watson, J. D. G., Frackowiak, R. S. J., Fong, K., & Zeki, S. (1997). The Activity in Human Areas V1/V2, V3, and V5 during the Perception of Coherent and Incoherent Motion. *NeuroImage*, *5*(1), 1–12.

Melcher, D., & Colby, C. L. (2008). Trans-saccadic perception. *Trends in Cognitive Sciences*, *12*(12), 466–473.

Melcher, D. (2009). Selective attention and the active remapping of object features in trans-saccadic perception. *Vision Research*, *49*(10), 1249–1255.

Melcher, D. (2011). Visual stability. *Philosophical Transactions of the Royal Society B: Biological Sciences*, *366*(1564), 468–475.

Merriam, E. P., & Colby, C. L. (2005). Active Vision in Parietal and Extrastriate Cortex. *The Neuroscientist*, *11*(5), 484 -493.

Merriam, E. P., Genovese, C. R., & Colby, C. L. (2007). Remapping in Human Visual Cortex. *Journal of Neurophysiology*, *97*(2), 1738–1755.

Meyer, K. (2012). Another Remembered Present. *Science*, *335*(6067), 415–416.

Milner, D. A., & Goodale, M. A. (2006). *The visual brain in action (2nd ed.)* (Vol. xxii). New York, NY, US: Oxford University Press.

Mountcastle, V. B. (1957). Modality and topographic properties of single neurons of cat's somatic sensory cortex. *Journal of Neurophysiology*, *20*(4), 408–434.

Muckli, L., Kriegeskorte, N., Lanfermann, H., Zanella, F. E., Singer, W., & Goebel, R. (2002). Apparent motion: event-related functional magnetic resonance imaging of perceptual switches and States. *The Journal of Neuroscience: The Official Journal of the Society for Neuroscience*, *22*(9), RC219.

Muckli, L., Kohler, A., Kriegeskorte, N., & Singer, W. (2005). Primary Visual Cortex Activity along the Apparent-Motion Trace Reflects Illusory Perception. *PLoS Biol*, *3*(8), e265.

Muckli, L. (2010). What are we missing here? Brain imaging evidence for higher cognitive functions in primary visual cortex V1. *International Journal of Imaging Systems and Technology*, *20*(2), 131–139.

Muckli, L., & Petro, L. S. (2013). Network interactions: non-geniculate input to V1. *Current Opinion in Neurobiology*, *23*(2), 195–201.

Muckli, L. (July, 2014). Layer resolution fMRI to investigate cortical feedback in the visual cortex. In A. Shmuel (Chair) *Biophysics, aquitition methods, and interpretation of laminar specific functional MRI*. Morning workshop conducted at the Human Brain Mapping conference, Hamburg, Germany.

Mumford, D. (1991). On the computational architecture of the neocortex. *Biological Cybernetics*, *65*(2), 135–145.

Mumford, D. (1992). On the computational architecture of the neocortex. *Biological Cybernetics*, *66*(3), 241–251.

Murray, S. O., Kersten, D., Olshausen, B. A., Schrater, P., & Woods, D. L. (2002). Shape perception reduces activity in human primary visual cortex. *Proceedings of the National Academy of Sciences*, *99*(23), 15164–15169.

Murray, S. O., Boyaci, H., & Kersten, D. (2006). The representation of perceived angular size in human primary visual cortex. *Nature Neuroscience*, *9*(3), 429–434.

Nakamura, K., & Colby, C. L. (2002). Updating of the visual representation in monkey striate and extrastriate cortex during saccades. *Proceedings of the National Academy of Sciences*, *99*(6), 4026–4031.

Nijhawan, R. (2008). Visual prediction: psychophysics and neurophysiology of compensation for time delays. *Behavioral and Brain Sciences*, *31*(2), 179-198.

O'Regan, J. K., & Noë, A. (2001). A sensorimotor account of vision and visual

consciousness. *Behavioral and Brain Sciences*, *24*(05), 939–973.

Olman, C. A., Harel, N., Feinberg, D. A., He, S., Zhang, P., Ugurbil, K., & Yacoub, E. (2012). Layer-Specific fMRI Reflects Different Neuronal Computations at Different Depths in Human V1. *PLoS ONE*, *7*(3), e32536.

Olsen, S. R., Bortone, D. S., Adesnik, H., & Scanziani, M. (2012). Gain control by layer six in cortical circuits of vision. *Nature*, *483*(7387), 47–52.

Olshausen, B. A., & Field, D. J. (2005). How Close Are We to Understanding V1? *Neural Computation*, *17*(8), 1665–1699.

Ostendorf, F., Fischer, C., Finke, C., & Ploner, C. J. (2007). Perisaccadic Compression Correlates with Saccadic Peak Velocity: Differential Association of Eye Movement Dynamics with Perceptual Mislocalization Patterns. *Journal of Neuroscience*, *27*(28), 7559 -7563.

Parks, N. A., & Corballis, P. M. (2008). Electrophysiological correlates of presaccadic remapping in humans. *Psychophysiology*, *45*(5), 776–783.

Parks, N. A., & Corballis, P. M. (2010). Human transsaccadic visual processing: Presaccadic remapping and postsaccadic updating. *Neuropsychologia*, *48*(12), 3451–3458.

Perrett, D. I., Xiao, D., Barraclough, N. E., Keysers, C., & Oram, M. W. (2009). Seeing the future: Natural image sequences produce 'anticipatory' neuronal activity and bias perceptual report. *The Quarterly Journal of Experimental Psychology*, *62*(11), 2081–2104.

Pertzov, Y., Avidan, G., & Zohary, E. (2009). Accumulation of visual information across multiple fixations. *Journal of Vision*, *9*(10), 2. 1-12.

Peterburs, J., Gajda, K., Hoffmann, K.-P., Daum, I., & Bellebaum, C. (2011). Electrophysiological correlates of inter- and intrahemispheric saccade-related updating of visual space. *Behavioural Brain Research*, *216*(2), 496–504.

Picard, F., & Friston, K. (2014). Predictions, perception, and a sense of self. *Neurology*, *83*(12), 1112–1118.

Pickering, M. J., & Clark, A. (2014). Getting ahead: forward models and their place in cognitive architecture. *Trends in Cognitive Sciences*, *18*(9), 451–456.

Piëch, V., Li, W., Reeke, G. N., & Gilbert, C. D. (2013). Network model of top-down influences on local gain and contextual interactions in visual cortex. *Proceedings of the National Academy of Sciences*, *110*(43), E4108–E4117.

Pourtois, G., Schettino, A., & Vuilleumier, P. (2013). Brain mechanisms for emotional influences on perception and attention: What is magic and what is not. *Biological*

Psychology, *92*(3), 492–512.

Powell, T. P., & Mountcastle, V. B. (1959). Some aspects of the functional organization of the cortex of the postcentral gyrus of the monkey: a correlation of findings obtained in a single unit analysis with cytoarchitecture. *Bulletin of the Johns Hopkins Hospital*, *105*, 133–162.

Prime, S. L., Niemeier, M., & Crawford, J. D. (2006). Transsaccadic integration of visual features in a line intersection task. *Experimental Brain Research*, *169*(4), 532–548.

Prime, S. L., Tsotsos, L., Keith, G. P., & Crawford, J. D. (2007). Visual memory capacity in transsaccadic integration. *Experimental Brain Research*, *180*(4), 609–628.

Pynn, L. K., & DeSouza, J. F. X. (2013). The function of efference copy signals: Implications for symptoms of schizophrenia. *Vision Research*, *76*, 124–133.

Rao, R. P. N., & Ballard, D. H. (1999). Predictive coding in the visual cortex: a functional interpretation of some extra-classical receptive-field effects. *Nature Neuroscience*, *2*(1), 79–87.

Reddy, L., & Kanwisher, N. (2006). Coding of visual objects in the ventral stream. *Current Opinion in Neurobiology*, *16*(4), 408–414.

Richmond, B. J., Hertz, J. A., & Gawne, T. J. (1999). The relation between V1 neuronal responses and eye movement-like stimulus presentations. *Neurocomputing*, *26–27*, 247–254.

Riesenhuber, M., & Poggio, T. (1999). Hierarchical models of object recognition in cortex. *Nature Neuroscience*, *2*(11), 1019–1025.

Riggs, L. A., Volkmann, F. C., Moore, R. K., & Ellicott, A. G. (1982). Perception of suprathreshold stimuli during saccadic eye movement. *Vision Research*, *22*(4), 423–428.

Rivaud, S., Müri, R. M., Gaymard, B., Vermersch, A. I., & Pierrot-Deseilligny, C. (1994). Eye movement disorders after frontal eye field lesions in humans. *Experimental Brain Research*, *102*(1), 110–120.

Rockland, K. S., & Pandya, D. N. (1979). Laminar origins and terminations of cortical connections of the occipital lobe in the rhesus monkey. *Brain Research*, *179*(1), 3–20.

Rockland, K. S., & Lund, J. S. (1982). Widespread periodic intrinsic connections in the tree shrew visual cortex. *Science*, *215*(4539), 1532–1534.

Rolfs, M., Jonikaitis, D., Deubel, H., & Cavanagh, P. (2011). Predictive remapping of attention across eye movements. *Nature Neuroscience*, *14*(2), 252–256.

Roopun, A. K., Middleton, S. J., Cunningham, M. O., LeBeau, F. E. N., Bibbig, A.,

Whittington, M. A., & Traub, R. D. (2006). A beta2-frequency (20–30 Hz) oscillation in nonsynaptic networks of somatosensory cortex. *Proceedings of the National Academy of Sciences*, *103*(42), 15646–15650.

Ross, J., Morrone, M. C., Goldberg, M. E., & Burr, D. C. (2001). Changes in visual perception at the time of saccades. *Trends in Neurosciences*, *24*(2), 113-121.

Royal, D. W., Sáry, G., Schall, J. D., & Casagrande, V. A. (2006). Correlates of motor planning and postsaccadic fixation in the macaque monkey lateral geniculate nucleus. *Experimental Brain Research*, *168*(1-2), 62–75.

Ruiz, O., & Paradiso, M. A. (2012). Macaque V1 representations in natural and reduced visual contexts: spatial and temporal properties and influence of saccadic eye movements. *Journal of Neurophysiology*, *108*(1), 324–333.

Saalmann, Y. B., Pigarev, I. N., & Vidyasagar, T. R. (2007). Neural Mechanisms of Visual Attention: How Top-Down Feedback Highlights Relevant Locations. *Science*, *316*(5831), 1612–1615.

Saenz, M., & Fine, I. (2010). Topographic organization of V1 projections through the corpus callosum in humans. *NeuroImage*, *52*(4), 1224–1229.

Schmidt, K. E., Lomber, S. G., Payne, B. R., & Galuske, R. A. W. (2011). Pattern motion representation in primary visual cortex is mediated by transcortical feedback. *NeuroImage*, *54*(1), 474–484.

Schroeder, C. E., Wilson, D. A., Radman, T., Scharfman, H., & Lakatos, P. (2010). Dynamics of Active Sensing and perceptual selection. *Current Opinion in Neurobiology*, *20*(2), 172–176.

Schölvinck, M. L., & Rees, G. (2010). Neural correlates of motion-induced blindness in the human brain. *Journal of Cognitive Neuroscience*, *22*(6), 1235-1243.

Schwiedrzik, C. M., Alink, A., Kohler, A., Singer, W., & Muckli, L. (2007). A spatio-temporal interaction on the apparent motion trace. *Vision Research*, *47*(28), 3424–3433.

Serences, J. T., & Boynton, G. M. (2007). Feature-Based Attentional Modulations in the Absence of Direct Visual Stimulation. *Neuron*, *55*(2), 301–312.

Sereno, M. I., Dale, A. M., Reppas, J. B., Kwong, K. K., Belliveau, J. W., Brady, T. J., Rosen, BR, & Tootell, R. B. (1995). Borders of multiple visual areas in humans revealed by functional magnetic resonance imaging. *Science*, *268*(5212), 889–893.

Serre, T., Wolf, L., Bileschi, S., Riesenhuber, M., & Poggio, T. (2007). Robust object recognition with cortex-like mechanisms. *IEEE Transactions on Pattern Analysis and Machine Intelligence*, *29*, 411–426.

Shepard, R. N., & Zare, S. L. (1983). Path-guided apparent motion. *Science*, *220*(4597), 632–634.

Shioiri, S., Yamamoto, K., Kageyama, Y., & Yaguchi, H. (2002). Smooth shifts of visual attention. *Vision Research*, *42*(26), 2811–2816.

Shipp, S. (2007). Structure and function of the cerebral cortex. *Current Biology*, *17*(12), R443–R449.

Sincich, L. C., & Horton, J. C. (2005). THE CIRCUITRY OF V1 AND V2: Integration of Color, Form, and Motion. *Annual Review of Neuroscience*, *28*(1), 303–326.

Smith, F. W., & Muckli, L. (2010). Nonstimulated early visual areas carry information about surrounding context. *Proceedings of the National Academy of Sciences*, *107*(46), 20099–20103.

Spaak, E., Bonnefond, M., Maier, A., Leopold, D. A., & Jensen, O. (2012). Layer-Specific Entrainment of Gamma-Band Neural Activity by the Alpha Rhythm in Monkey Visual Cortex. *Current Biology*, *22*(24), 2313–2318.

Sperry, W. R. (1950). Neural basis of the spontaneous optokinetic response produced by visual inversion. *Journal of Comparative and Physiological Psychology*, *43*(6), 482–489.

Spratling, M. W. (2008). Predictive coding as a model of biased competition in visual attention. *Vision Research*, *48*(12), 1391–1408.

Spratling, M. W. (2010). Predictive Coding as a Model of Response Properties in Cortical Area V1. *The Journal of Neuroscience*, *30*(9), 3531–3543.

Sterzer, P., Haynes, J.-D., & Rees, G. (2006). Primary visual cortex activation on the path of apparent motion is mediated by feedback from hMT+/V5. *NeuroImage*, *32*(3), 1308–1316.

Sterzer, P., Frith, C., & Petrovic, P. (2008). Believing is seeing: expectations alter visual awareness. *Current Biology*, *18*(16), R697–R698.

Sugita, Y. (1999). Grouping of image fragments in primary visual cortex. *Nature*, *401*(6750), 269–272.

Summerfield, C., Trittschuh, E. H., Monti, J. M., Mesulam, M.-M., & Egner, T. (2008). Neural repetition suppression reflects fulfilled perceptual expectations. *Nature Neuroscience*, *11*(9), 1004–1006.

Summerfield, C., & Egner, T. (2009). Expectation (and attention) in visual cognition. *Trends in Cognitive Sciences*, *13*(9), 403–409.

Summerfield, C., & de Lange, F. P. (2014). Expectation in perceptual decision making: neural and computational mechanisms. *Nature Reviews Neuroscience*, *15*(11), 745–

756.

Supèr, H., Togt, C. van der, Spekreijse, H., & Lamme, V. A. F. (2004). Correspondence of presaccadic activity in the monkey primary visual cortex with saccadic eye movements. *Proceedings of the National Academy of Sciences of the United States of America*, *101*(9), 3230–3235.

Sylvester, R., Haynes, J.-D., & Rees, G. (2005). Saccades Differentially Modulate Human LGN and V1 Responses in the Presence and Absence of Visual Stimulation. *Current Biology*, *15*(1), 37–41.

Synofzik, M., Thier, P., Leube, D. T., Schlotterbeck, P., & Lindner, A. (2010). Misattributions of agency in schizophrenia are based on imprecise predictions about the sensory consequences of one's actions. *Brain*, *133*(1), 262–271.

Szinte, M., & Cavanagh, P. (2011). Spatiotopic apparent motion reveals local variations in space constancy. *Journal of Vision*, *11*(2), 4. 1-20

Temereanca, S., Hämäläinen, M. S., Kuperberg, G. R., Stufflebeam, S. M., Halgren, E., & Brown, E. N. (2012). Eye Movements Modulate the Spatiotemporal Dynamics of Word Processing. *The Journal of Neuroscience*, *32*(13), 4482–4494.

Thorpe, S. J., & Fabre-Thorpe, M. (2001). Seeking Categories in the Brain. *Science*, *291*(5502), 260–263.

Todorovic, A., Ede, F. van, Maris, E., & Lange, F. P. de. (2011). Prior Expectation Mediates Neural Adaptation to Repeated Sounds in the Auditory Cortex: An MEG Study. *The Journal of Neuroscience*, *31*(25), 9118–9123.

Tolias, A. S., Moore, T., Smirnakis, S. M., Tehovnik, E. J., Siapas, A. G., & Schiller, P. H. (2001). Eye Movements Modulate Visual Receptive Fields of V4 Neurons. *Neuron*, *29*(3), 757–767.

Tootell, R. B. H., Mendola, J. D., Hadjikhani, N. K., Ledden, P. J., Liu, A. K., Reppas, J. B., Sereno, M.I., & Dale, A. M. (1997). Functional Analysis of V3A and Related Areas in Human Visual Cortex. *The Journal of Neuroscience*, *17*(18), 7060–7078.

Treisman, A. (1982). Perceptual grouping and attention in visual search for features and for objects. *Journal of Experimental Psychology: Human Perception and Performance*, *8*(2), 194–214.

Tse, P. U., Baumgartner, F. J., & Greenlee, M. W. (2010). Event-related functional MRI of cortical activity evoked by microsaccades, small visually-guided saccades, and eyeblinks in human visual cortex. *NeuroImage*, *49*(1), 805–816.

Ulanovsky, N., Las, L., & Nelken, I. (2003). Processing of low-probability sounds by cortical neurons. *Nature Neuroscience*, *6*(4), 391–398.

Umeno, M. M., & Goldberg, M. E. (1997). Spatial processing in the monkey frontal eye field. I. Predictive visual responses. *Journal of Neurophysiology*, *78*(3), 1373–1383.

Umeno, M. M., & Goldberg, M. E. (2001). Spatial Processing in the Monkey Frontal Eye Field. II. Memory Responses. *Journal of Neurophysiology*, *86*(5), 2344 -2352.

Vallines, I., & Greenlee, M. W. (2006). Saccadic Suppression of Retinotopically Localized Blood Oxygen Level-Dependent Responses in Human Primary Visual Area V1. *The Journal of Neuroscience*, *26*(22), 5965–5969.

Van Essen, D., Newsome, W. T., & Bixby, J. L. (1982). The pattern of interhemispheric connections and its relationship to extrastriate visual areas in the macaque monkey. *The Journal of Neuroscience*, *2*(3), 265–283.

Van Lier, R., van der Helm, P., & Leeuwenberg, E. (1994). Integrating global and local aspects of visual occlusion. *Perception*, *23*(8), 883–903.

Vandenbroucke, A. R. E., Fahrenfort, J. J., Sligte, I. G., & Lamme, V. A. F. (2013). Seeing without Knowing: Neural Signatures of Perceptual Inference in the Absence of Report. *Journal of Cognitive Neuroscience*, *26*(5), 955–969.

Verghese, A., Kolbe, S. C., Anderson, A. J., Egan, G. F., & Vidyasagar, T. R. (2014). Functional size of human visual area V1: A neural correlate of top–down attention. *NeuroImage*, *93, Part 1*, 47–52.

Vetter, P., Edwards, G., & Muckli, L. (2012). Transfer of Predictive Signals Across Saccades. *Frontiers in Psychology*, *3*: 176. 1-10.

Vetter, P., Grosbras, M.-H., & Muckli, L. (2013). TMS Over V5 Disrupts Motion Prediction. *Cerebral Cortex*, bht297.

Vetter, P., Smith, F. W., & Muckli, L. (2014). Decoding Sound and Imagery Content in Early Visual Cortex. *Current Biology*, *24*(11), 1256–1262.

Vezoli, J., Falchier, A., Jouve, B., Knoblauch, K., Young, M., & Kennedy, H. (2004). Quantitative Analysis of Connectivity in the Visual Cortex: Extracting Function from Structure. *The Neuroscientist*, *10*(5), 476–482.

Vincent, J. L., Patel, G. H., Fox, M. D., Snyder, A. Z., Baker, J. T., Van Essen, D. C., Zempel, J.M., Snyder, L.H., Corbetta, M., & Raichle, M. E. (2007). Intrinsic functional architecture in the anaesthetized monkey brain. *Nature*, *447*(7140), 83–86.

Volkmann, F. C., Schick, A. M., & Riggs, L. A. (1968). Time course of visual inhibition during voluntary saccades. *Journal of the Optical Society of America*, *58*(4), 562–569.

von Helmholtz, H. (1962). *Treatise on Physiological Optics.* Dover Publications: New York, vol. 3.

Wacongne, C., Labyt, E., Wassenhove, V. van, Bekinschtein, T., Naccache, L., & Dehaene, S. (2011). Evidence for a hierarchy of predictions and prediction errors in human cortex. *Proceedings of the National Academy of Sciences*, *108*(51), 20754–20759.

Wexler, M. (2005). Anticipating the three-dimensional consequences of eye movements. *Proceedings of the National Academy of Sciences of the United States of America*, *102*(4), 1246–1251.

Wibral, M., Bledowski, C., Kohler, A., Singer, W., & Muckli, L. (2009). The Timing of Feedback to Early Visual Cortex in the Perception of Long-Range Apparent Motion. *Cerebral Cortex*, *19*(7), 1567–1582.

Wittenberg, M., Bremmer, F., & Wachtler, T. (2008). Perceptual evidence for saccadic updating of color stimuli. *Journal of Vision*, *8*(14), 1-9.

Wolfe, J. M. (1998). Visual memory: What do you know about what you saw? *Current Biology*, *8*(9), R303–R304.

Wurtz, R. H. (2008). Neuronal mechanisms of visual stability. *Vision Research*, *48*(20), 2070–2089.

Wurtz, R. H., Joiner, W. M., & Berman, R. A. (2011). Neuronal mechanisms for visual stability: progress and problems. *Philosophical Transactions of the Royal Society B: Biological Sciences*, *366*(1564), 492–503.

Wyatte, D., Jilk, D. J., & O'Reilly, R. C. (2014). Early recurrent feedback facilitates visual object recognition under challenging conditions. *Frontiers in Psychology*, *5*. 1-10.

Yantis, S., & Nakama, T. (1998). Visual interactions in the path of apparent motion. *Nature Neuroscience*, *1*(6), 508-512.

Yi, D.-J., Turk-Browne, N. B., Flombaum, J. I., Kim, M.-S., Scholl, B. J., & Chun, M. M. (2008). Spatiotemporal object continuity in human ventral visual cortex. *Proceedings of the National Academy of Sciences*, *105*(26), 8840–8845.

Zacharie, M. (2007). Adaptive Resonance Theory 1 (ART1) Neural Network Based Horizontal and Vertical Classification of 0-9 Digits Recognition. *Journal of Computer Science*, *3*(11), 869–873.

Zimmermann, E., Morrone, M. C., & Burr, D. C. (2014). The visual component to saccadic compression. *Journal of Vision*, *14*(12), 13.

Zuber, B. L., & Stark, L. (1966). Saccadic suppression: Elevation of visual threshold associated with saccadic eye movements. *Experimental Neurology*, *16*(1), 65–79.